THE CALCULATION OF SOLAR RADIATION OVER LAKE ONTARIO

THE CALCULATION OF SOLAR
RADIATION OVER LAKE ONTARIO

by

MANUEL NUNEZ, B.Sc.

A Thesis
Submitted to the Faculty of Graduate Studies
in Partial Fulfilment of the Requirements
for the Degree
Master of Science

McMaster University
September 1971

MASTER OF SCIENCE (1971)
(Physics)

McMASTER UNIVERSITY
Hamilton, Ontario

TITLE: The calculation of solar radiation over Lake Ontario

AUTHOR: Manuel Nunez, B.Sc. (University of Montreal)

SUPERVISOR: Dr. J. A. Davies

NUMBER OF PAGES: ix, 116

SCOPE AND CONTENTS:

Simultaneous solar radiation and meteorological observations were taken from an instrumented tower located in southwestern Lake Ontario. During the four month period of this study (July-November, 1969) it was found that short-term fluxes of incoming global radiation could be predicted with a standard error which was better than 0.05 cal $cm^{-2}min^{-1}$ under cloudless conditions. Under cloudy conditions the lowest standard of prediction error (0.14 cal $cm^{-2}min^{-1}$) was obtained using a model which takes into account cloud type transmission. Under cloudless conditions the Fresnel curve underpredicts the albedos observed for low zenith angles and overpredicts when the zenith angle is high. This is mostly due to a backscatter effect estimated to be between 1.5 to 2% and to the albedo of diffuse radiation which was confirmed to be 6.5 to 7%.

ACKNOWLEDGEMENTS

I would like to gratefully acknowledge the excellent guidance given by my supervisor, Dr. J. A. Davies. Special thanks to the Canada Center for Inland Waters who lent valuable assistance and support during the field program; to Mr. R. Latimer of the National Radiation Laboratory for calibrating the sensors used in the study; to members of the Department of Geography at McMaster for their assistance and many fruitful discussions and to Messrs. R. and L. Martin for the use of their property during the field season. The author is also indebted to Mr. H. Fritz who prepared the figures and to Miss J. Hillen who typed the final draft.

TABLE OF CONTENTS

LIST OF FIGURES

LIST OF TABLES

CHAPTER I

INTRODUCTION

Depletion problem

In most energy balance systems in the natural world solar radiation is the forcing function (Lettau, 1969). This input is subjected to large variations due to astronomical and environmental factors. These two effects have generated a large number of studies on depletion processes in the atmosphere and the calculation of solar radiation at the earth's surface.

Direct measurements of solar radiation are sparce relative to other meteorological parameters. Even when these measurements are made their accuracy is often questionable. In fact only recently has it been possible to obtain reliable measurements of solar radiation due to improved sensor designs (Robinson, 1966).

Simultaneous meteorological observations are of course essential in depletion estimates and careful consideration must be given to their quality and frequency. Most of the depletion studies have been confined to monthly estimates (Monteith, 1962, London, 1957, Houghton, 1954) and only give insight into mean values of the processes. There is a need to consider shorter term variation. Studies on the diurnal variation of atmospheric transmission under special conditions of overcast skies have been conducted by Haurwitz (1948) and Vowinckel and Orwig (1962).

Recently Lettau (1969) used data collected near solar noon to study solar depletion but his estimates were few and he did not attempt to generalize for all possible conditions.

A theoretical approach to depletion has also been attempted. Deirmendjian and Sekera (1954), calculated the direct and diffuse radiation incident on a plane parallel atmosphere. Deirmendjian (1969) solved the radiative transfer equations for a turbid atmosphere containing aerosols of different sizes and concentration. Feigel'son (1966) obtained theoretical transmissions for different types of stratus clouds. The writer considers that at present, attempts at a theoretical description of the entire depletion of solar radiation are limited by two considerations. Firstly, experimental verification of the model is difficult because of the type of data that have to be obtained. Very often the instrumentation has not been developed or the cost of conducting such an operation is prohibitive. Secondly, and more fundamental, certain depletion processes in the atmosphere are inherently statistical in nature and cannot be easily modelled on a strict analytical basis. For example, although a complete theoretical description of the radiation transmitted by a particular cloud might be possible, the statistics of the cloud distribution would have to be analyzed to obtain an overall atmospheric transmission.

Prediction problem

Apart from depletion analyses, the problem of predicting* solar radiation fluxes is an important one in meteorology. Although it can be argued that a model which describes solar depletion correctly at a location can be used as a predictor, the space and time dependence of

* in this study the word prediction is synonymous with calculation.

the prediction cannot be neglected. This aspect of prediction has been largely ignored. The usual procedure has been to apply depletion relations obtained at defined locations, to predict solar fluxes over an arbitrary area. Houghton (1954), using data from the Smithsonian Institution's Astrophysical Laboratory derived a set of solar transmission curves. These relations along with cloud data were then used to predict daily global radiation over the northern hemisphere. Similar studies have been carried out by London(1957) and Budyko (1956). Hay (1970) using climatic data across Canada predicted mean monthly values of short-wave and long-wave radiation which agreed well with individual station measurements. Prediction models of this nature must rely on the horizontal distribution of the meteorological parameters. If the parameter depletes solar radiation strongly, its distribution over the given area could have a critical effect on the prediction. A proper assessment of the model would be obtained by comparing predicted with measured values of solar radiation over the area in question. The time dependence of the prediction is of course related to the variation with time of the parameters controlling the depletion. If a significant parameter varies faster than the frequency of observation, then large prediction errors could be expected.

Aims of the study

During the period of July to November 1969 an instrumented tower was located in the southwestern end of Lake Ontario. Incoming and outgoing fluxes of solar and long-wave radiation were recorded on a continuous basis. In addition routine meteorological measurements were taken for most days. This study, which is based on their data, will have two aims:

a) The depletion and modification of the solar fluxes by the marine environment will be examined in detail. The relative importance of each parameter in causing depletion will be calculated and it is hoped that this work will isolate critical parameters. This analysis will concentrate specially on half-hourly fluxes since short-term depletion studies can give a realistic view of all the processes occurring in the atmosphere.

b) Different models will be tested for their ability to predict solar radiation at the tower location. There will be no attempt to predict solar radiation over an area. This is a separate problem. In brief the problem can be stated as follows: Given a particular location, which is typical of Lake Ontario, how well can a model predict solar radiation for different time intervals and what effect will the frequency of meteorological sampling have on the prediction?

Organization of thesis

The content of this work has been divided into four main sections. Chapter II discusses the depletion processes and predictive models of solar radiation under both cloudless and cloudy conditions. Chapter III deals with the site location and instrumentation used to collect the experimental data. The data are analyzed in Chapter IV and the computed depletion estimates are discussed. Predictive models for both cloudless and cloudy conditions are compared with experimental measurements under different time periods. Finally, the theory and experimental results of the albedo of water are discussed in Chapter V.

CHAPTER II

DEPLETION PROCESSES AND PREDICTIVE MODELS OF SOLAR RADIATION IN THE ATMOSPHERE

A. DEPLETION PROCESSES IN CLOUDLESS CONDITIONS

Direct radiation

The global radiation Ge measured at the earth's surface is given as:

$$Ge = Ie \cos Z + D \tag{1}$$

where, Ie = direct beam radiation,

D = diffuse radiation,

Z = solar zenith angle.

This flux is the residual after the atmosphere has depleted the extra-terrestrial radiation intensity Io' (Figure 1). Since the sun-earth distance changes throughout the year Io' will undergo small changes according to the inverse power law. Thus, it can be written,

$$Io' = Io/r^2, \tag{2}$$

in which, r = radius vector (the ratio of the instantaneous sun-earth distance to the annual mean),

Io = mean annual intensity or solar constant = $\int Io\lambda d\lambda$,

$Io\lambda$ = solar spectral intensity of emission.

Although the radius vector is well known (List, 1966), an accurate

Figure 1
SPECTRAL INTENSITY OF SOLAR RADIATION FOR CLOUDLESS CONDITIONS (GATES 1965)

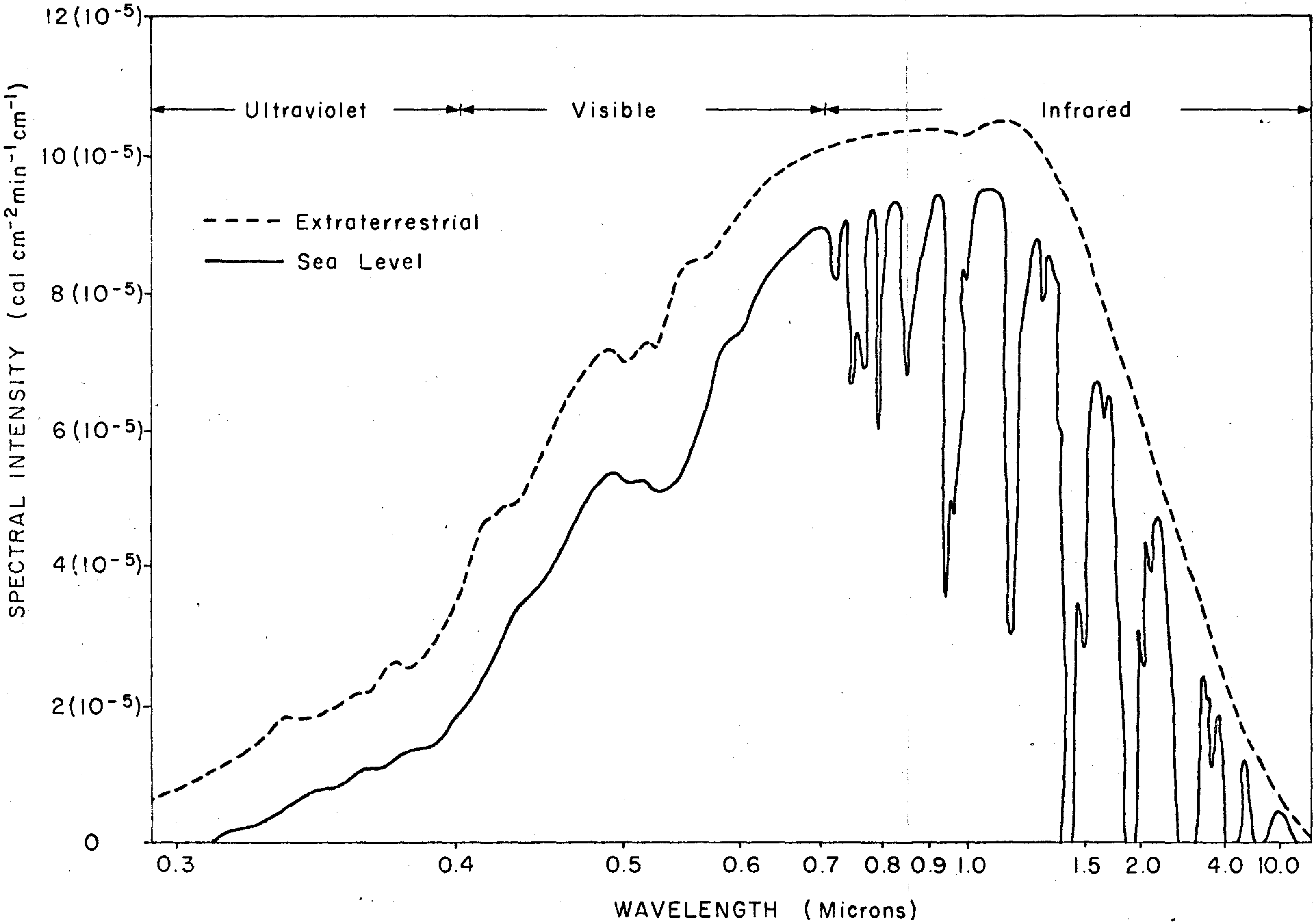

determination of the solar constant has been difficult. Experimental measurements have shown that its spectral distribution approximates that from a 6000 °K black body but with lower values in the ultraviolet and infrared. Estimates of the solar constant have yielded values ranging from 1.94 cal cm^{-2} min^{-1}, Abbot, et al. (1932, 1954) to 2.05 cal cm^{-2} min^{-1} (Stair and Johnston, 1956). Drummond (1970) attributes the measurements problems mainly to:-

a) differences in the spectral response of the sensors,

b) variation in atmospheric attenuation of solar radiation,

c) uncertainty in the spectral windows of the sensors used.

However, recent determinations above the earth's atmosphere using high altitude balloons (Kondrat'yev and Nikolsky, 1970) and satellite data (Drummond, 1970) have indicated a consistent value of Io = 1.94 cal cm^{-2} min^{-1}.

The depletion of Io' in the earth's atmosphere is mostly caused by neutral air molecules, ozone, water vapor and aerosols. Using Beer's law an incremental change dI_λ in the intensity of a monochromatic beam I_λ in the atmosphere is given as:-

$$dI_\lambda = -I_\lambda k_\lambda dL,$$

where, k_λ = monochromatic extinction coefficient,

dL = incremental path length.

Integrating this equation with respect to path length an approximate expression can be obtained for the direct beam monochromatic intensity at the earth's surface:-

$$I_\lambda = Io'_\lambda \exp\{-m[\rho'_{\lambda R} L_R + \alpha'_{\lambda o} O_3 + (\alpha'_{\lambda w} + \rho'_{\lambda w})W + (\alpha'_{\lambda d} + \rho'_{\lambda d})d]\}, \tag{3}$$

in which, Io'_{λ} = extra-terrestrial spectral intensity,

m = optical air mass ≃ sec Z,

$\rho'_{\lambda R}$ = monochromatic exponential Rayleigh scatter extinction coefficient per unit path length,

L_R = vertical path length for Rayleigh scatter,

$\alpha'_{\lambda o}$ = exponential monochromatic ozone absorption coefficient per unit path length at normal temperature and pressure,

O_3 = total depth of ozone in a vertical path length in the atmosphere at normal temperature and pressure,

$\alpha'_{\lambda w}, \rho'_{\lambda w}$ = exponential monochromatic absorption and scattering coefficients for unit path length of water vapor at normal temperature and pressure,

W = total depth of precipitable water vapor in a vertical path length in the atmosphere,

$\alpha'_{\lambda d}, \rho'_{\lambda d}$ = exponential monochromatic absorption and scattering coefficients per unit aerosol path length,

d = total aerosol depth in a vertical path length in the atmosphere.

Studies which model the extinction of solar radiation in a cloudless atmosphere must involve knowledge of the extinction coefficients, depletion agents and the diffuse radiation generated by direct beam scattering. It is evident that not all the processes are known equally well nor do they affect the solar radiation in a similar manner.

The Rayleigh scattering coefficient $\rho'_{\lambda R}$ can be treated as essentially constant in the atmosphere (Robinson, 1966) and equal to:-

$$\rho'_{\lambda R} = 32\pi^3(n_{\lambda a} - 1)/3N\lambda^4, \quad (4)$$

where, $n_{\lambda a}$ = index of refraction of air,

N = correction factor to take into account the non-spherical nature of air molecules,

λ = wavelength of light.

Equation 4 states that the scatter is continuous and large for small wavelengths in the violet and blue portions of the solar spectrum. Furthermore, theoretical work also show symmetry of scatter about the direction of the incoming beam and strong polarization at right angles to the direction of the incoming beam with equal amounts being scattered in the forward and back direction.

Unlike Rayleigh scattering which is a continuous process, absorption of ozone occurs in discreet absorption bands which are a result of electronic transitions in the element. The dominant bands are known as the Hartley bands (0.2-0.3μ), the Huggins bands (0.3-0.36μ) and the visible Chappuis bands (0.4-0.8μ). Since the depletion of solar radiation by ozone is not very large and essentially constant, some authors (Dave and Sekera, 1959, Robinson, 1963) treat the depletion by Rayleigh scatter and ozone as being representative of a moist-free clean atmosphere. If W and d are omitted from 3 and the results integrated over wavelength, the direct beam I_{Ro} received at the earth's surface under these idealized conditions can be obtained from:-

$$I_{Ro} = \int_{0.28\mu}^{4\mu} I'_{o\lambda} \exp[-\rho'_{\lambda R} L_R m - m\alpha'_{\lambda o} O_3] d_\lambda. \qquad (5)$$

The water vapor and aerosol terms show large variations in magnitude for given locations and times. In fact the vibrational and rotational absorption bands of water vapor cause the largest and most significant absorption of solar radiation in the atmosphere. Most present estimates of water vapor depletion are based on the experimental data derived by Fowle (1912, 1915). Using absorption data at Mount Wilson along with laboratory measurements with folded water vapor path lengths, he was able to calculate the water vapor absorption by the principal infrared bands and scattering by water vapor molecules. His results have been widely used. Kimball (1928, 1930) used Fowle's data to develop a set of curves describing the depletion of the direct beam in the atmosphere by Rayleigh scatter, water vapor scatter and water vapor absorption. Similar studies also using Fowle's data have been carried out by Mügge and Möller (1932) and Yamamoto-Onishi (1952). Houghton (1954) after expressing doubts as to the consistency of the Kimball curves and the original Fowle data, carried out an independent analysis of the water vapor transmission data published by the Smithsonian Institution. His resultant absorptivity, expressed as a percentage of the extra-terrestrial beam Io is shown in Figure 2. In a review of previous work McDonald (1960) presents the following relation to describe the absorptivity α_w:-

$$\alpha_w = 0.077(wm)^{0.30}; \tag{6}$$

It gives different results from Houghton's (Figure 2) but McDonald could not explain the discrepancy. He lists slight disagreements in the solar constant as being the main cause of the differences between his results and those of Mügge-Möller and Yamamoto-Onishi. Finally an attempt was made to reconcile the McDonald and Houghton results by Yamamoto (1962) who pointed out that the difference could be due to extra water vapor, carbon dioxide and oxygen bands apparently not considered by McDonald (Figure 2). Considering all the absorption bands Lettau (1969) fitted the Yamamoto data with the expression:-

$$\alpha_w = 0.102(wm)^{0.276}. \tag{7}$$

Figure 2

WATER VAPOR ABSORPTIVITY VS. PRECIPTABLE WATER (W)*

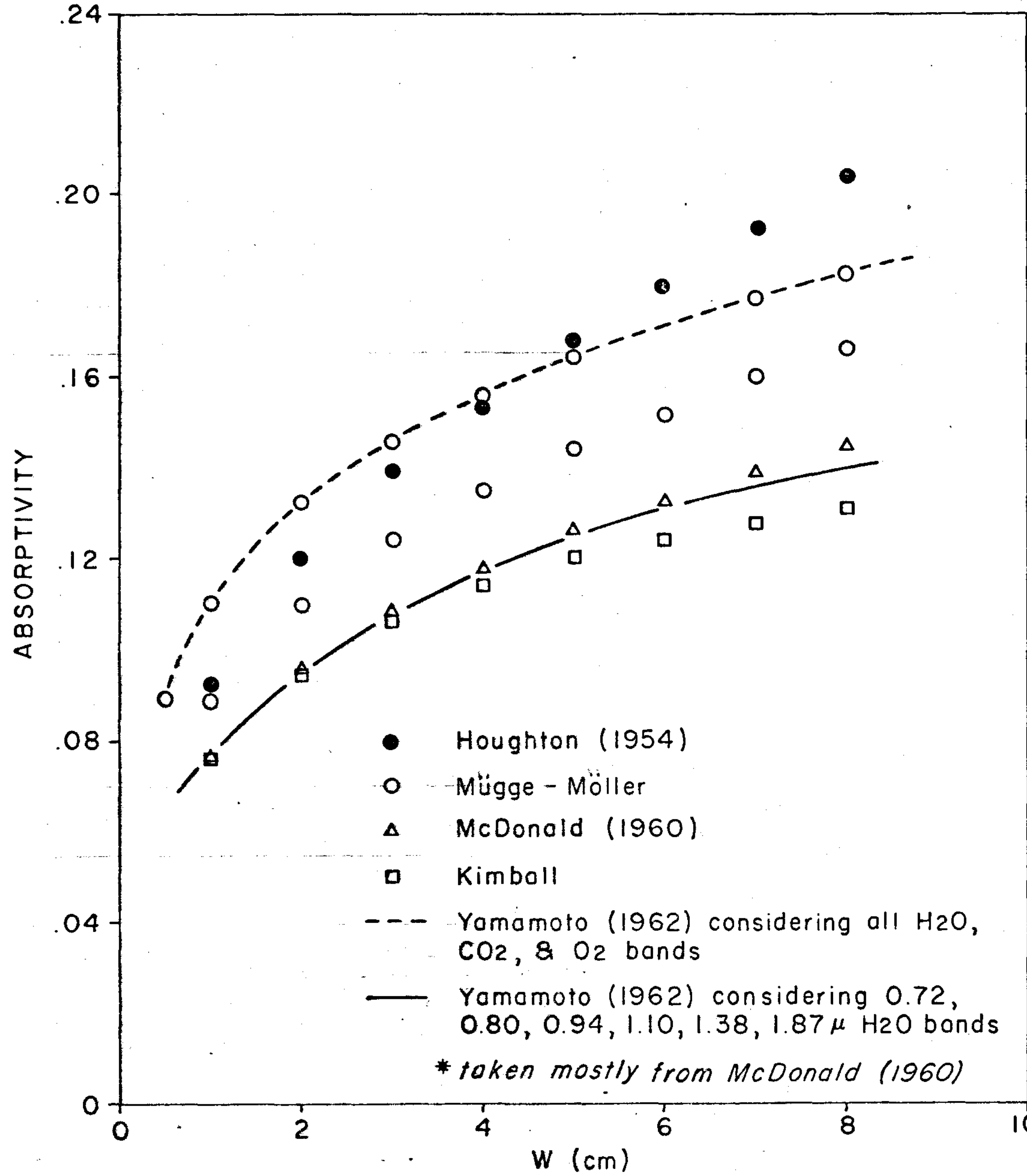

The influence of the aerosols, d, is without a doubt the most uncertain of all the depletion terms. This is of course due to the great variability in size and composition of the aerosol as well as the lack of experimental measurements of this parameter. Thus, incorporation of d, $\alpha'_{\lambda d}$ and $\rho'_{\lambda d}$ in equation 3 is not practical. In this study all gaseous or particulate matter not included in a hypothetical Rayleigh atmosphere containing known amounts of water vapor and ozone will be treated as aerosols. As there is evidence to suggest that the size of a large portion of natural aerosols over land is of the same order of magnitude, or larger, than the wavelength of light (Mason, 1962), Mie scatter with its larger forward scatter and inverse linear dependence on wavelength is expected to be a dominant process for aerosols (Robinson, 1966). However, uncertainties in the size, distribution and refractive index of the aerosols make this theory, at present, not applicable for regular use. There have been a number of empirical relations which describe the effect of the aerosols as an added depletion of the direct beam (Ångström, 1964, 1962, Linke, 1942). These approaches rely on experimental measurements of the direct radiation and a comparison of the results under aerosol-free conditions. In the most general case the depletion due to aerosols ΔI is obtained using the residual equation:-

$$\Delta I = I_{Ro} - I\acute{o}\alpha_{w} - Ie \; ; \qquad (8)$$

Experimental measurements to determine the aerosol depletion using residual methods are scarce. Houghton (1954) found this term was exceedingly variable. Given an air mass m, a mean value of $(0.95)^{m}$ was assigned as the aerosol transmission term for the entire northern hemisphere. He assumed that half of this depletion was due to absorption and the other half due to scattering. A similar value was used by London (1957). Monteith (1962) used this term along with an extra depletion term which he attributed to smoke. Robinson (1963) found a considerable variation in the aerosol depletion depending on whether measurements were made over industrialized or non-industrialized areas.

Diffuse radiation

This term comprises all the solar radiation which has been scattered from the direct beam and is incident at the earth's surface. In the actual case the scattered beam will undergo further scattering so that the diffuse radiation incident on the surface represents the net effect of a multiple scattering atmosphere. This is further complicated by possible absorption of the scattered radiation by water vapor, ozone and aerosols. Nevertheless it is expected that this term will not be large under clear conditions since scattering will occur mostly in the blue portion of the spectrum and water vapor bands occupy the near infrared and infrared. On the other hand, in areas with heavy industrial pollution this effect might be noticeable.

Diffuse radiation in most physical models has been predicted by assigning a bulk coefficient to the total radiation scattered from the direct beam. Houghton (1954) assumes that half the radiation scattered from the beam reaches the earth's surface undepleted. Similar assumptions were made by Klein (1948). Robinson (1963) using a simplified aerosol-free model showed that the use of a bulk coefficient of $^1/2$ resulted in a prediction of diffuse radiation which agreed well with more complicated predictions using multiple Rayleigh scattering. In the presence of large aerosols Mie scattering will dominate and the individual particle will scatter more in the forward direction than in the backward direction. These considerations have led to the development of a separate bulk scattering coefficient for aerosols. Robinson (1963) uses an experimentally determined ratio of total forward scatter to back scatter which was found to depend on the solar altitude. London (1957) assumed a bulk coefficient for aerosols which was twice as large in the forward than in the back direction. His treatment also included absorption of diffuse radiation by water vapor. Lettau (1969) assumed that $^2/3$ of the total radiation scattered from the direct beam reached the earth's surface while $^1/3$ was reflected back to space. Absorption of diffuse radiation was not considered in his model.

In the absence of theoretical and experimental verification of aerosol scattering, all these coefficients can at best be considered tentative. It is possible that under clear conditions the bulk scattering coefficient might approach $^1/2$. Yet it is not reasonable to expect this coefficient to remain the same for one particular location under all conditions. The same argument could be applied to the Lettau coefficient of $^2/3$. Nevertheless, as will be seen later, practical considerations impose the condition that the bulk scattering coefficient remain constant when used in prediction models.

B. DEPLETION PROCESSES IN CLOUDY CONDITIONS

The radiation depletion processes inside the cloud structure are sufficiently complex to have warranted separate studies. The large variations in cloud thickness, water vapor amount and water droplet size and distribution make the cloud extinction coefficients varied and generally larger than those observed under cloudless conditions. This section will discuss some of the theoretical and experimental attempts at learning the reflection, absorption and transmission of solar radiation by the cloud structure. The general problem of predicting global radiation under cloudy or partially cloudy conditions will be discussed in the later section.

As a beam of direct radiation enters a cloud layer and travels through the saturated or supersaturated medium, water vapor absorption will deplete part of the radiation. When the beam finally encounters a water droplet, a fraction of the radiation will be absorbed by the droplet while the remainder is scattered. Since a large percentage of the cloud droplets are within the 0.1-25μ range (Feigel'son, 1966) Mie scattering will occur. Thus the scattered radiation will travel in new directions constantly being absorbed by water vapor until scattered and absorbed by other droplets. If the cloud is thick enough all the direct radiation will be depleted so that the radiation inside the cloud is diffuse but not necessarily isotropic. Some of the scattered light will return to the cloud top and appear as reflected radiation, some of it will leave the cloud base as transmitted radiation.

There have been several theoretical models which have attempted to represent the above phenomenon. Hewson (1942) considered the cloud structure as composed of identical water sphere in suspension. He then assumed that the radiation could be described by two "currents" of diffuse radiation travelling in an upward and downward direction respectively. The effect of absorption and scattering was calculated over a thin horizontal slab inside the cloud. This resulted in a differential equation which could be solved over the entire thickness. The resultant cloud albedo and transmission was found to depend on the density of the liquid water inside the cloud, the droplet radius, the thickness of the cloud and the zenith angle of the incoming radiation.

A different approach was taken by Fritz (1958, 1954) who studied clouds of large droplets. He visualized the scattering process from a single droplet a number of photons emerging radially from the drop. These are superimposed upon a large stream of photons travelling in a forward direction with respect to the incoming beam (Mie scatter). The radiation field could then be described by a diffusion equation with absorption caused by water vapor and scattering by droplets. His solution of the diffusion equation showed that cloud albedo depends on solar zenith angle. For a cloud of infinite thickness an absorption of between 19% and 30% was obtained. This depended on the water content and droplet radius. The remaining percentage would evidently be reflected from the cloud.

Using the equations of radiative transfer with multiple scattering Feigel'son (1966) calculated the reflection, absorption and transmission of stratus clouds using typical cloud properties, an experimentally derived scattering coefficient and a known optical thickness. Her results for the albedo of different cloud types are shown in Table 1. The absorption estimates using this model ranged from 2.5% for a cloud of 2 Km. thickness to 8.9% for one 4.5 Km. thick.

A comparison of these theoretical models is not appropriate since different water content, drop radii and thicknesses were used. Nevertheless it is relevant to note that all models exhibited much larger albedos than absorption estimates. All three models exhibit a dependence of albedo on zenith angle and cloud type.

TABLE 1

THEORETICAL ALBEDO CALCULATIONS FOR DIFFERENT CLOUD TYPES

Feigel'son (1966)

Cloud Type	Zenith angle		
	30°	50°	70°
Stratus	0.59	0.63	0.69
Strato-cumulus	0.68	0.72	0.76
Nimbostratus-altostratus	0.85	0.88	0.90
Altostratus	0.63	0.68	0.73

The limited experimental measurements of cloud albedo also show a variation with cloud type. Most measurements of this nature are made from an aircraft outfitted with upward and downward facing sensors. Such airborne measurements usually ignore the effect of the earth's surface on the albedo. A wide range of values occur even for clouds of the same type (Fritz and McDonald, 1951, Robinson, 1958, Conover, 1965, Griggs, 1968). Albedo values for low clouds seem to range between 50% to 68% judging from these measurements. Neiburger's (1949) albedo measurements of stratus clouds in California show that albedo varies with cloud thickness as predicted by the theoretical models. Measurements ranged from a value of 30% for a 60 meters thick cloud to 75%

for a 500 meter stratus. Little can be said regarding the albedo properties of high and middle clouds because of insufficient measurements.

Aircraft absorption measurements are even more scarce than the albedo observations. Fritz and McDonald (1951) report values of 17, 27, and 14% for nimbostratus clouds. Griggs (1968) obtained a value of 4% for stratus clouds in California and Robinson (1958) obtained a mean value of 22% for low clouds in Britain.

Because of their cost and irregularity it would seem that aircraft observations have only limited usefulness in providing continuous measurements of cloud albedo and absorption estimates. A more practical approach to the problem of understanding cloud transmission would be obtained by measurements of global radiation under completely overcast skies. The global radiation measured can then be related to the transmission of the cloud - atmosphere system. Haurwitz (1948) using data for an 8 year period computed the instantaneous global radiation, G_c', received at Blue-Hill, Massachusetts under overcast conditions and for different air masses, m. He was able to fit the following exponential relation to his data:-

$$G_c' = ({}^{a}/m) \exp(-bm), \tag{9}$$

in which a and b are empirical constants which depend on the cloud type (Table 2).

TABLE 2

EMPIRICAL CONSTANTS USED IN HAURWITZ (1948) MODEL

	Ci	Cs	Ac	As	Sc	S	Ns
a	82.2	87.1	52.5	39.0	34.7	23.8	11.2
b	0.079	0.148	0.112	0.063	0.104	0.159	-0.167

Vowinckel and Orwig (1962) used cloud and solar radiation data from North American and Arctic stations. They defined the cloud transmission Tc as:-

$$Tc = G'c/G'o, \tag{10}$$

where, $G'o$ = instantaneous global radiation for cloudless conditions. They found that cloud transmission varied with type, location and season. A general northward increase in Tc was obtained as well as a decrease with zenith angle. They concluded that cloud albedo was the most important factor affecting the transmission and that its variation with solar altitude was a phenomenon predicted by theoretical models.

C. PREDICTIVE MODELS OF SOLAR RADIATION IN CLOUDLESS CONDITIONS

In the previous section most of the depletion processes of solar radiation in the atmosphere were described. However, the prediction of solar radiation at the earth's surface involves a number of assumptions with regards to the order and manner in which processes occur and how diffuse radiation should be handled.

There are many models which predict global radiation at the earth's surface. In this study three models were considered. These are the Houghton (1954), London (1957) and Lettau (1969) models. These were selected because they are physical models from which information can be drawn even though they utilize different assumptions.

Both the Houghton and London models were derived in an attempt to predict solar radiation on a global scale. Houghton derived his own transmission curves neglecting any anomalies that could arise in non-isotropic aerosol depletion. London, on the other hand, attempted to model such secondary effects as diffuse radiation absorption, non-isotropic water vapor and aerosol scattering. The Lettau model differs from the other two in its attempt to describe the radiation balance relations at a location. Using a minimum number of assumptions it is possible to gain an insight into the absorption and scattering processes that would otherwise have been assumed. Therefore this model will be examined in detail. Using the Lettau model, the effect of depletion errors on the global radiation will be examined and a detailed radiation budget will be performed using global radiation data collected at the Lake Ontario tower site as discussed in Chapter III. Finally all three models will be tested for their ability to predict short-term fluxes.

Lettau model

Lettau treated the atmosphere as a slab where the fluxes at its top and bottom could be defined. All the radiation processes occurring inside the slab were expressed in terms of four independent equations. With the aid of these equations it is possible to express the global radiation in terms of its depletion parameters.

The following assumptions are involved in the model:-

1. Individual absorption and scattering coefficients can be added to give overall estimates. Thus, referring to all processes as percent of I_o',

$$\alpha = \alpha_w + \alpha_d + \alpha_{o3}, \tag{11}$$

$$\rho = \rho_R + \rho_d, \tag{12}$$

where, α = total direct beam absorption,

α_{o3} = direct beam absorption by ozone,

α_d = direct beam absorption by aerosols,

ρ = total direct beam scattering coefficient,

ρ_d = direct beam aerosol scattering coefficient,

ρ_R = direct beam Rayleigh scattering coefficient.

2. In addition it seems to this writer that the model implicitly assumes no absorption of diffuse radiation. This point will be discussed later.

The entire solar radiation budget in the slab can then be described by four equations which use the following terms:-

A = fraction of the extra-terrestrial flux, $I_o' \cos z$, returned to space,

G* = relative global radiation or the ratio of the global radiation received at the surface to the extra-terrestrial flux,

D* = relative diffuse radiation or the ratio of diffuse radiation received at the surface to the extra-terrestrial flux,

H* = fraction of the extra-terrestrial flux absorbed in the atmosphere,

a = albedo of the lower boundary,

ξ = bulk scattering coefficient describing the effective scattering to space of the radiation scattered from the direct beam,

κ = fraction of the reflected radiation that is backscattered to the surface of the earth;

$$1 - A = G^*(1 - a) + H^*, \tag{13}$$

$$1 - G^* + D^* = \alpha + \rho, \tag{14}$$

$$A = \xi\rho + (1 - \alpha)aG^*(1 - \kappa\rho), \tag{15}$$

$$D^* = (1 - \xi)\rho + (1 - \alpha)aG^*\kappa\rho. \tag{16}$$

Equation 13 states that the fraction of the radiation not reflected to space is absorbed by the ground and the atmosphere. Equation 14 shows that the fraction of the direct radiation depleted in the atmosphere must equal its depletion by absorption and scattering. Equation 15 states that the fraction of the radiation reflected to space equals the total radiation backscattered from the atmosphere plus the amount reflected from the earth's surface that is not backscattered or absorbed. Finally, in equation 16, the diffuse radiation received at the earth's surface must equal the amount scattered forward from the direct beam plus the fraction of the reflected radiation that is backscattered by the atmosphere.

From equations 15 and 16 the total radiation scattered from the direct beam and which reaches the outer surfaces of the slab can be given as:-

$$\xi\rho + (1 - \xi)\rho = \rho, \tag{17}$$

which implies that there is no absorption of the diffuse radiation.

In the four equations there are nine unknowns. Values of G*, D* and a can be obtained from surface radiation data. The coefficients ξ, κ, A, α, ρ and H* have to be determined. Lettau's procedure is to assign arbitrary values of κ and ξ which depend on the geographical location. The remaining unknowns can then be calculated. Lettau assigned an arbitrary value of $\xi = {}^1/3$ and values of κ equal to ${}^3/8$, ${}^3/3$ or ${}^3/4$ depending on whether the model applied to an urban, desert, or prairie environment. He restricted himself to conditions close to solar noon. In this study a value of $\xi = {}^1/3$ will also be used. It will also be assumed that the reflected solar radiation from the water surface can be replaced by a direct beam whose effective backscatter coefficient is also ${}^1/3$. Hence,

$$\kappa = \xi = {}^1/3; \tag{18}$$

This value of κ will correspond closely to the value of ${}^3/8$ which Lettau used for Kew. If equations 14 and 16 are solved for ρ, a quadratic equation in ρ will be obtained:-

$$\rho^2\{aG^*\xi\} + \rho\{(G^* - D^*)aG^*\xi + 1 - \xi\} - D^* = 0. \tag{19}$$

This can be solved for ρ and if substituted into equations 11 and 12 the values of ρ_D and α_D will be obtained provided the precipitable water vapor is known.

Using equations 14 and 16 the global radiation is given by:-

$$G^* = \frac{(1 - \alpha - \xi\rho)}{1 - a\xi\rho(1 - \alpha)}, \tag{20}$$

where it has been assumed that $\kappa = \xi$.

Figure 3 shows the sensitivity of global radiation as expressed in equation 20 to changes in depletion parameters. Changes in direct beam absorption will affect global radiation most strongly. The scattering coefficients ρ_R and ρ_D, have a lesser effect. The model shows very little sensitivity to large changes in albedo. As an example let us suppose that global radiation is predicted using equation 20. It is possible that an error of 5% could occur from an under-estimation of the aerosol absorption or use of a precipitable water vapor absorption which is unrepresentative. This is equivalent to a 25% change from the value of $\alpha = 20\%$. This will produce 7% over-estimation of the global radiation. Similarly, an error in the scattering coefficient of 5% will result in a corresponding error of 2%. An error in the albedo 5% will have a negligible effect on G*. This last result is of course a consequence of the small albedo and scattering coefficient considered and does not apply to all conditions (Moeller, 1965).

Using records of G*, D* a and W available for Kew (England), La Joya (Peru), and O'Neill (Nebraska) Lettau solved equations 13 to 16 for the unknowns, A, α, ρ and H*. It was then possible to partition the ρ term into the respective Rayleigh and aerosol components and the α term into its ozone, water vapor and aerosol component. ρ_R and α_w were obtained from a model by Dave and Sekera (1959) and α_w was calculated using the Yamamoto - Onishi relation (equation 7). A comparison of the radiation budget for the different climatic locations revealed that:-

Figure 3

THE RELATIVE EFFECT OF EACH PARAMETER ON THE DEPLETION OF INCOMING GLOBAL RADIATION (LETTAU MODEL)

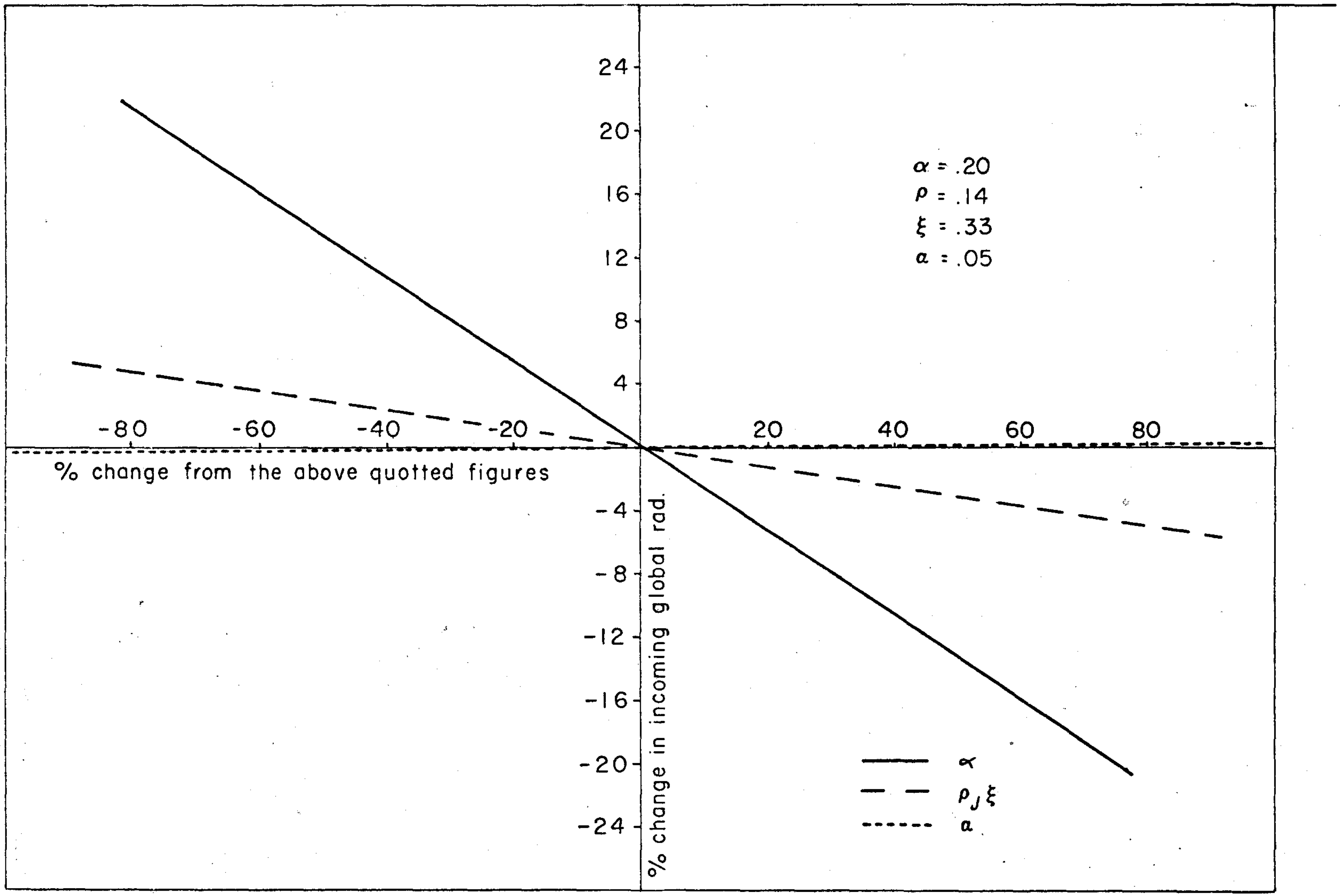

1. City aerosol (Kew) is a more efficient absorber than desert aerosol (La Joya).

2. Given an increase in surface albedo, diffuse radiation and planetary albedo show the largest increase in the desert atmosphere while the heating rate is largest in the urban area.

3. The addition of aerosol peculiar to each location would result in a small increase in diffuse radiation, planetary albedo and atmospheric heating for O'Neill and La Joya. Kew on the other hand would exhibit a large increase in atmospheric heating and a considerable decrease in surface heating and direct radiation at the surface.

These results were based on data for a few continuous cloudless days at the respective locations. In the next chapter the experimental data obtained at the Lake Ontario tower site will be subjected to such an analysis and compared with Lettau's observations.

Comparison of the Houghton, London and Lettau models

Table 3 shows the principal assumptions involved in each of the models considered in this study. Listed also are the main sources used in each model to obtain the depletion relations.

Houghton assumed that the direct beam would first encounter absorption followed by scattering. Thus, the direct beam arriving at the earth's surface can be expressed as the product of four transmissions:-

1. water vapor absorption,
2. water vapor scattering,
3. atmospheric Rayleigh scattering,
4. aerosol depletion.

The first three transmission relations were derived by Houghton after an

TABLE 3

DETAILS ON SOLAR RADIATION MODELS

	Houghton (1954)	London (1957)	Lettau (1969)
ORDER OF PROCESSES	1 absorption 2 scattering	not specified	not specified
DIRECT BEAM DEPLETION			
ozone absorption	none	yes. Calculated using Pressman (1954)	yes. Calculated using Dave and Sekera (1959)
water vapor absorption	yes. Calculated using Smithsonian data.	yes. Calculated using Mügge and Möller (1932)	yes. Calculated using Yamamoto (1962)
water vapor scattering	yes. Calculated using Smithsonian data.	yes. Calculated using Houghton (1954)	none
dry air scattering	yes. Calculated using Smithsonian data.	yes. Calculated using Houghton (1954)	yes. Calculated using Dave and Sekera (1959)
aerosol scattering	yes. Assumed average value: $(1-(.95)^m)/2$	yes. Assumed average value: $3/4 \times [1-(.95)^m]$	yes. Obtained experimentally
aerosol absorption	yes. Assumed average value: $(1-(.95)^m)/2$	yes. Assumed average value: $1/4 \times [1-(.95)^m]$	yes. Obtained experimentally

continued.......

TABLE 3 continued .....

	Houghton (1954)	London (1957)	Lettau (1969)
ORDER OF PROCESSES	1 absorption 2 scattering	not specified	not specified
SCATTERED RADIATION			
water vapor	1/2 scattered upwards 1/2 scattered downwards	3/4 scattered downwards 1/4 scattered upwards	none
dry air	1/2 scattered upwards 1/2 scattered downwards	1/2 scattered upwards 1/2 scattered downwards	1/3 scattered upwards 2/3 scattered downwards
aerosol	1/2 scattered upwards 1/2 scattered downwards	2/3 scattered downwards 1/3 scattered upwards	1/3 scattered upwards 2/3 scattered downwards
absorption	none	yes. By water vapor 3/2 vertical absorption	none

analysis of the Smithsonian data. The last one was calculated as a residual term and represented a global average. The global radiation at the earth's surface has the form:-

$$G_o' = I_o' \cos Z[(1 - \alpha_w)(1 - \rho_w)(1 - \rho_R)T_d + 0.5(1 - \alpha_w)T_D'(1 - (1 - \rho_w)(1 - \rho_R)T_D')] \quad (21)$$

where, ρ_w = scattering coefficient for water vapor,

T_d = direct beam transmission due to aerosols,

T_d' = direct beam transmission due to aerosol absorption or scattering.

London did not consider the order of the processes but instead assumed that the transmission relations which Houghton used could be added to give an overall depletion. Taking into account the non-isotropic properties of the water vapor and aerosol scattering as well as diffuse absorption, London expressed the direct and diffuse radiation at the earth's surface as:-

$$I = I_o'[1 - \alpha_{o3} - \alpha_w - \rho_R - \rho_w - (1 - T_d)],$$

$$D = I_o' \cos z[0.75\rho_w(1 - 1.5\alpha_w') + 0.5\rho_R + 0.5(1 - T_d)],$$

Therefore the global radiation is given by:-

$$G_o' = I_o' \cos Z[1 - \alpha_o - \alpha_w - 0.5\rho_R - \rho_w - 0.5(1 - T_d) + 0.75\rho_w(1 - 1.5\alpha_w')], \quad (22)$$

and α_w' = direct beam absorptivity by a vertical column of precipitable water vapor.

In a similar manner the Lettau model also assumes that the absorption and scattering coefficients can be added. From equation 20 the global radiation at the earth's surface is:-

$$G_o' = I_o' \cos Z \frac{1 - \alpha - \xi\rho}{1 - a\xi\rho(1 - \alpha)} . \tag{23}$$

There appears to be some uncertainty regarding water vapor scattering. Fowle's original clear day calculations over Mount Wilson (1913) showed that the amount of actual water vapor scattering was far too large to be accounted for using molecular scattering alone. This effect as well as the departure of the water vapor transmission coefficients from the inverse fourth power law led him to the conclusion that the water vapor was loaded with something in size larger than the molecule. He attributed this effect to dust or nuclei formed by ultraviolet radiation interacting with moist air. Kimball (1928, 1930) who used Fowle's data to derive his transmission curves, refers to this effect as "water vapor scattering". A similar procedure seems to have been followed by Houghton in his analysis of the Smithsonian data. London expressed the view that "at very high levels, the water vapor scattering is probably molecular scattering and should follow an isotropic law. However, in the lower atmosphere it is probable that the scatterers are small condensed droplets of water vapor." A similar view is expressed in Haltiner and Martin (1957). London hoped to take into account these properties of the water vapor by assigning a larger forward scatter than backscatter. This effect has been ignored in the model by Lettau as well as by Robinson (1963) who implicitly treated this effect as aerosol scattering.

Finally, it should be mentioned that all three models assume that diffuse radiation is dependent on cos Z. This implies non-isotropic radiation concentrated in a narrow cone about the direct beam (Klein, 1948).

D. PREDICTIVE MODELS OF SOLAR RADIATION IN CLOUDY CONDITIONS

The problem of solar radiation interaction with clouds was considered earlier from the point of view of the physical processes. Idealized models of constant physical characteristics were discussed. Experimental studies on cloud albedo and transmission were examined under conditions of uniform or near uniform overcast. Although studies of this nature are essential in understanding solar radiation in the atmosphere, predictive models must take into account certain processes not considered in these idealized studies. They are the following:-

a) variation in cloud amount,

b) variation in cloud type,

c) further depletion by the atmosphere.

Hence a theoretical model describing individual cloud transmission does not necessarily represent the transmission of the entire atmosphere. This is a statistical problem which will depend mainly on the nature and amount of cloud present.

Even if a description of the global radiation at the surface were possible, the problem of predicting the flux for different time intervals remains. It will probably depend on the variation in time of the cloud distribution and the frequency of cloud observations.

Ångström (1924) proposed that a linear relation could be used to predict daily values of global radiation received at the earth's surface. This relationship employs a sunshine recorder to measure the total number of hours, s, during the day in which a beam of radiation is not intercepted by a cloud. The formula proposed is:-

$$Gc \quad = \quad Go(\varepsilon + (1 - \varepsilon)s/S), \tag{24}$$

in which, Gc = daily predicted global radiation in cloudy conditions,

ε = an empirical term found experimentally and related to a mean transmissivity under overcast conditions,

S = maximum number of sunshine hours during the day,

Go = daily predicted global radiation under cloudless conditions.

In terms of cloud cover, c, the above equation takes the form

$$Gc \quad = \quad Go(1 - (1 - \varepsilon)c); \tag{25}$$

This relationship ignores any anomalies due to cloud type, transmission or height. Furthermore, any variations in atmospheric turbidity other than the one caused by the cloud must somehow be taken into consideration by Go. When c = 0, Ge reduces to the standard clear day global radiation. Similarly when c = 1,

$$Gc \quad = \quad Go\varepsilon; \tag{26}$$

The term ε then reduces to a mean cloud transmissivity under overcast conditions. ε is usually obtained by a least square fit of experimentally determined values of Gc/Go and c. Previous considerations indicate that if cloud type varies considerably there will be scatter in the regression line. Similarly two geographical regions with different cloud type regimes might exibit anomalies in ε. The following are a few of the determined forms of the relation:-

$$Gc = Go(1 - 0.71c) \qquad \text{(Kimball, 1928)} \tag{27}$$

$$Gc = Go(1.275 - 1.02c) \qquad \text{(Houghton, 1954)} \tag{28}$$

$$Gc = Go(1 - 0.54c) \qquad \text{(Neumann, 1954)} \tag{29}$$

$$Gc = Go(1 - 0.65c) \qquad \text{(Budyko, 1956)} \tag{30}$$

$$Gc = Go(1 - 0.61c) \qquad \text{(Monteith, 1962).} \tag{31}$$

Other investigators have found that the experimental relationship between Gc/Go and c can best be described in a non-linear form. Some of the best known are:-

$$Gc = Go(1 - 0.6c^3) \qquad \text{(Laevastu, 1960)} \tag{32}$$

$$Gc = Go(1 - 0.38c - 0.38c^2) \qquad \text{(Berliand, 1962)} \tag{33}$$

$$Gc = Go\left(1.02 - \frac{0.1831}{1.27 - c}\right) \qquad \text{(Mateer, 1963).} \tag{34}$$

Multiple reflection from the side of the clouds has been considered as a possible cause of the non-linearity. Tabata (1964) added a zenith angle dependence to the linear transmission relation. According to Tabata such a dependence would arise as a result of the variation of cloud albedo and absorption with Z. The results of his multiple regression relation was:-

$$Gc = Go(1 - 0.0945c + 0.00357h), \tag{35}$$

where, h = solar elevation = 90 - Z.

Finally a brief mention should be made of the London (1957) and Lettau (1969) models. These take into account cloud type transmission. However,no attempt is made in either model to account for the simultaneous presence of two or more cloud types located at different heights. Because of their complexity and uncertain physical basis they will not be analyzed in this study.

E. PROBLEM AREAS

The preceeding discussion on the theory and previous measurements of global radiation has illustrated the need to proceed along certain lines of investigation. They are as follows:-

a) The ability of the Houghton, London and Lettau models to predict short-term fluxes must be investigated in view of some of the different processes considered.

b) Since there is still considerable uncertainty as to the exact form of the water vapor absorption, its effect on the predicted fluxes must be estimated.

c) The magnitude and temporal variation of the aerosol depletion terms must be established.

d) In the case of global radiation prediction under cloudy weather, suitable comparison with experimental data must be performed to determine which of the linear or non-linear models predict best for the Grimsby site.

e) An improvement of the empirical prediction relations under cloudy conditions will be attempted by using some of the results of cloud-type transmission under idealized conditions.

CHAPTER III

INSTRUMENTATION AND DATA ACQUISITION

All radiation measurements were made from a guyed tower anchored to the lake bottom at a depth of 4 meters. The structure was located 400 meters from shore in the vicinity of Grimsby, Ontario. An aluminum platform at the top of the structure permitted easy access to the instruments and provided a suitable working area (Figure 4). The sensors were located at the platform level which was located at a height of 4 meters above the water surface.

Two Eppley pyranometers (model 6-90) were used to measure the incoming and reflected solar fluxes. The sensor, shown in Figure 5, consists of 20 junctions of radially wound thermopile obtained by copper plating constantan wire (Monteith, 1959). The white surface (barium sulphate) is in good thermal contact with the cold junctions and the black surface (Parson's optical black) with the hot junctions. When radiation is incident on the instrument, the glass dome filters out the long-wave portion of the spectrum while allowing solar radiation to penetrate. Differential heating of the two horizontal surfaces occurs and it can be shown from heat balance considerations (Davies, Robinson, Nunez, 1970) that the output signal of the instrument is proportional to the temperature difference of the two surfaces. Any dependence of the output on ambient air temperature is rectified by a temperature -

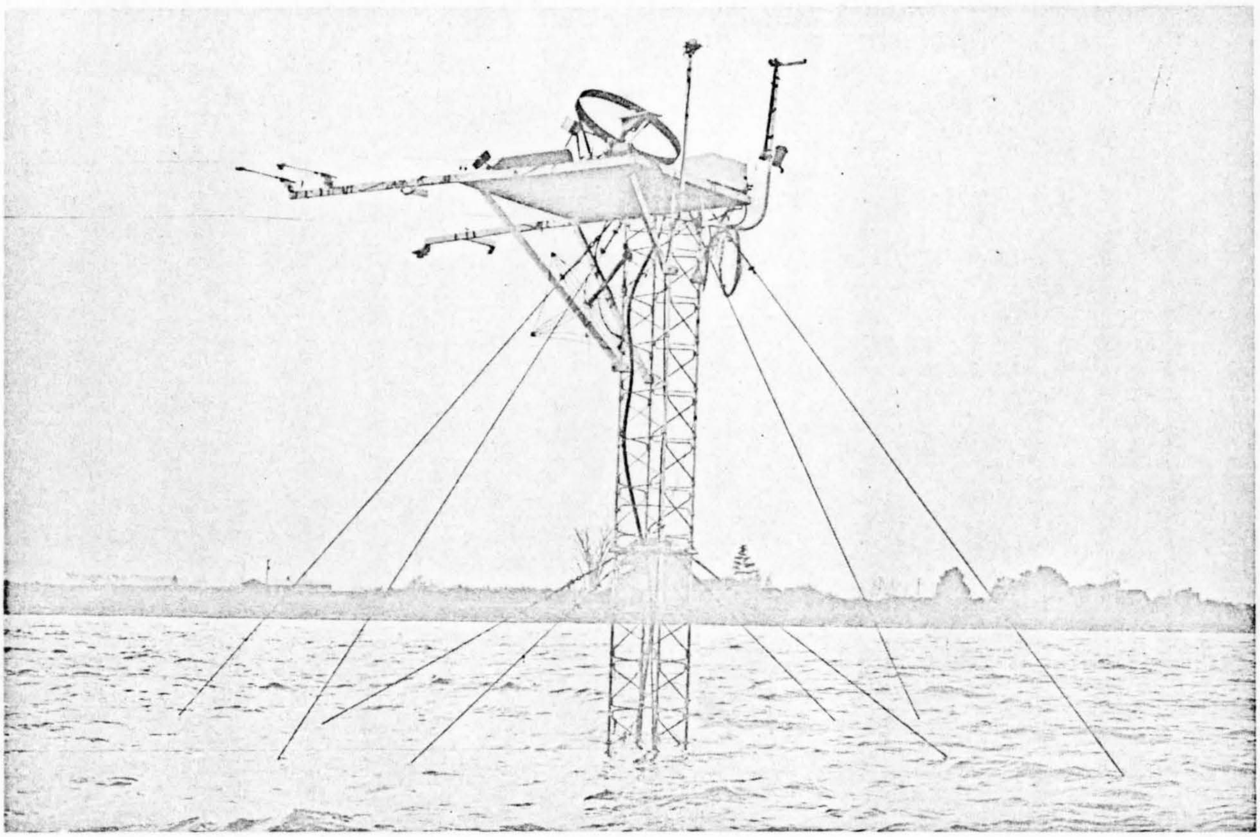

Figure 4 THE TOWER

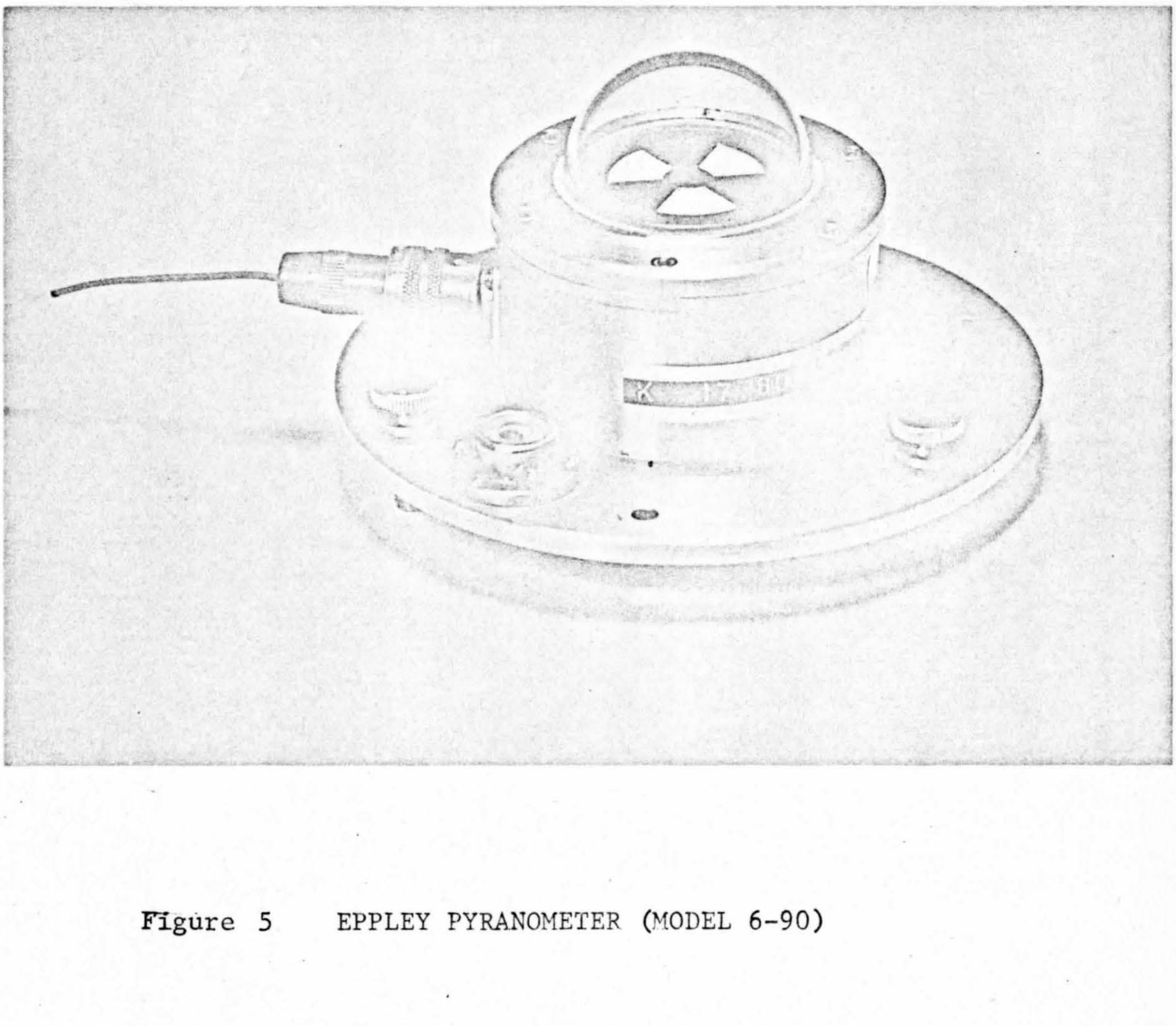

Figure 5   EPPLEY PYRANOMETER (MODEL 6-90)

compensating circuit built in the instrument which utilizes a thermistor to monitor ambient air temperature. By proper calibration with a known source of radiation, the instrument is made to measure the direct and diffuse solar radiation incident on a unit horizontal area.

It was possible to measure the diffuse radiation directly by means of a diffusograph. This device, which is of the standard type used by the Canadian Meteorological Branch, consists of a baseplate, a supporting column, a platform to support a pyranometer and a shading ring (Figure 6). The angle between the base plate and the column was adjusted to correspond to the station latitude. The column was then oriented towards the north celestial pole. After suitable centering of the pyranometer and adjustment of the sliding collar, the shading ring intercepted the direct rays of the sun throughout the entire day. It was of course necessary to adjust the position of the sliding collar at regular intervals to compensate for variation in the solar declination.

Multiple reflections from the glass dome were avoided by ensuring that the dome was always in the shadow of the shading ring. A correction must be made for the fraction of the sky that is obstructed by the shading ring. Although the ring is designed to minimize this effect by employing a large radius (101.6 cm) and a small width (8.8 cm), this discrepancy cannot be neglected. A theoretical correction has been developed by A. J. Drummond (1956). He assumed that an isotropic radiation intensity I existed over the entire hemisphere seen by the sensor. The total radiation intensity from the whole hemisphere incident on the sensor would be:-

$$q_h = \pi I \tag{36}$$

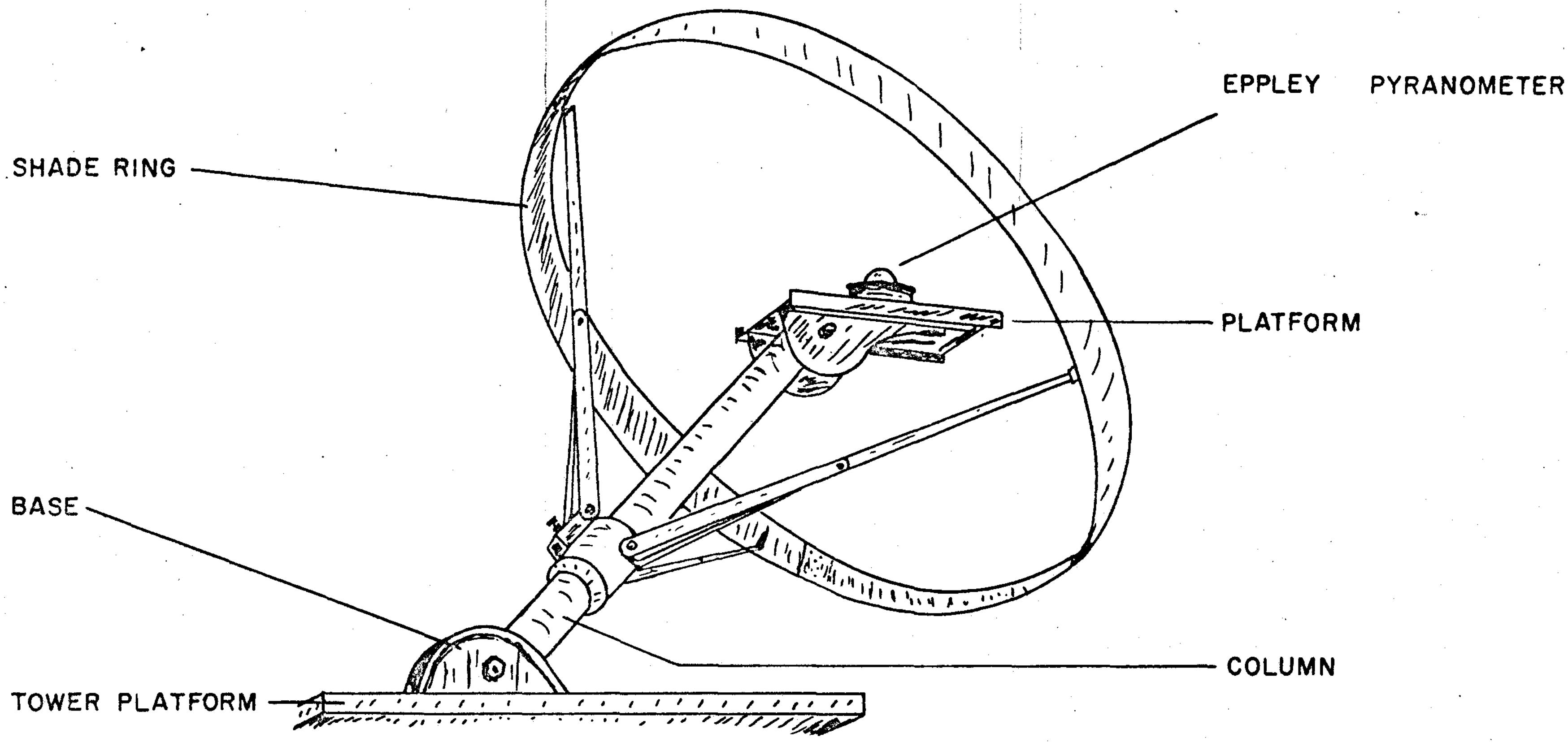

Figure 6 **CANADIAN METEOROLOGICAL BRANCH DIFFUSOGRAPH**

Drummond showed that the flux from the portion of the hemisphere obstructed by the ring is:-

$$q_D = \frac{2I}{r_o} T \cos^3\sigma(\sin\phi \sin\delta' ho + \cos\phi \cos\delta' \sin ho), \qquad (37)$$

where, T = width of the shading ring,

r_o = radius of the shading ring,

δ' = solar declination,

ϕ = station latitude,

ho = hour angle of the sun.

The fraction of the diffuse radiation that will be observed by the ring is:-

$$\frac{q_D}{q_h} = \frac{2T}{\pi r_o} \cos^3\delta'[\sin\phi \sin\delta' ho + \cos\delta' \sin ho], \qquad (38)$$

and the correction factor β to be applied is:-

$$\beta = \frac{1}{(1 - q_D/q_h)} . \qquad (39)$$

Knowing the constants T, r_o, ϕ and the variables δ' and ho, β can be calculated. This factor was computed for the period of this study and is shown in Figure 7. Both daylength and declination data were obtained from the Smithsonian Meteorological Tables (List, 1966). The correction factor ranges from 5% to 11%. It is nevertheless questionable whether isotropic conditions can be expected in the real case and an experimental method was devised to check the validity of the correction. Days in July and August were picked which contained cloudy overcast conditions. The

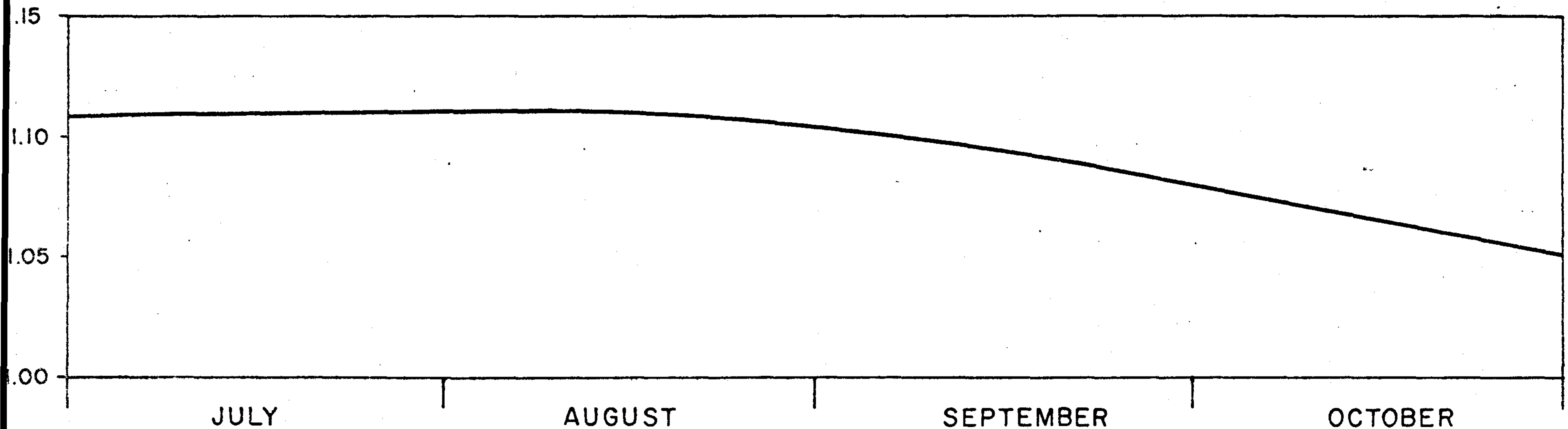

Figure 7 THEORETICAL CORRECTION FOR DIFFUSE RADIATION MEASUREMENT

data were selected rather subjectively by searching for periods of large solar radiation depletion and with little variation. In some cases there were visual cloud observations to verify the selection. The diffuse data for these selected intervals were then corrected using Drummond's results. If the ratio of the corrected diffuse to the total solar radiation exceeded 0.90 then the data were arbitrarily considered to be representative of overcast conditions. These ratios were then plotted against the mean zenith angle observed in the intervals (Figure 8). Of the 40 observations selected, 85% of the ratios were between 0.90 and 0.96 with a mean close to 0.93. Therefore a further correction of 7% is indicated over Drummond's results. However it is not known whether the correction would also apply for clear or partially cloudy conditions. In the absence of complete experimental verification of this correction it was decided to use Drummond's values as sole correction to be applied to the data.

The signals from all radiometers were fed into three two-channel potentiometric strip chart recorders (Hewlett Packard Model 7100 B) located in a building near the shore. The individual signal cable consisted of 16 gauge stranded copper wire with ground. All signal cables were passed through a heavy PVC tube along the lake bottom. Thus, possible damage by abrasion was minimized. All signals were grounded to a water pipe on shore.

Sensors were checked on a daily basis to insure the instruments were clean and the sensing surfaces level. Discounting minor difficulties in the recording the performance of both the instruments and the recorders proved satisfactory. The pyranometers, which were calibrated at the

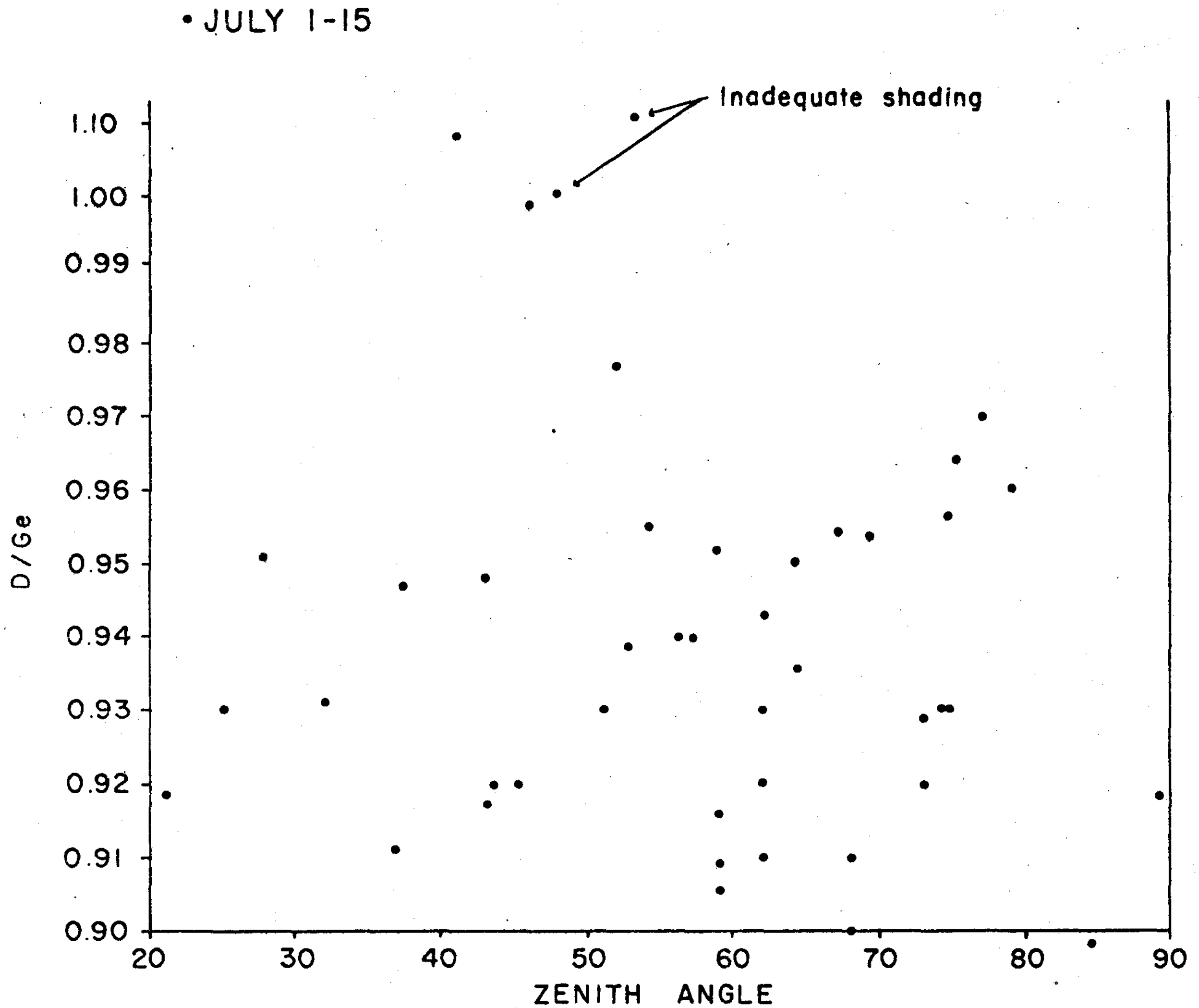

Figure 8 RATIOS OF MEASURED DIFFUSE TO GLOBAL RADIATION UNDER COMPLETE CLOUD COVER

National Radiation Centre (Scarborough, Ontario) before and after the field season, showed little change in their calibration constant. The recorders proved reliable and required only a small amount of supervision.

Solar flux data were collected on a continuous basis from July 1 until November 18, 1969. In addition meteorological observations were obtained on an hourly basis on most days. These observations are listed in Table 4 below:-

TABLE 4

METEOROLOGICAL OBSERVATIONS COLLECTED ON AN HOURLY BASIS

cloud type	visibility	wind speed	dominant wave height
cloud cover		wind direction	dominant wave direction
total fraction of sky covered by clouds			

Since it was not practical to take hourly meteorological observations from the tower structure, most were taken from the shore. The assumption was made that this change in location would not affect the observations. Cloud, visibility and wave observations were taken using the Manual of Marine Weather Observing (Department of Transport) as a guide. Wind speed and direction were obtained by means of a Nassau Windmaster System (Science Association) which was mounted on a 2 meter mast on the roof of the building housing the recorders. Thus, the sensors had a clear view of the lake and immediate surroundings.

On selected clear days radiosonde ascents were made. These gave pressure, temperature and relative humidity at various levels in the atmosphere. Standard Meteorological Branch ascent procedures as discussed in the Manual of Upper Air Observations were followed. A 403 Mc radiosonde,a radio receiver SCR - 658, an audio amplifier, recorder and baseline box were used.

All the radiation data were integrated by planimeter for half-hourly (TST) periods. Average fluxes (cal cm^{-2} min^{-1}) were obtained for every half hour. These values were stored in computer cards along with the relevant astronomical and meteorological parameters.

CHAPTER IV

ANALYSIS OF EXPERIMENTAL DATA

A. CLOUDLESS CONDITIONS

As an initial step to the evaluation of the prediction relations, a knowledge of the radiation balance at the Grimsby site is desirable. In particular, the aerosol absorption and scattering properties must be determined and compared to Lettau's results for different climatic conditions.

Half-hourly and daily fluxes will then be compared with some of the predictive models and different depletion relations will be discussed.

A total of three cloudless days and four cloudless half-days were available with precipitable water records. These are shown in Table 5.

TABLE 5

AVAILABLE CLOUDLESS DAYS WITH RADIOSONDE ASCENTS

Date	Morning	Afternoon	Total Day	Origin of Radiosonde Ascent
July 1		X		Buffalo
August 21			X	Grimsby
August 22			X	Buffalo
September 13	X			Grimsby

TABLE 5 continued ......

Date	Morning	Afternoon	Total Day	Origin of Radiosonde Ascent
September 22		X		Buffalo
October 5			X	Buffalo
October 10	X			Buffalo

Radiation budget

Lettau's budget equations were applied to the values of Ge, D and a collected at the site. Prior to such an analysis it is necessary to have estimates of α_w, α_{o3} and ρ_R. The Yamamoto-Onishi relation as expressed in equation 7 was used to obtain α_w. Lettau used the Dave and Sekera model to obtain values of ρ_R and α_{o3}. However, as this model does not describe in detail the effect of the depletion parameters with air mass, it was decided instead to compute α_{o3} and ρ_R using equation 5. Equation 5 was solved using $I'_{\lambda o}$ and $\rho'_{\lambda R}$ obtained from List (1966). These scattering coefficients ranged from 0.28 to 4.0 μ. The coefficients of ozone absorption were also obtained from List. These values were taken from experimental results by Ny and Choong (1933) but have been confirmed by later experimental studies (Robinson, 1966). To determine the amount of ozone at the site, mean monthly averages were obtained from data presented by Robinson (1966) for a latitude of 45°. The air mass was considered to be equal to the secant of the zenith angle as a first approximation. In the actual case atmospheric refraction and the change in air density with height causes the air mass to be less than sec Z. However, as this departure is only noticeable for zenith angles greater than 70° (Robinson, 1966) it will be neglected in this work.

Table 6 gives the direct beam transmission for an atmosphere containing Rayleigh scattering and ozone absorption. The effect of the ozone change on the transmission over the five-month period of this study is negligible. Table 7 shows the atmospheric transmission due to ozone only. The absorption is not particularly sensitive to air mass changes. An overall ozone absorption of 2% can be considered representative of this location during the period of this study.

Table 8 shows the radiation budget near noon during the seven clear days. For comparison Lettau's results for Kew, La Joya and O'Neill are shown. An interesting feature is the large variation in the aerosol scatter and absorption. Aerosol absorption ranges from a negligible amount on July 1 to a calculated maximum of 6.7% on August 22. This value approaches the value of 10.3% which Lettau calculated for the industrialized area of Kew. Similarly, the aerosol scattering term shows magnitudes of up to 11% of the incoming direct beam and compares with values of 13.5% which Lettau reported for the desert atmosphere of La Joya.

The surface albedo values (4%-5%) are consistently smaller than those quoted by Lettau for land (15%-22%). Hence the planetary albedo (7%-11%) will be lowered and the fraction of the incoming solar radiation that is absorbed by the water surface will be large. The total energy absorption by the atmosphere is between 17% and 21%. Generally this represents values larger than La Joya or O'Neill but less than the observed value of 25% at Kew.

The large variance in the aerosol term seems to justify a closer study of the diurnal variation of these terms. Figure 9 shows the total

TABLE 6

TRANSMISSION OF DIRECT BEAM SOLAR RADIATION DUE

TO RAYLEIGH SCATTER AND OZONE ABSORPTION AT A LATITUDE OF 45°

Month	Zenith Angle (degrees)									
	0	10	20	30	40	50	60	70	80	
July	1.745	1.743	1.736	1.723	1.702	1.670	1.618	1.525	1.322	cal cm^{-2} min^{-1}
0.32 cm O_3	0.90	0.90	0.89	0.89	0.88	0.86	0.83	0.79	0.68	transmission (I/I_o')
August	1.746	1.743	1.736	1.724	1.703	1.671	1.618	1.526	1.323	cal cm^{-2} min^{-1}
0.31 cm O_3	0.90	0.90	0.89	0.89	0.88	0.86	0.83	0.79	0.68	transmission (I/I_o')
September	1.747	1.744	1.737	1.724	1.704	1.672	1.620	1.527	1.326	cal cm^{-2} min^{-1}
0.29 cm O_3	0.90	0.90	0.89	0.89	0.88	0.86	0.83	0.79	0.68	transmission (I/I_o')
October	1.747	1.745	1.738	1.725	1.705	1.673	1.622	1.529	1.328	cal cm^{-2} min^{-1}
0.27 cm O_3	0.90	0.90	0.90	0.89	0.88	0.86	0.84	0.79	0.68	transmission (I/I_o')
November	1.747	1.745	1.738	1.725	1.705	1.673	1.621	1.529	1.327	cal cm^{-2} min^{-1}
0.28 cm O_3	0.90	0.90	0.89	0.89	0.88	0.86	0.83	0.79	0.68	transmission (I/I_o')

TABLE 7

TRANSMISSION OF DIRECT BEAM SOLAR

RADIATION DUE TO OZONE ABSORPTION (5-MONTH AVERAGE)

Zenith Angle (degrees)

0	10	20	30	40	50	60	70	80	
1.900	1.900	1.899	1.898	1.895	1.891	1.884	1.872	1.836	cal cm^{-2} min^{-1}
0.98	0.98	0.98	0.98	0.98	0.98	0.97	0.96	0.95	transmission (I/I_o')
0.02	0.02	0.02	0.02	0.02	0.02	0.03	0.04	0.05	absorption ($(I_o' - I)/I_o'$)

TABLE 8

LETTAU MODEL FOR NEAR NOON CONDITIONS ($\xi = {}^1/_3$)

	air mass	global radiation	diffuse radiation	albedo	water vapor	Rayleigh scatter	aerosol scatter	water vapor absorp.
	m	G^*	D^*	a	W (cm)	ρ_R	ρ_d	α_w
Kew[1] (industrial)	1.25	0.728	0.110	0.150	2.0	0.095	0.062	0.102
La Joya (desert)	1.11	0.808	0.189	0.180	0.84	0.103	0.135	0.100
O'Neil (prairie)	1.16	0.804	0.134	0.220	2.10	0.107	0.063	0.130
<u>Grimsby</u>								
July 1	1.10	0.816	0.075	0.04	2.90	0.087	0.024	0.132
August 21	1.17	0.769	0.084	0.04	1.74	0.090	0.035	0.124
August 22	1.18	0.760	0.091	0.04	1.00	0.091	0.066	0.107
September 13	1.29	0.735	0.120	0.04	1.70	0.099	0.080	0.127
September 22	1.37	0.736	0.140	0.05	2.25	0.103	0.100	0.139
October 5	1.47	0.729	0.147	0.05	2.17	0.109	0.104	0.140
October 10	1.52	0.752	0.152	0.05	1.27	0.112	0.111	0.122

cont'd...

TABLE 8 continued .....

	ozone absorp. α_o	aerosol absorp. α_d	α_d/ρ_d	albedo to space A	absorb. by atmosphere H*	absorb. by surface (1-a)G*
Kew[1] (industrial)	0.020	0.103	1.66	0.129	0.252	0.619
La Joya (desert)	0.016	0.027	0.20	0.175	0.162	0.663
O'Neil (prairie)	0.018	0.012	0.19	0.187	0.186	0.627
<u>Grimsby</u>						
July 1	0.022	0.00	0.00	0.066	0.154	0.780
August 21	0.023	0.043	1.23	0.066	0.196	0.738
August 22	0.023	0.067	1.01	0.069	0.203	0.728
September 13	0.023	0.057	0.71	0.084	0.213	0.705
September 22	0.025	0.036	0.36	0.094	0.206	0.700
October 5	0.025	0.038	0.36	0.100	0.207	0.693
October 10	0.025	0.029	0.26	0.104	0.183	0.713

aerosol depletion (in % of extra-terrestrial radiation I_o') calculated from equation 8 and the aerosol depletion and absorption term using the Lettau Model. Depletion was plotted against air mass for all seven days of data (1/2 hourly mean fluxes) using a log-log scale since a non-linear dependence of depletion with air mass was expected. The large scatter observed in all three terms illustrates the variability of the aerosol. Not only does this parameter vary for individual days but there are no consistent daily trends. The regular increase in total depletion with air mass which is exhibited in the trace of July 1 is not evident in the remaining traces. Indeed the traces of October 5 and 10 show a constant depletion with air mass whereas data on the afternoon of September 22 show a decrease with increasing air mass. However, these results are not unique. Robinson (1963) observed an increase in aerosol depletion of global solar radiation with increasing air mass in clean non industrial areas. This effect was not evident at Kew and Vienna where the absorption and scattering were found to be independent of air mass. Absorption and scattering coefficients ranged from 18% to 15% and from 7% to 12% of the extra-terrestrial radiation for urban areas. Similar non-dependence on air mass was found by Paltridge, Hamilton and Collingbourne (1969) for direct beam depletion by aerosols. Although the total depletion graph seems to suggest a seasonal increase in depletion, it is not possible to come to any conclusion on the basis of seven days' data. This possible seasonal effect is also evident (although less clearly) in the scatter graphs but disappears altogether for the absorption relation. Furthmore, most of the absorption and scatter estimates are of the same order of magnitude (between 1 and 10 per cent).

Figure 9

DEPLETION OF THE DIRECT BEAM BY AEROSOLS

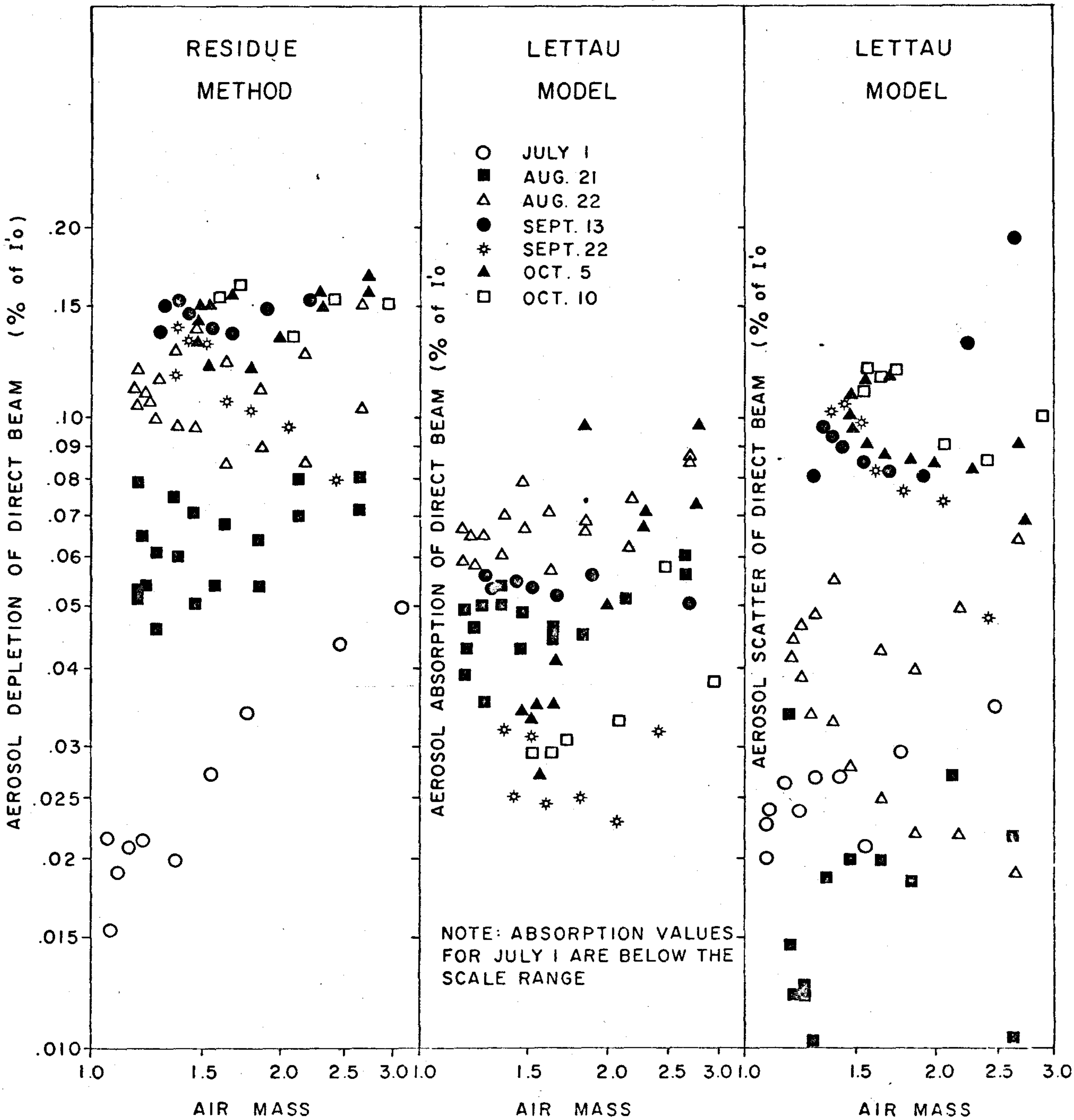

It should be kept in mind that these results are not necessarily representative of only one type of aerosol. It is possible that two or more types of different optical properties are represented in this chart with the results that the scatter and absorption graphs will not behave in a similar manner.

The large variance of the aerosol depletion term seems to warrant independent measurements of the diurnal and seasonal variation of the aerosol content in the atmosphere. In conjunction with detailed spectral measurements of solar radiation of the Ångström type, it might be possible to answer some of the questions raised in this study. Without an independent measurement of the aerosol content of the atmosphere it does not seem possible to predict the aerosol depletion of solar radiation accurately.

Finally, it should be emphasized that these results are approximate since they assume a scattering coefficient of 1/3 which represents a best estimate by Lettau. In fact it is not possible on a strict basis to describe the entire radiation budget using only surface measurements of radiation. It is necessary to bring in certain assumptions regarding the nature of the absorption or scattering processes. It is possible that this problem will be solved through satellite measurements of the planetary albedo. Simultaneous measurements of A, G*, D* and a could be used in equations 13 to 16 to yield values of ρ, α and ξ.

Prediction of fluxes

The global radiation predicted by the Houghton, London and Lettau models were compared with the 1/2 hourly mean fluxes collected for the seven cloudless days. ρ_R, ρ_w and α_w in equations 21 and 22 were obtained from the Houghton curves. In the absence of any clearcut way of predicting α_D and ρ_D in the Lettau model, it was decided to use the computed seasonal averages of $\alpha_D = 4\%$ and $\rho_D = 8\%$. These values were then substituted into equation 23 along with values of ρ_R and α_{03} computed from Tables 6 and 7 and α_w computed from equation 7. Figures 10, 11 and 12 show the relation between the predicted and experimental fluxes. Table 9 gives the result of a linear regression analysis.

TABLE 9

RESULTS OF A LINEAR REGRESSION ANALYSIS ON THE PREDICTED AND OBSERVED HALF HOURLY FLUXES UNDER CLOUDLESS CONDITIONS

Model	Relation	Correlation Coefficient	Standard Error (cal cm^{-2} min^{-1})
Lettau	$G'o=0.03 + 0.955$ Ge	0.996	0.035
London	$G'o=-0.08 + 0.899$ Ge	0.989	0.053
Houghton	$G'o=-0.04 + 1.007$ Ge	0.994	0.044

The London relation underpredicts considerably as indicated by the low slope and intercept. With respect to this model the main conclusion is that the allowance for certain secondary effects, such as diffuse radiation absorption and Mie scatter, does not significantly improve the prediction over the simpler Houghton model. Figure 13 shows how the models predict for individual days. Both the Houghton and Lettau models predict extremely well.

Corrections to the Houghton relation have been used by several

Figure 10

LETTAU MODEL

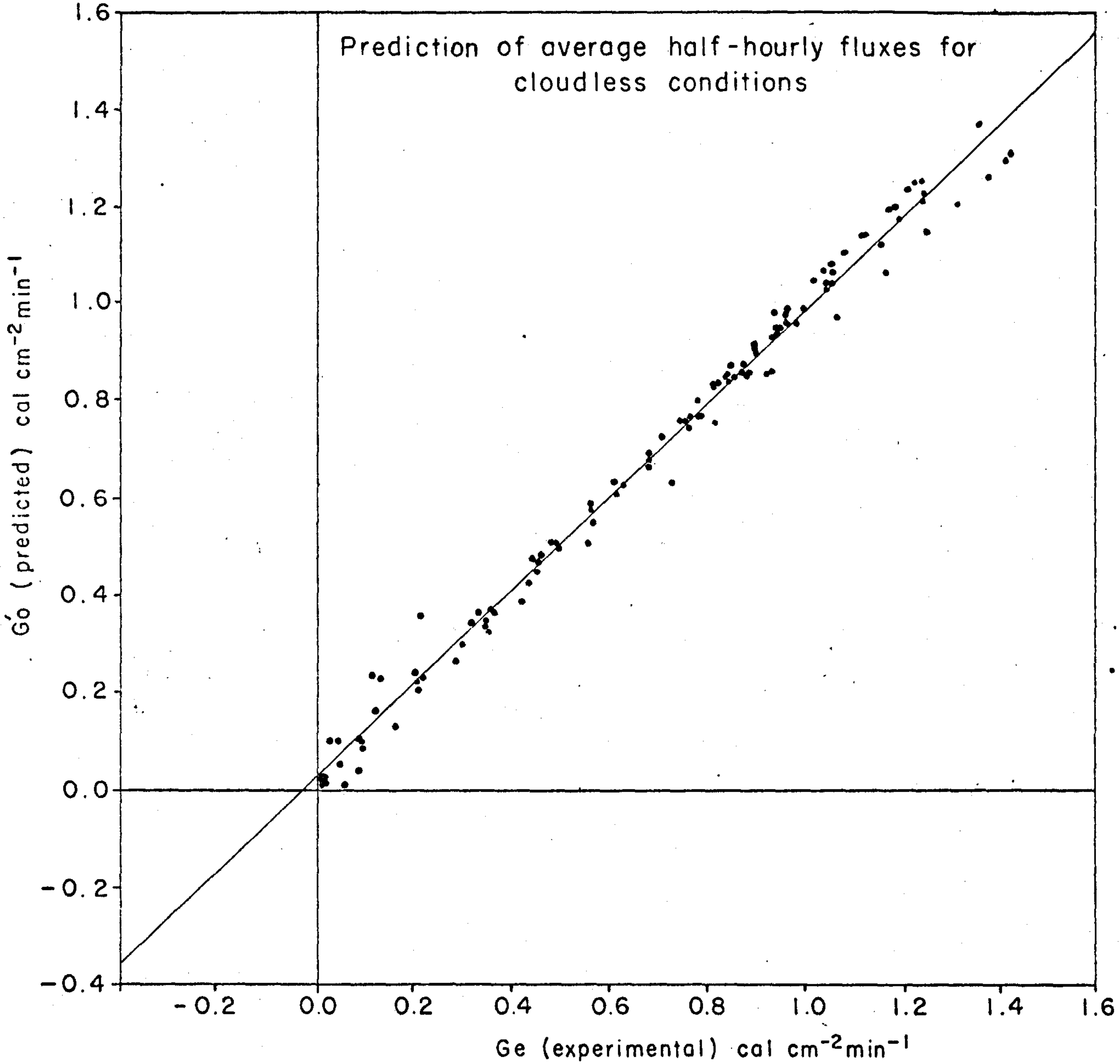

Figure 11
LONDON MODEL

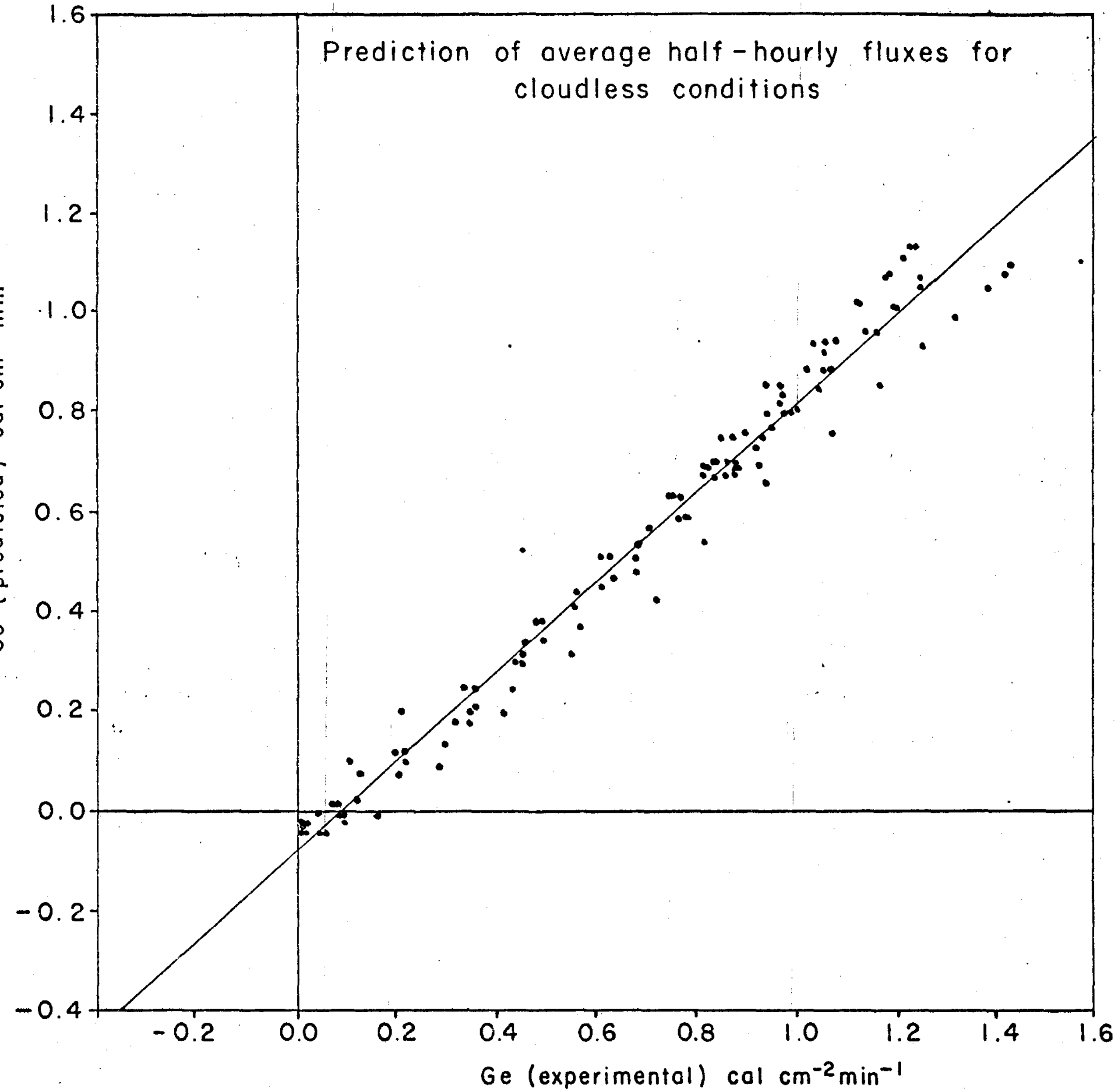

Figure 12

HOUGHTON MODEL

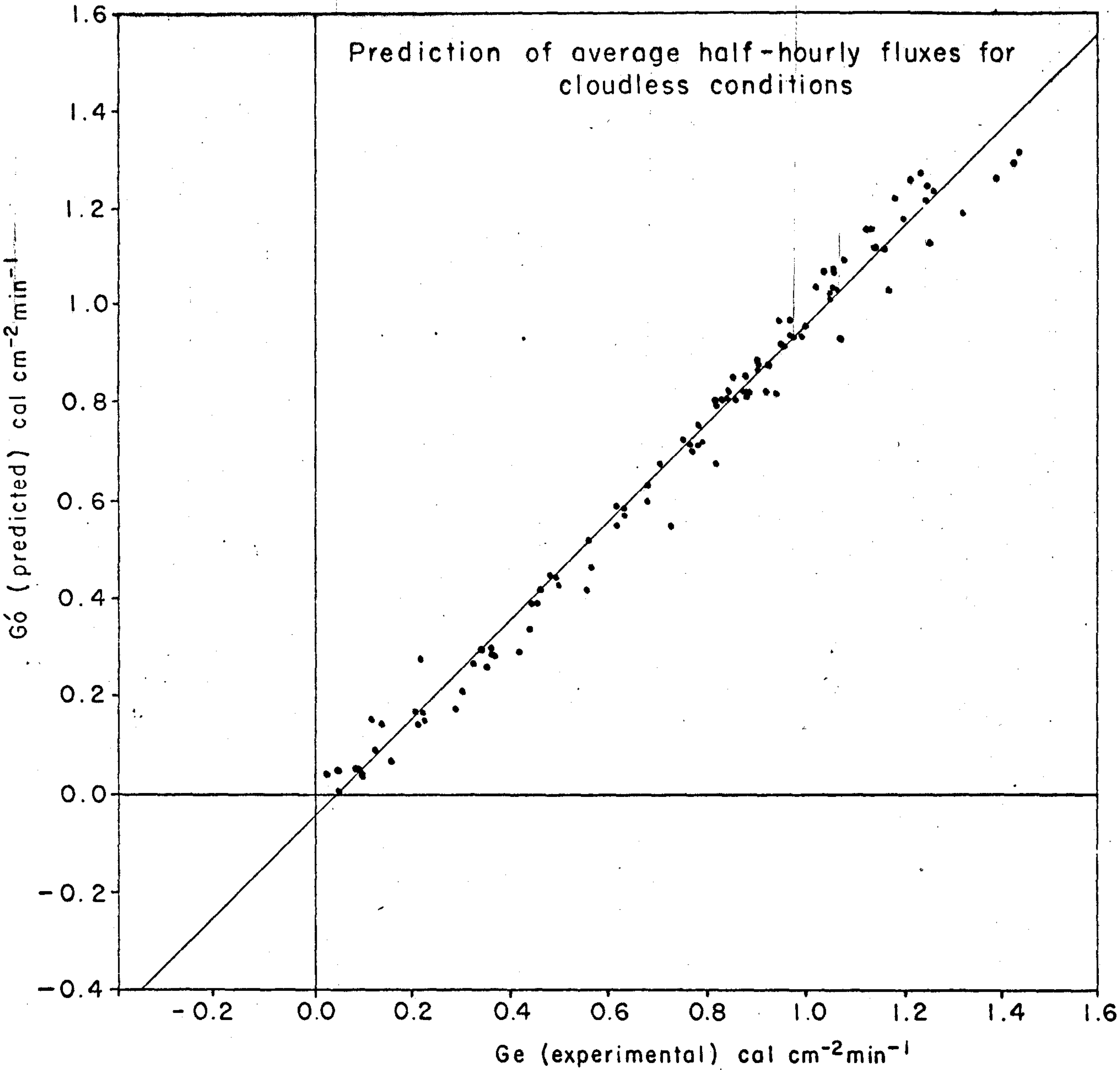

Figure 13
PREDICTION OF MEAN HALF HOURLY GLOBAL RADIATION FLUXES FOR INDIVIDUAL DAYS

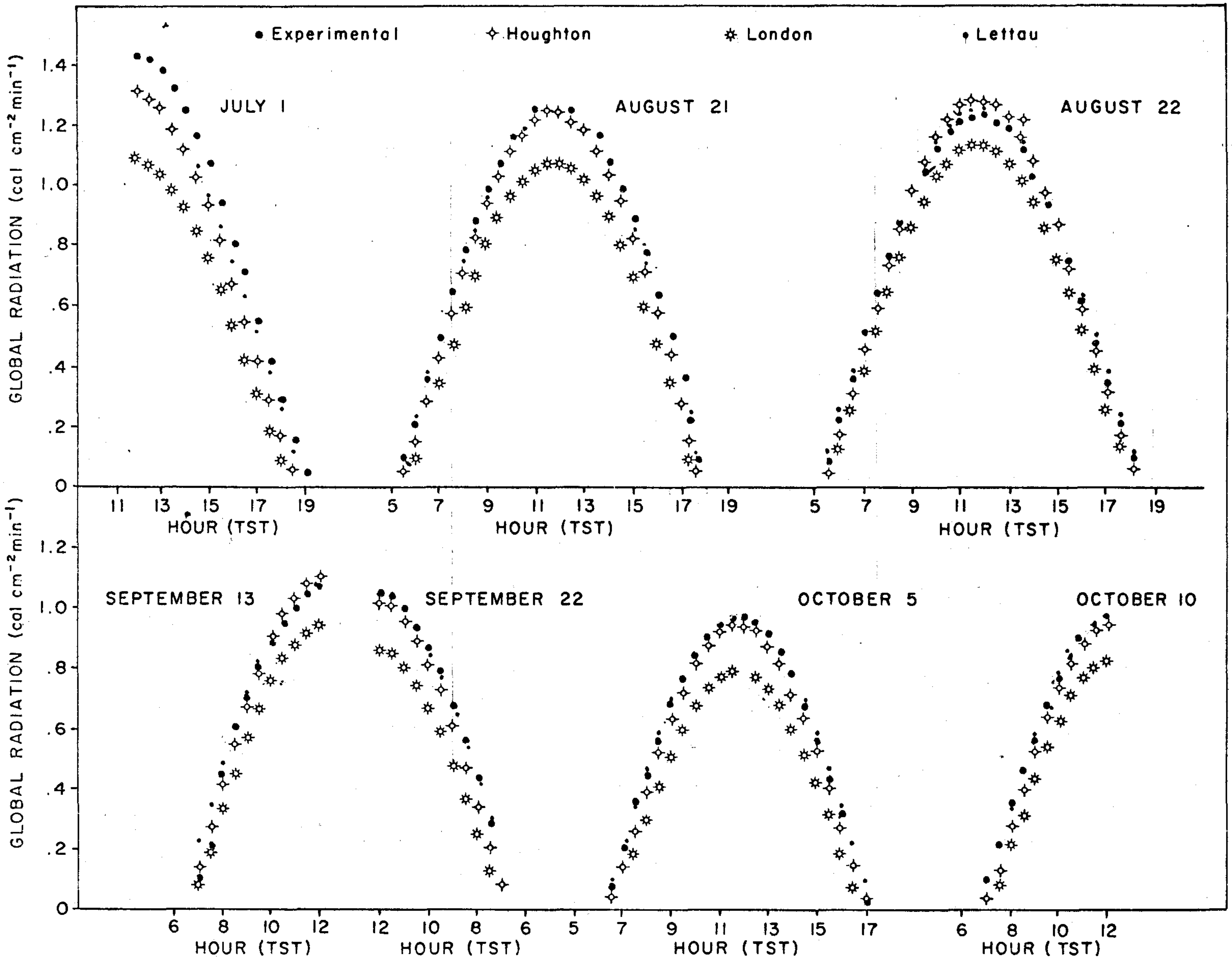

workers (eg. Hay, 1970, Idso, 1969, 1970). These workers favour the McDonald relation for water vapor absorption. Hay also uses a solar constant of 2.00 cal cm^{-2} min^{-1} in his work dealing with modelling of the radiation fluxes over Canada. At this stage it was found appropriate to compare the effect of these widely used values on the prediction. Table 10 listed, observed and calculated daily total fluxes.

TABLE 10

PREDICTED AND OBSERVED DAILY FLUXES UNDER CLOUDLESS CONDITIONS

(cal cm^{-2} day^{-1})

	Observed	Lettau	London	Houghton	Houghton (McDonald) absorption)	Houghton (McDonald absorption + Io=2.0)
July 1*	778	669	538	669	682	704
August 21	618	609	491	585	594	612
August 22	605	621	538	606	610	629
September 13*	477	508	401	480	488	503
September 22*	468	465	346	430	438	451
October 5	400	412	301	374	382	394
October 10*	379	404	316	375	381	393

*half day clear sky observations have been used

It is evident from the table that the use of the McDonald absorption relation will only increase daily fluxes by approximately 1-2%. However, the additional use of a solar constant of 2 cal cm^{-2} min^{-1} will increase the flux by a total of approximately 4-6%. In view of the uncertainty in the aerosol depletion the use of these modified terms cannot be meaningful. If the aerosol depletion is consistently underestimated the use of these "corrected" terms will give correct results and vice versa.

It should finally be emphasized that this analysis was conducted using seven days of data and thus cannot be considered complete. Nevertheless the results indicate that during the period of this study and under a variety of conditions both the Houghton and Lettau models can estimate average 1/2 hourly fluxes with a standard error of better than 0.05 cal cm^{-2} min^{-1}. Similar good agreement has been found for daily fluxes. This is confirmed by the measurements of Idso (1970).

Conclusion

This analysis has considered the depletion of solar radiation both as a study of the individual depletion terms and the incorporation of the results in a logical model to predict solar radiation in cloudless conditions.

There is at present still a considerable uncertainty regarding some of the depletion terms which in turn are going to affect the prediction. It seems to this writer that a proper knowledge of the solar constant and water vapor absorption is important since it will affect the magnitude of the aerosol depletion term which is calculated as a residue. Furthermore, although there seems to be two accepted water vapor absorption relationships (Houghton's and McDonald's) these results seem to indicate that either of these relations make little difference in the prediction of daily fluxes of solar radiation at the surface. Time variation of water vapor and aerosol seem to be more important.

Residual calculations point out that there are large variations in the aerosol scattering and absorption coefficients throughout the season. An independent method of estimating the aerosol content in the atmosphere would be beneficial. The Lettau model was employed to partition the aerosol depletion into scattering and absorption terms. This method however, assumes a bulk coefficient describing the fraction of the diffuse radiation scattered to space. Simultaneous satellite measurements of the planetary albedo could solve the problem and also could indicate the effect of aerosols on the albedo.

Finally, it should be stated that the prediction of solar radiation over water surfaces is not particularly sensitive to albedo but is sensitive to absorbers and scatterers. Nevertheless the variation in the global radiation is small compared to large changes in the turbid media. Thus, solar radiation is a conservative quantity. Short-term fluxes can be predicted with good accuracy.

B. CLOUDY CONDITIONS

Since short-term and daily fluxes of global radiation can be predicted with good accuracy, errors that arise in the prediction of global under cloudy weather cannot be attributed to Go. Thus, further refinements in the prediction of Go, such as empirical observations of aerosol depletion, are not relevant in view of the large errors that could arise in the cloud transmission relations.

This section will concentrate on the ability of present models to predict global radiation in cloudy conditions at the Grimsby site. A study of the individual cloud transmission properties will not be attempted and previous work will be relied upon for such knowledge. The ability of these models to predict 1/2 hourly, five-day and monthly fluxes will be examined.

Prediction of half-hourly fluxes

Cloud observations were taken every hour during most days of the study. To make the data compatible with the half-hourly integrated fluxes, the cloud observations were interpolated every hour to yield half hourly estimates of cloud and amount as well as total cover. A total of 1894 half hourly observations were obtained with radiation and cloud cover data.

Prior to the use of the prediction equations, a knowledge of the global radiation under cloudless conditions is necessary. The Houghton relation (equation 21) was used with monthly estimates of precipitable water vapor obtained from Reitan's (1960) ten year averages for the Buffalo station. To take into account the reduction of precipitable water under cloudless conditions, a correction factor χ developed empirically by Hay (1970) was employed. It has the form:-

$$\chi = -22.373 + 0.02275P, \tag{40}$$

where, P = monthly mean sea level pressure in millibars. Thirty year mean values of sea level pressure for the Buffalo station were obtained from the "CLIMATIC ATLAS OF THE UNITED STATES" (1968). Substitution of the correction factor into the original precipitable water vapor values yields the results in Table 11.

TABLE 11

MONTHLY MEAN PRECIPITABLE WATER VAPOR FOR CLOUDLESS CONDITIONS

July	2.04 cm
August	2.09 cm
September	1.69 cm
October	1.31 cm
November	0.84 cm

The above precipitable water vapor values were used in conjunction with the Houghton relation to predict individual half hourly and daily fluxes.

Table 12 shows the result of the half hourly prediction for the linear and non-linear models discussed in Chapter II. The linear models of the Ångström type exibit a correlation coefficient of between 0.905 to 0.918 with standard errors of estimates between 0.16 to 0.17 cal cm^{-2} min^{-1}. The Kimball model (Figure 14) with a lower ε (lower cloud transmission) underpredicts considerably for medium to high cloud cover while providing a reasonable prediction for low cloud cover. This effect is apparent to a lesser extent in the Neumann model (Figure 15) which employs a larger ε (higher cloud transmission).Although the prediction for large cloud cover is improved, the model overpredicts for low cloud cover. This suggests that the relationship between cloud cover and global radiation is non-linear. The non-linear models of Mateer and Laevastu (Figures 16 and 17) show a significant improvement in the correlation and standard error of estimate while the Tabata and Berliand relations do not. In addition the slope of the linear regression equation

Figure 14
KIMBALL MODEL

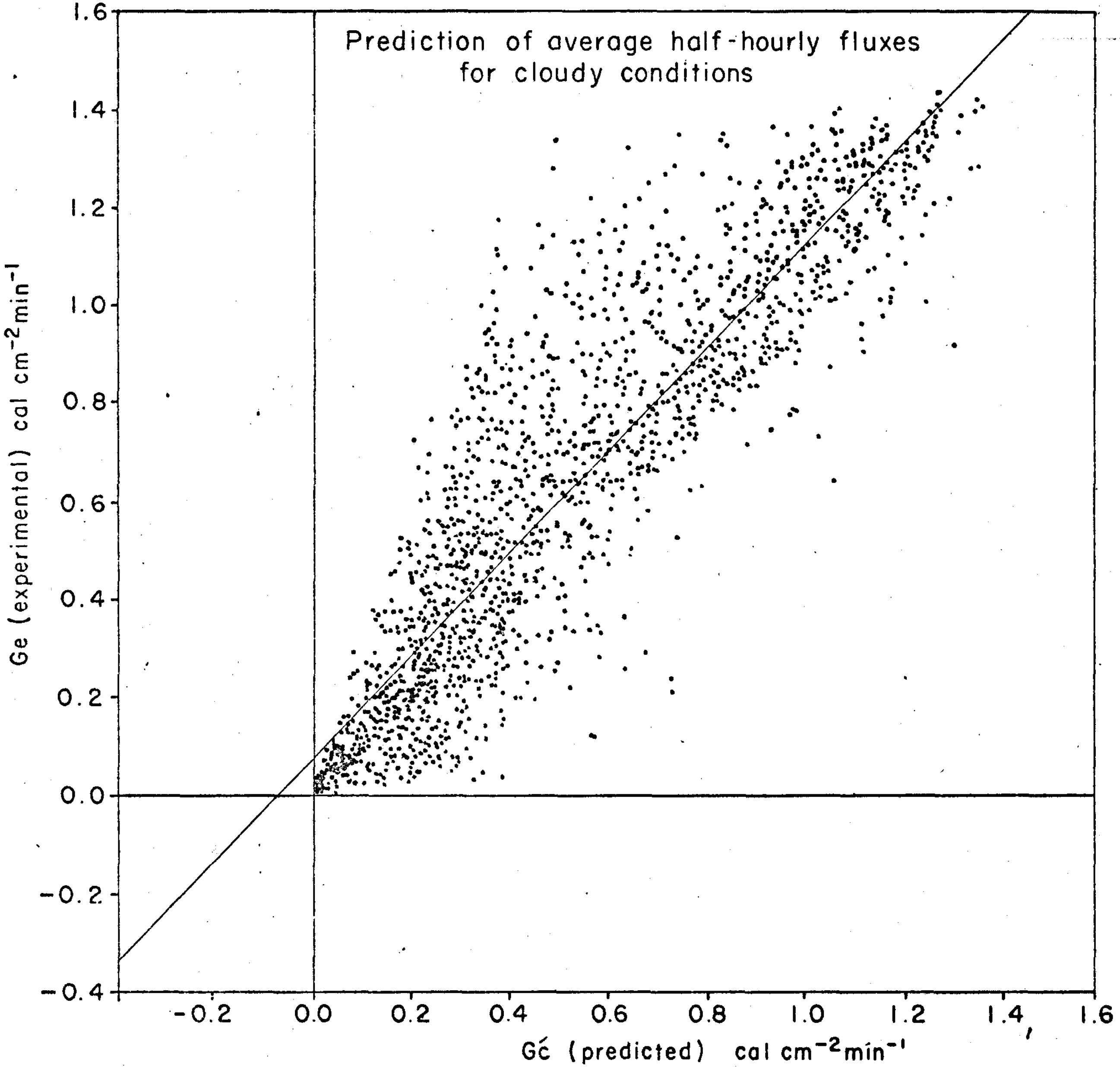

Figure 15

NEUMANN MODEL

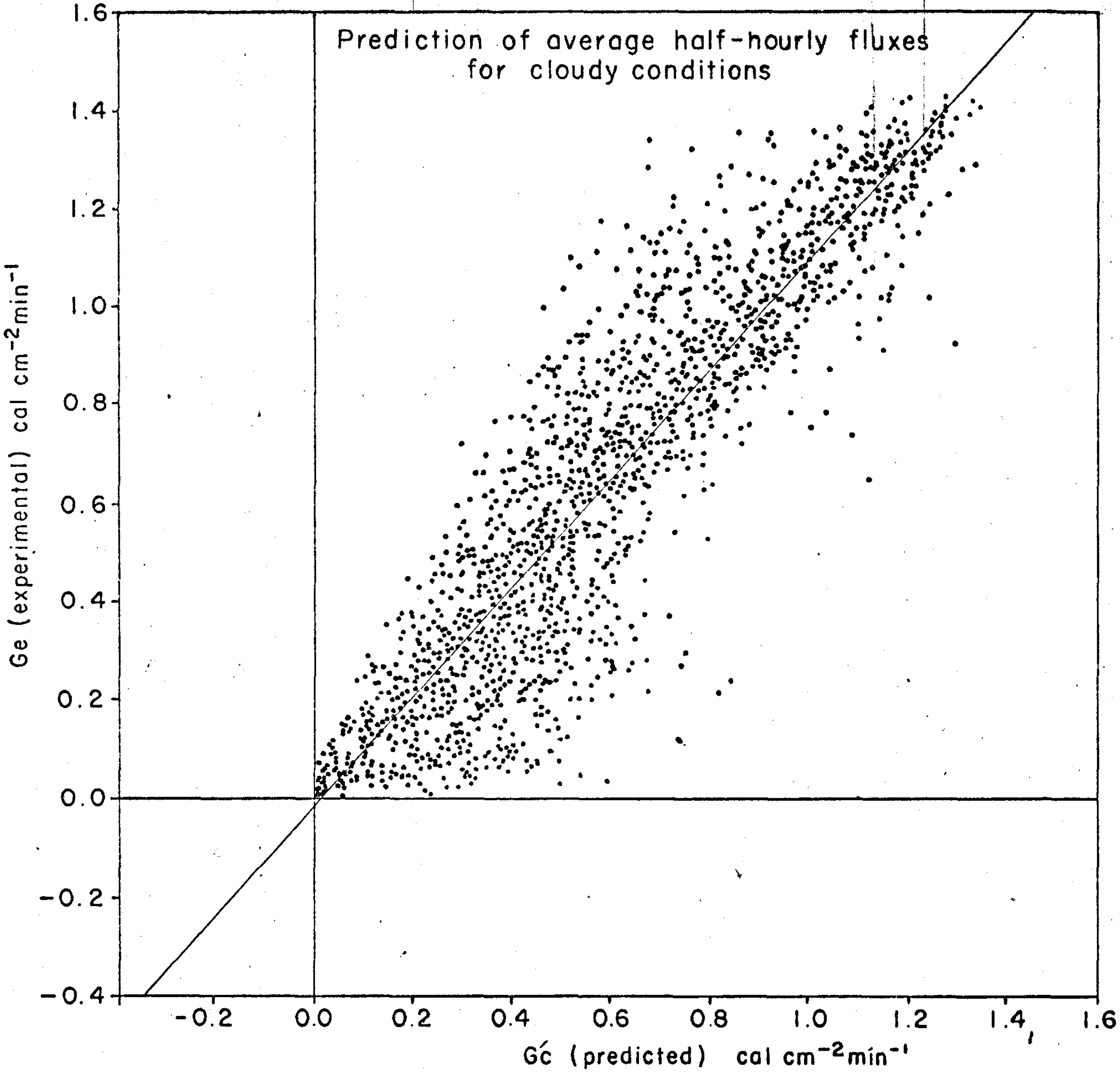

Figure 16

MATEER MODEL

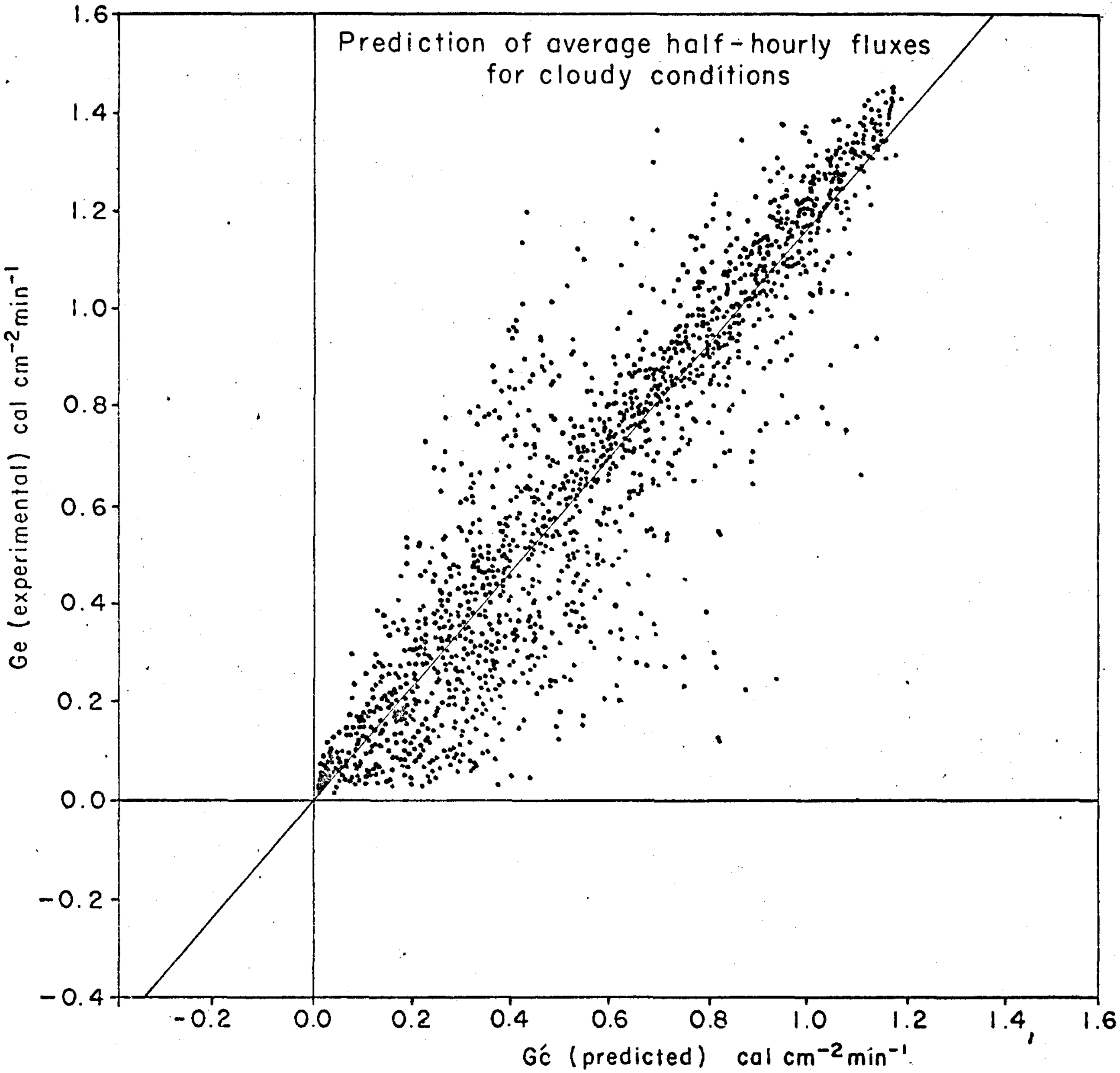

Figure 17

LAEVASTU MODEL

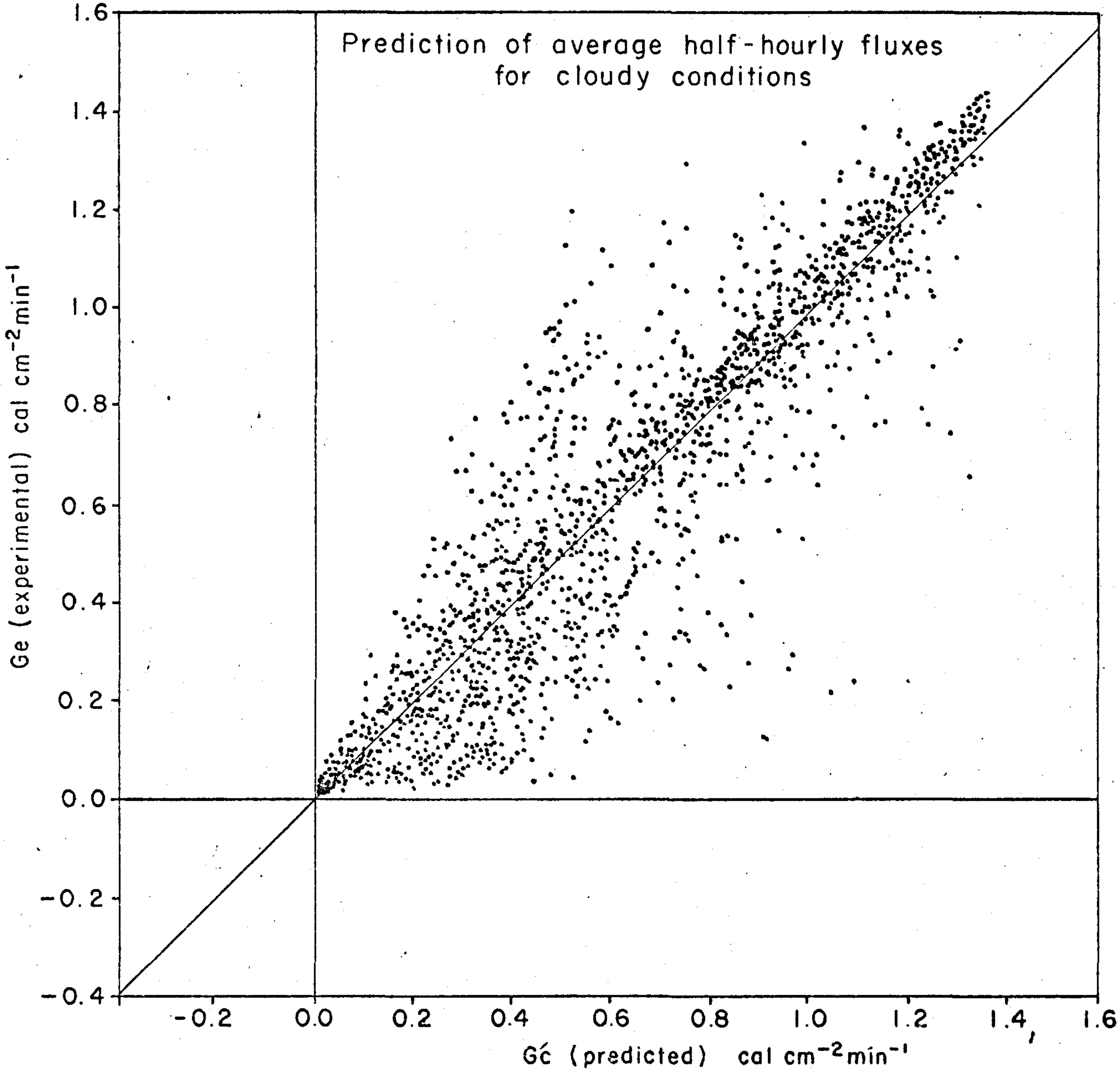

for the Laevastu model is 0.99 which indicates no over or under prediction. We can thus conclude that the Laevastu equation with a correlation of 0.927 is the best predictor for short-term fluxes.

TABLE 12

RESULTS OF A LINEAR REGRESSION

ANALYSIS ON THE PREDICTED AND OBSERVED HALF HOURLY FLUXES

Model	Relation	Correlation	Standard Error $cal\ cm^{-2}\ min^{-1}$
Budyko	$Ge = 1.07\ Gc' + 0.059$	0.912	0.16
Houghton	$Ge = 0.79\ Gc' + 0.152$	0.888	0.18
Kimball	$Ge = 1.05\ Gc' + 0.09$	0.905	0.17
Monteith	$Ge = 1.09\ Gc' + 0.03$	0.916	0.16
Neumann	$Ge = 1.10\ Gc' - 0.01$	0.918	0.16
Berliand	$Ge = 0.87\ Gc' - 0.04$	0.765	0.26
Laevastu	$Ge = 0.99\ Gc' + 0.01$	0.927	0.15
Mateer	$Ge = 1.15\ Gc' - 0.01$	0.922	0.15
Tabata	$Ge = 0.75\ Gc' - 0.06$	0.824	0.23
Layer	$Ge = 1.07\ Gc' - 0.01$	0.939	0.14

The question still remains as to the cause of the non-linearity. Although side reflection from the clouds could be a likely possibility, it is possible that the allowance of transmission for particular cloud types might effectively remove the non-linearity. Keeping these considerations in mind a new model was developed and is described below.

Layer model

This model was derived using the premise that clouds of different type exist simultaneously. The model is composed of three layers of randomly distributed cloud cover. The total transmission of the cloud layers is then given as the product of the individual transmission for each regime.

$$T = \nu_h \cdot \nu_m \cdot \nu_l , \tag{41}$$

where, ν_h = transmission of the high cloud regime,

ν_m = transmission of the middle cloud regime,

ν_l = transmission of the low cloud regime.

The individual transmission of each cloud regime ν_i is given as:-

$$\begin{aligned} \nu_i &= (C_i T_i + 1 - C_i) \\ &= 1 - (1 - T_i) C_i , \end{aligned} \tag{42}$$

in which, T_i = transmission of cloud layer i,

C_i = cloud cover of layer i.

Since $T_i = \varepsilon$ the formula reduces to the linear form of equation 25. The model must receive as inputs the cloud type and the fraction of the sky covered by each cloud type. In the case of the middle and high clouds, the values of cloud cover are only approximate if low cloud cover is present. The assumption must be made that the fraction of the unobstructed sky covered by the middle or high cloud is representative of the total sky covered by the cloud layer.

It is evident that T_i must refer to the cloud transmission under overcast conditions. Originally it was intended to derive this parameter using data collected at the site. However, because of insufficient data, it was decided to use the more reliable estimates from Haurwitz' work (Table 2). Dividing equation 9 by the global radiation expected under cloudless conditions we obtain:-

$$T_i = \frac{G_c'}{G_o'} = \frac{a}{m} \cdot e^{-bm}, \tag{43}$$

and thus T_i is expressed as a function of cloud type and air mass. The global radiation in the presence of all three cloud layers is:-

$$G_c' = G_o'[1 - (1 - T_l)C_l]\,[1 - (1 - T_m)C_m]\,[1 - (1 - T_h)C_h], \tag{44}$$

and, T_w = transmission of the high cloud layer,

T_m = transmission of the middle cloud layer,

T_l = transmission of the low cloud layer.

For purposes of computation it has been assumed that if two or more cloud types exist at the same level, they can be replaced by a single and most abundant type. Since Haurwitz did not compute the transmission of cumulus and cirro cumulus clouds, it has also been assumed that these transmissions can be given by the transmissions of the stratocumulus and cirrostratus clouds respectively.

Application of this model to half hourly fluxes collected yields the highest correlation of 0.939 with a slope of 1.07 and a standard error of 0.14 cal cm^{-2} min^{-1} (Figure 18). Thus it seems that the non-linearity

Figure 18

LAYER MODEL

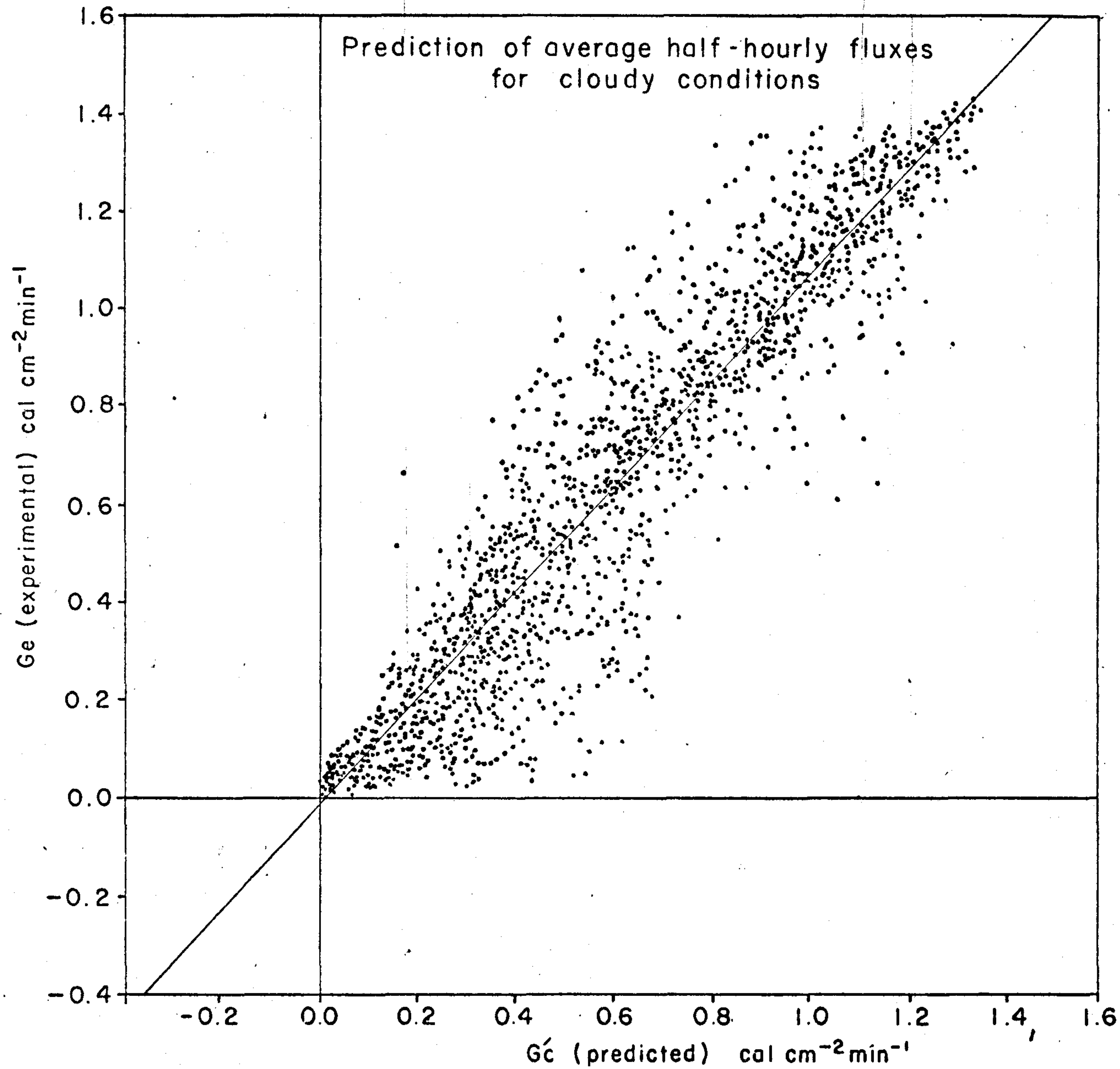

can be largely accounted for by selective transmission of different cloud types. The fit however, still leaves a considerable scatter about the regression line which must be explained. There seems to be two possible explanations:

a) The sampling interval of cloud measurement is not representative of the cloud regime during the interval.

b) There are consistent differences in the transmission for clouds of the same type.

If the first case were to be the only effect, it is reasonable to expect better results after daily integration of the half-hourly transmission coefficients. On the other hand if there were consistent long-term (daily) anomalies in the cloud transmission, a better fit cannot be expected.

Prediction of daily fluxes

Thirty days of half-hourly interpolated cloud observations from dawn to dusk were available. These data were analyzed in two ways:-

a) A mean daily cloud cover was assigned to each layer as well as to the total cloud cover. This value was then applied to the corresponding daily total global radiation under cloudless conditions. The predictive models were then tested. In the case of the layer model each cloud layer was characterized by the most frequent cloud type. A mean solar angle equal to half the noon solar angle was assumed.

b) Half hourly fluxes were calculated using cloud data over the half hour period. The resultant fluxes were then summed over the entire day so as to give daily totals.

Tables 13 and 14 show the results of the regression relations. A maximum correlation of 0.88 was obtained for the Laevastu and Mateer models using daily average cloud observations. These values were slightly lower than the correlations of 0.90 using the sum of the half hourly fluxes. However, it was found that the increase was statistically not significant at the 5% level. The linear models of Houghton, Neumann, Monteith, Budyko and Kimball all exibit correlation coefficients between 0.876 (Neumann) to 0.852 (Houghton) in the half-hourly transmission relation. Again no significant difference could be found between these predictions at the 5% level nor was there any significant difference in the correlation between these results and the ones using a daily average cloud observation. The non-linear models of Tabata and Berliand show a significant lower correlation coefficient than the Mateer, Laevastu or linear models. Again no significant difference existed at the 5% level between the two methods. Finally the Layer model predicts with a correlation of 0.82 using the sum of the half-hourly fluxes but shows a significantly poorer prediction using average daily cloud cover. The inability of the Layer model to predict with a higher accuracy indicates that consistent differences exist in the cloud transmission on a daily basis. A more complex dependence on cloud structure and general climatic properties is suggested.

Although generally the correlation coefficient did not show large differences in the two methods of prediction, the slope of the regression lines do. All models except the Layer model and the Berliand model exhibit an increase in the slope when mean daily cloud observations are used. The difference is significant to within 5% in the case of the

TABLE 13

RESULTS OF A LINEAR REGRESSION ANALYSIS ON THE PREDICTED AND OBSERVED DAILY FLUXES USING INTEGRATED HALF HOURLY PREDICTIONS

Model	Relation	Correlation	Standard Error cal $cm^{-2}day^{-1}$
Budyko	Ge = 1.00 Gc + 77	0.865	71
Houghton	Ge = 0.66 Gc + 176	0.852	74
Kimball	Ge = 0.94 Gc + 116	0.860	72
Monteith	Ge = 1.07 Gc + 34	0.870	70
Neumann	Ge = 1.18 Gc - 36	0.876	68
Berliand	Ge = 1.02 Gc - 96	0.394	131
Laevastu	Gc = 1.00 Gc - 3	0.899	62
Mateer	Ge = 1.18 Gc - 15	0.901	62
Tabata	Ge = 0.99 Gc - 211	0.603	113
Layer	Ge = 1.09 Gc - 38	0.821	81

TABLE 14

RESULTS OF A LINEAR REGRESSION ANALYSIS ON THE PREDICTED AND OBSERVED DAILY FLUXES USING DAILY AVERAGE CLOUD OBSERVATIONS

Model	Relation	Correlation	Standard Error cal $cm^{-2} day^{-1}$
Budyko	Ge = 1.42 Gc - 115	0.843	67
Houghton	Ge = 0.97 Gc + 16	0.824	105
Kimball	Ge = 1.35 Gc - 63	0.836	72
Monteith	Ge = 1.50 Gc - 171	0.849	61
Neumann	Ge = 1.63 Gc - 262	0.855	55
Berliand	Ge = 1.04 Gc - 124	0.409	130
Laevastu	Ge = 1.39 Gc - 268	0.882	56
Mateer	Ge = 1.79 Gc - 350	0.881	44
Tabata	Ge = 2.77 Gc - 1551	0.591	73
Layer	Ge = 0.73 Gc + 246	0.766	95

the Mateer, Houghton, Neumann, Monteith and Tabata models and to within 10% in the case of the Laevastu, Budyko, Kimball and the Layer model. Figures 19 and 20 show the daily prediction of the Mateer model using the two methods. An examination of the data revealed that the difference lies in the non-random distribution of clouds during the day. Using the linear prediction equation:-

$$G_c' = G_o'[1 - (1 - \varepsilon)C],$$

we require that:-

$$\int G_o'[1 - (1 - \varepsilon)c]dt = G_o[1 - (1 \varepsilon)\bar{c}], \tag{45}$$

where $\bar{c}$ refers to a mean daily cloud cover and the integration is performed over the entire day. The above equation can be simplified to give:-

$$\int G_o' c\,dt = G_o\bar{c}; \tag{46}$$

If c is constant throughout the day, the equality will hold. However, on the days with overcast near noon and partial overcast in the early morning or late afternoon the right hand side of the equation will obviously overpredict. Since there were six days with these conditions out of a total of thirty days, it is certain that these six days influenced considerably the slope of the regression line. The two different results illustrate the discrepancies that can arise in taking mean daily cloud cover.

An investigation of Figure 19 revealed that for nine days model values did not agree with measured values to within 10% of the regression

Figure 19
MATEER MODEL
Daily Prediction Using Sum Of Half-Hourly Fluxes

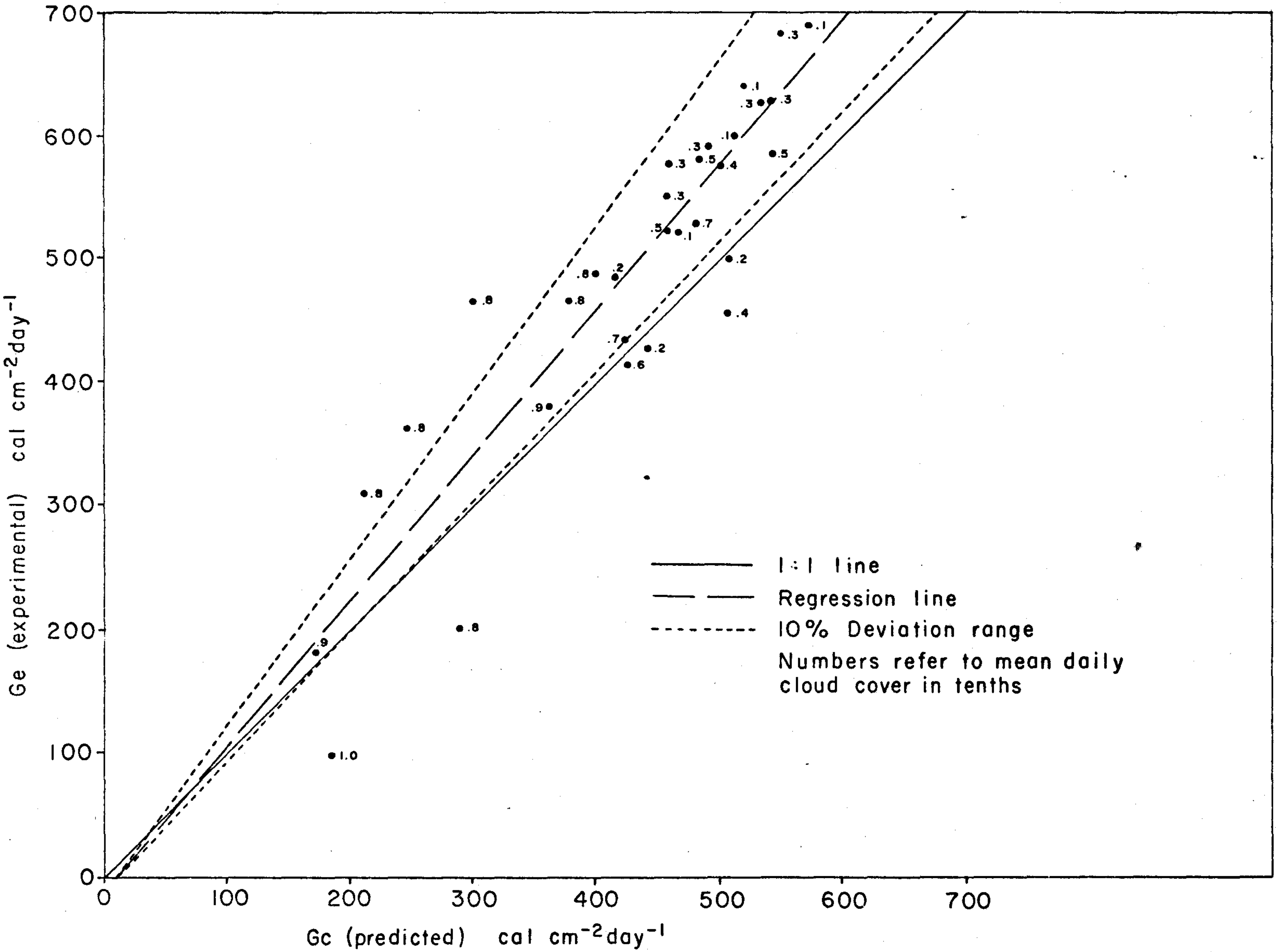

Figure 20
MATEER MODEL
Daily Prediction Using Daily Average Cloud Data

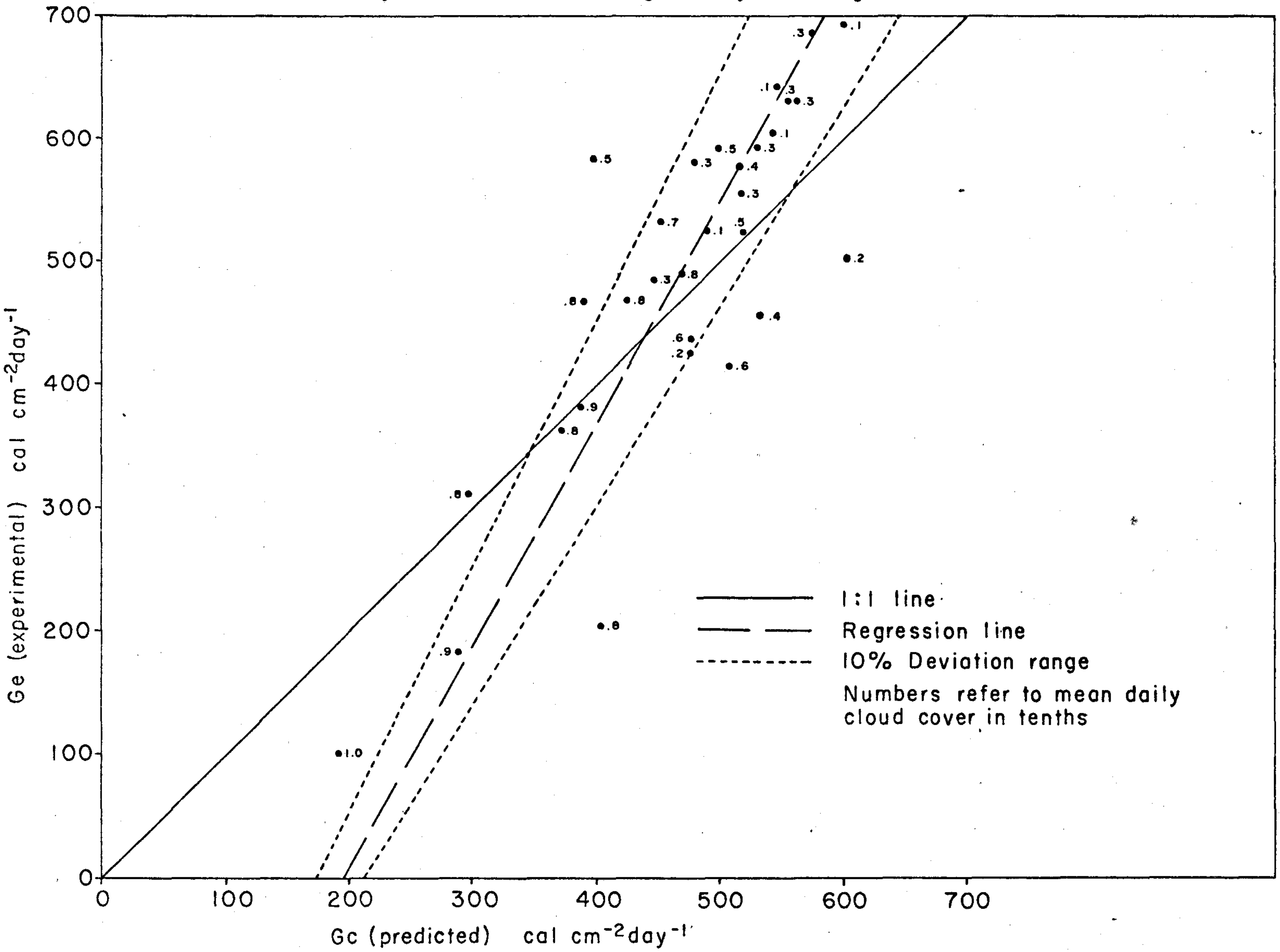

line. Of these, five days had a mean daily cloud cover of 0.8 or larger. It is probable then that changes in cloud transmission properties are felt more strongly under overcast conditions as opposed to partial overcast conditions where periods of large radiation input might obscure any variations in cloud transmission. Figure 21 shows the result of the Layer model using integrated half hourly fluxes. It is evident that allowance for cloud type transmission does not remove the discrepancy. In a similar fashion to the Mateer model, there were twelve days in which model values did not agree with measured values to within 10% of the regression line. Five days out of the twelve days had a mean daily cloud cover of 0.8 or larger. Clearly the prediction error is strongly influencedby systematic variations in cloud transmission under overcast conditions which show a variability even for clouds of the same type.

The effect of using one noon cloud observation rather than three daily observations was also investigated. A total of 68 days were available in which observations were taken at 9:00, 12:00 and 15:00 hours TST. An average cloud value was computed for these three observations and the resultant prediction compared with the noon observations. Tables 15 and 16 show the results of the predictions. There is no significant difference in the correlation coefficients (0.893 and 0.897 for three observations) for the Laevastu and Mateer predictions. All the linear models and the Layer model show a significant improvement in the correlation using the average of the three observations while the Tabata and Berliand models do not. There is a consistent increase in the slope of the regression line when the average of the cloud observations are used.

Figure 21

LAYER MODEL

Daily Prediction Using Sum Of Half-Hourly Fluxes

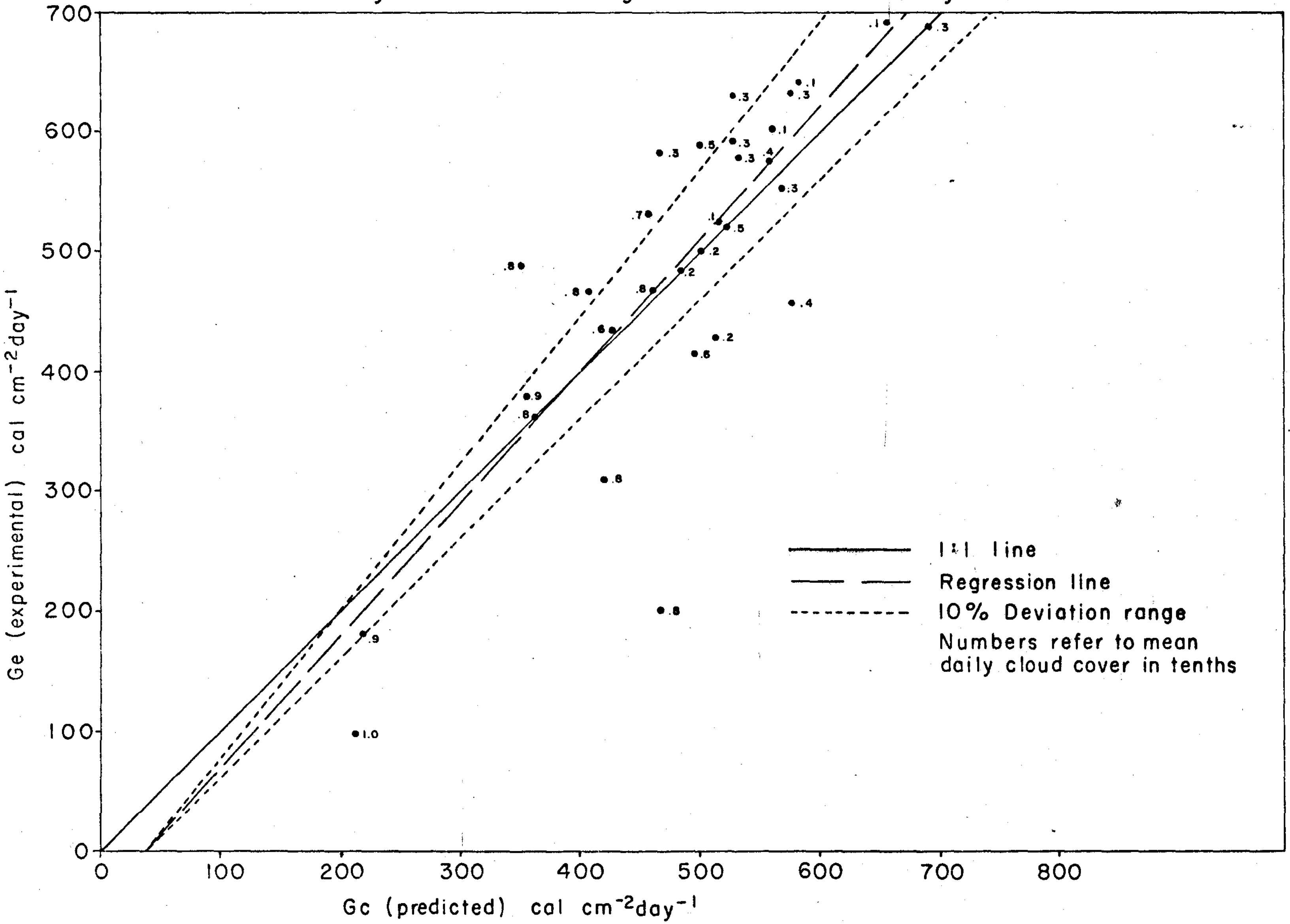

TABLE 15

RESULTS OF A LINEAR REGRESSION ANALYSIS ON THE PREDICTED AND OBSERVED DAILY FLUXES USING NOON CLOUD OBSERVATIONS

Model	Relation	Correlation	Standard Error
			cal cm^{-2} day^{-1}
Budyko	Ge = 0.83 Gc + 108	0.846	91
Houghton	Ge = 0.56 Gc + 180	0.820	98
Kimball	Ge = 0.78 Gc + 136	0.837	94
Monteith	Ge = 0.87 Gc + 79	0.854	89
Neumann	Ge = 0.94 Gc + 36	0.864	86
Berliand	Ge = 0.94 Gc - 86	0.644	130
Laevastu	Ge = 0.83 Gc + 48	0.873	83
Mateer	Ge = 1.00 Gc + 30	0.882	83
Tabata	Ge = 0.76 Gc - 78	0.742	11
Layer	Ge = 0.59 Gc + 250	0.759	111

TABLE 16

RESULTS OF A LINEAR REGRESSION ANALYSIS ON THE PREDICTED AND OBSERVED DAILY FLUXES USING THE AVERAGE OF THREE CLOUD OBSERVATIONS

Model	Relation	Correlation	Standard Error
			cal cm^{-2} day^{-1}
Budyko	Ge = 1.22 Gc - 39	0.898	68
Houghton	Ge = 0.89 Gc - 41	0.882	103
Kimball	Ge = 1.19 Gc - 9	0.893	72
Monteith	Ge = 1.26 Gc - 71	0.901	65
Neumann	Ge = 1.32 Gc - 119	0.904	61
Berliand	Ge = 2.31 Gc - 800	0.660	84
Laevastu	Ge = 1.11 Gc - 104	0.893	77
Mateer	Ge = 1.34 Gc - 123	0.897	63
Tabata	Ge = 1.40 Gc - 491	0.738	111
Layer	Ge = 1 14 Gc + 85	0.845	95

The difference is significant in all models except in the Laevastu and Mateer relations. Figure 22 shows how the Mateer relation predicts using noon observations. Again out of the 43 observations outside of the 10% deviation range, 27 had a noon cloud cover of 0.8 or larger.

Five day averages

A five day time interval was arbitrarily chosen as representing a period larger than a day but still considerably smaller than a month. The noon cloud observations were averaged over the five day period and related to the average daily global radiation for cloudless skies. In the case of the Layer model an average noon solar altitude was obtained which was halved and this was used to obtain the average air mass describing the cloud transmission. The results show a marked improvement in the prediction with a correlation coefficient of 0.95 for the three best fits which were the Mateer, Neumann and Layer model. Figure 23 shows how these three relations predict five day average fluxes throughout the season. Out of the 23 five day periods considered, the Layer model predicted 18 values within 10% of the observed which compares with the 16 values using the Neumann model and 14 values with the Mateer.

Monthly averages

Monthly averages of Go were considered along with averages of noon cloud observations. In the case of the Tabata model the noon solar altitude was taken at the 15th of each month. Similarly the "mean air mass", to calculate the cloud transmission relations for the Layer model, was taken as half the noon solar altitude at the 15th of each month.

Figure 22

MATEER MODEL

Daily Predictions Using Noon Cloud Observations

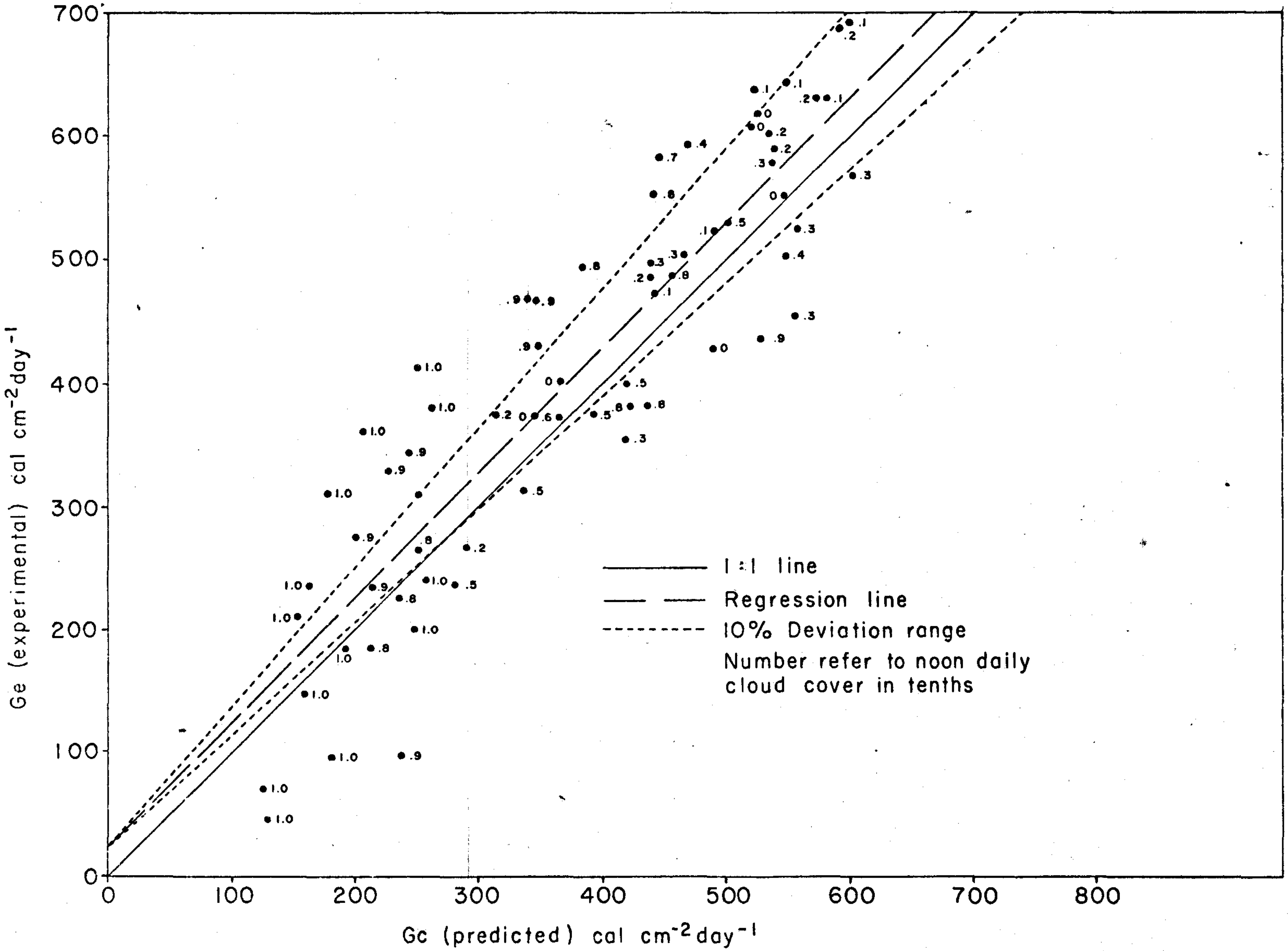

Figure 23
FIVE - DAY PREDICTION USING AVERAGE NOON CLOUD OBSERVATIONS

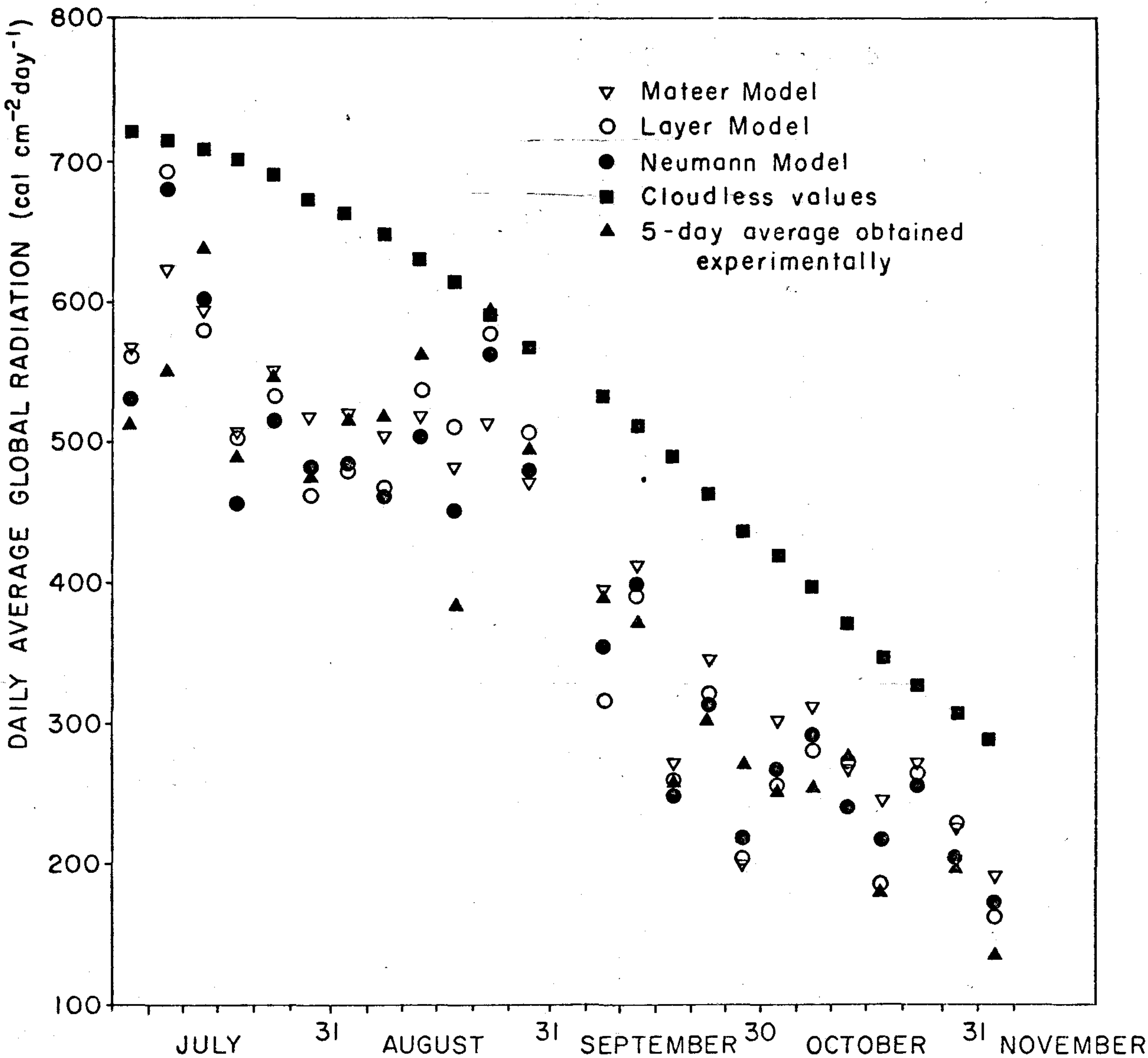

TABLE 17

COMPARISON OF THE OBSERVED AND PREDICTED MONTHLY MEAN FLUXES

($cal\ cm^{-2} day^{-1}$)

Model	July	August	September	October
Budyko	510	476	276	215
Houghton	598	567	293	234
Kimball	494	466	259	204
Monteith	525	488	292	227
Neumann	546	504	316	244
Berliand	641	570	453	336
Laevastu	674	596	405	313
Mateer	568	512	353	271
Tabata	506	468	376	296
Layer	537	537	306	244
Observed	539	517	323	230

Table 17 shows the result. Although a proper comparison is not possible due to lack of data, there are nevertheless some results that are evident. The non-linear models of Laevastu and Berliand tend to overestimate these range of values. The Layer and Neumann models show the best prediction with an error less than 5% in all four predictions. This is followed by the Mateer and the linear models of Budyko, Monteith and Houghton.

Conclusion

At present the problem of short-term prediction of global radiation in cloudy conditions has not been solved. It was hoped that allowance for transmission according to cloud type might solve some of the uncertainties in the prediction. Although the Layer model gave the best correlation, the large standard error observed indicates that the results are far from conclusive. Furthermore, it is evident that the discrepancies must arise from consistent changes in cloud type transmission that cannot be characterized properly using visual observations alone. The results of integrating half-hourly fluxes using the Layer model show large deviations above and below the experimental values. In a large number of cases the discrepancy arises under conditions of high overcast where changes in cloud transmission are most apparent. A logical direction for future work must be to consider the mesoscale climatic conditions at the time of the observations. In particular daily precipitable water vapor estimates might solve some of the anomalies in cloud-type transmission.

It seems that noon observations can be used to predict monthly and five day averages of global radiation satisfactorily. For daily totals it is likely that daily averages of cloud measurements can lead to serious errors under conditions of partial to high overcast.

The non-linear model of Mateer predicts most satisfactorily for all time periods. The Laevastu model can predict correctly for short time periods but is unsatisfactory for five-day or monthly averages. With regards to the linear models, it seems that the Neumann relation gives the best prediction for monthly averages although not enough data are available to discriminate between them.

Finally, it should be mentioned that if total cloud cover is used in the prediction, it seems unlikely that a universal formula, linear or otherwise, will be applicable. At a location the distribution of cloud type will influence the form of the prediction. It might be possible to obtain a universal relationship if cloud type transmission is considered together with a local dependence on precipitable water vapor.

CHAPTER V

THE ALBEDO OF WATER BODIES

A. THEORY AND PREVIOUS MEASUREMENTS

The amount of solar energy reflected from surfaces is a particularly relevant process in the case of lakes or oceans. Their relatively large energy storage capacity as well as the ability of solar radiation to penetrate to large depths make the solar energy input an important parameter.

It is customary in meteorology to characterize the reflection of solar energy from surfaces as the albedo. This term is defined as the ratio of the solar energy reflected from a surface to the incident solar energy. Both are referred to a horizontal surface. The albedo will then be given as:-

$$a = GR/Ge, \tag{47}$$

where, GR = solar flux leaving the surface.

If the surface in question is assumed to be smooth and horizontal the albedo, in the absence of diffuse radiation, can be expressed as:-

$$a = \frac{Ie \cdot R \cdot \cos Z}{Ie \cdot \cos Z} = R, \tag{48}$$

in which, R = direct beam reflectivity. R can be readily calculated since it is the Fresnel reflection for unpolarized light (Kondrat'yev, 1969):-

$$R_F(Z,n) = {}^1/_2 \left[\frac{\sin^2(Z - n)}{\sin^2(Z + n)} + \frac{\tan^2(Z - n)}{\tan^2(Z + n)} \right] , \qquad (49)$$

where, n = index of refraction for the medium.

It has been shown (Centeno, 1941) that n is essentially constant and equal to 1.33 for the visible range in water. Substituting this value into equation 49, the reflectivity of a smooth horizontal water surface can be obtained as a function of the zenith angle (Figure 24).

Experimental estimates of the albedo of water bodies are made using upright and inverted pyranometers. The few results obtained under cloudless skies reveal consistent departures from the Fresnel relation (Kondrat'yev, 1959; Anderson, 1954; Powell and Clarke, 1936). For low zenith angles the theoretical relation is overestimated by a few percent while for high zenith angles the reverse occurs. There can be several factors which could produce this effect;

a) Atmospheric turbidity,

b) Backscatter of radiation from subsurface depths,

c) Surface wave geometry.

Anderson (1954) studied the effect of atmospheric turbidity over Lake Hefner in Oklahoma. After extensive comparisons of the albedo under a turbid and non-turbid air mass and cloudless skies, he concluded that no significant difference existed between the two.

The subject of the albedo of diffuse isotropic solar radiation has also been under investigation. A widely accepted theoretical estimate of 17% was proved incorrect by Burt (1953) who pointed out that the former treatment did not consider the reflected radiation as being incident on a

Figure 24
ALBEDO FOR CLOUDLESS SKIES

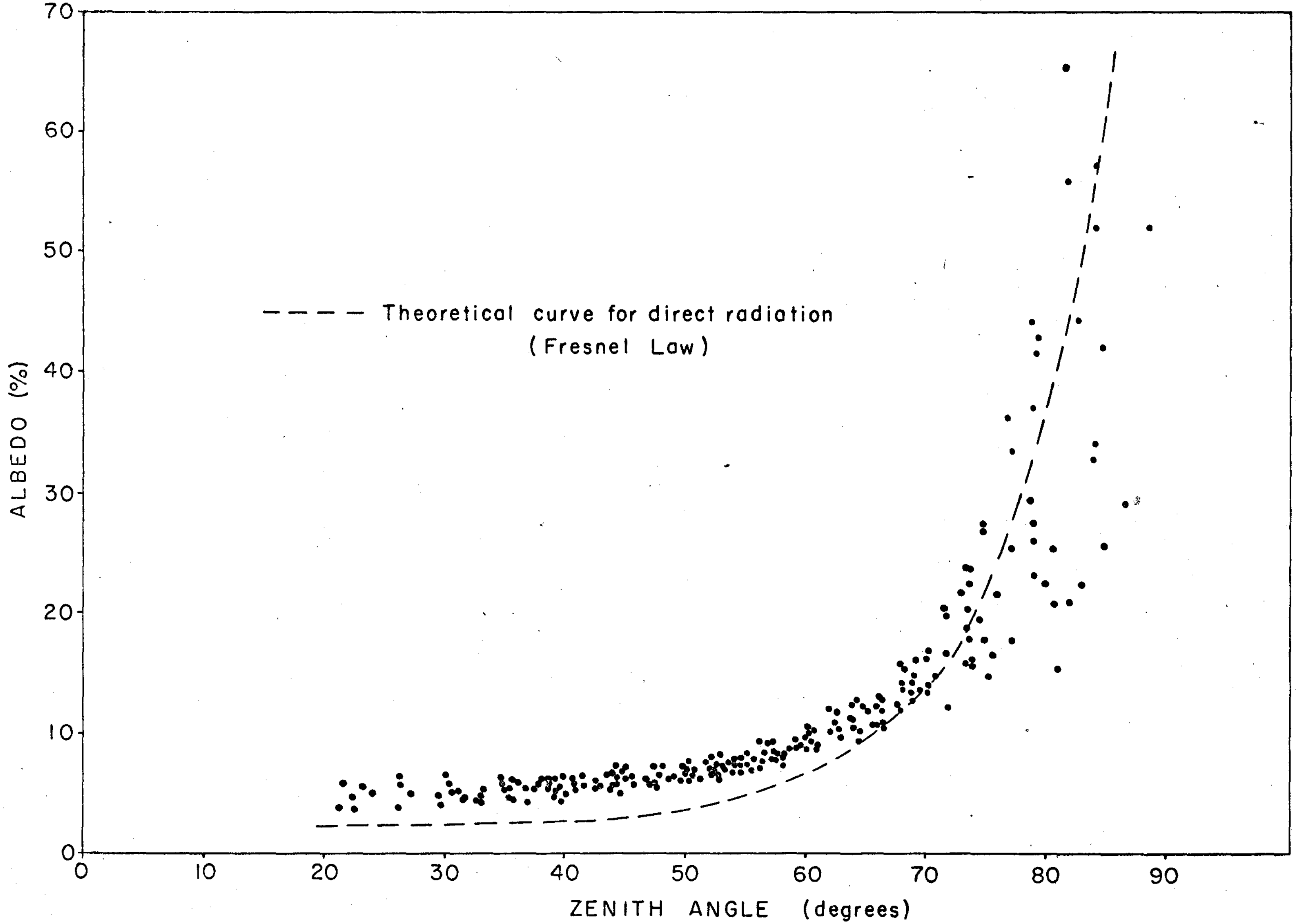

horizontal surface. He calculated a corrected estimate of 6.6% Experimental measurements by Powell and Clarke (1936) and Neumann and Hollman (1961) agree with this value.

Measurements under different cloud conditions have been undertaken by Anderson (1954) as well as Neiburger (1948). The results show a dependence of albedo on zenith angle which is lessened with increasing cloud amount and decreasing cloud height.

Direct observations of the upward scattered solar radiation in the subsurface layers have been studied by several workers, among them are Atkins and Poole (1940), Powell and Clarke (1936) and Jerlov (1968). A value of between 2 to 3% was obtained by Powell and Clarke over deep coastal waters. Jerlov lists a similar result for turbid ocean waters as compared to 6% for the clear case. According to Jerlov not all the upward travelling radiation escapes into the atmosphere since approximately 1/2 is internally reflected. No appreciable diurnal change in this quantity was observed by Powell and Clarke.

The effect of waves on the albedo cannot be computed theoretically without a previous assumption on the wave geometry. Burt (1954) used a statistical distribution of wave facets whose individual reflections could be calculated. A similar model using multiple reflection has been formulated by Cox and Munk (1956). The models predict an increase in albedo under rough conditions for low zenith angles (1 - 2%) and a decrease for large zenith angles (16% for a zenith angle of 80°). Beard and Wiebelt (1966) using a sinusoidal wave shape, show a dependence on solar azimuth as well as on the ratio of wave amplitude to height. Contrary to theoretical predictions, the dependence of albedo on wave height has not been observed experimentally to this writer's knowledge. In fact the extensive studies of Anderson failed to show any dependence. It is possible that the wave effect might be obscured by other significant factors. These will be discussed later.

B. ALBEDO ANALYSIS

The previous discussion has shown that the albedo of a water body cannot be represented accurately by a simple Fresnel reflection. A more accurate representation of the albedo is:-

$$a = \frac{IeR' + DR_D' + B}{Ge}, \tag{50}$$

where, R' = the fraction of the incoming direct radiation that is reflected and is incident on a horizontal surface. In the case of a perfectly smooth horizontal water surface, it can be described as $R_F \cos Z$,

R_F = Fresnel reflection,

R_D' = the fraction of the incident diffuse radiation that is reflected and incident on a horizontal surface,

B = the fraction of the incoming global radiation that is backscattered from the subsurface layers.

The direct, diffuse and backscattered components of the albedo will always be present simultaneously and therefore individual observations of these quantities is difficult. Nevertheless, under certain conditions it is possible to minimize the effect of certain individual components on the albedo.

Under cloudless skies it is logical to expect the diffuse component D to be minimal and thus the curve will approximate Fresnel reflection. Figure 24 shows how the experimental albedo measurements vary as a function of the zenith angle. For purposes of comparison the theoretical Fresnel curve is shown. In agreement with previous observations the measurements are higher than the theoretical curve by about 2% for low zenith angles. At zenith angles greater than 70° there is considerable scatter above and below the theoretical curve. Anderson (1954) also observed a scatter at large zenith angles and attributed it to errors associated with measurement of small radiation values. However, it seems to this writer that diffuse radiation cannot be neglected for large zenith angles. Figure 25 describes the daily variation of diffuse radiation for the seven cloudless days used in this study. For a zenith angle of 70° between 20 to 30% of the radiation is diffuse and increases rapidly for larger zenith angles with considerable scatter. It is thus possible that the albedo values which lie below the Fresnel curve at large zenith angles represent the contribution of the lower albedo of diffuse radiation.

An attempt was made to determine the albedo of diffuse radiation. The technique is essentially the same as that used by Neumann and Hollman (1961). The ratio of the diffuse to total global radiation was plotted as a function of albedo. Two zenith angle ranges of 20° to 25° and 60° to 63° were used. The direct beam albedo was taken as essentially constant in these two ranges. As the Fresnel reflection changes rapidly for zenith angles greater than 60°, the second range was only given a three degree span (Figure 26). The data points were generalized with lines obtained by linear regression. The regression line for the lower zenith angles gives an albedo of 7.4% for totally diffuse radiation and an approximate value of 8.2% was obtained for the higher zenith angle.

Figure 25
RATIO OF DIFFUSE TO GLOBAL RADIATION FOR CLOUDLESS CONDITIONS

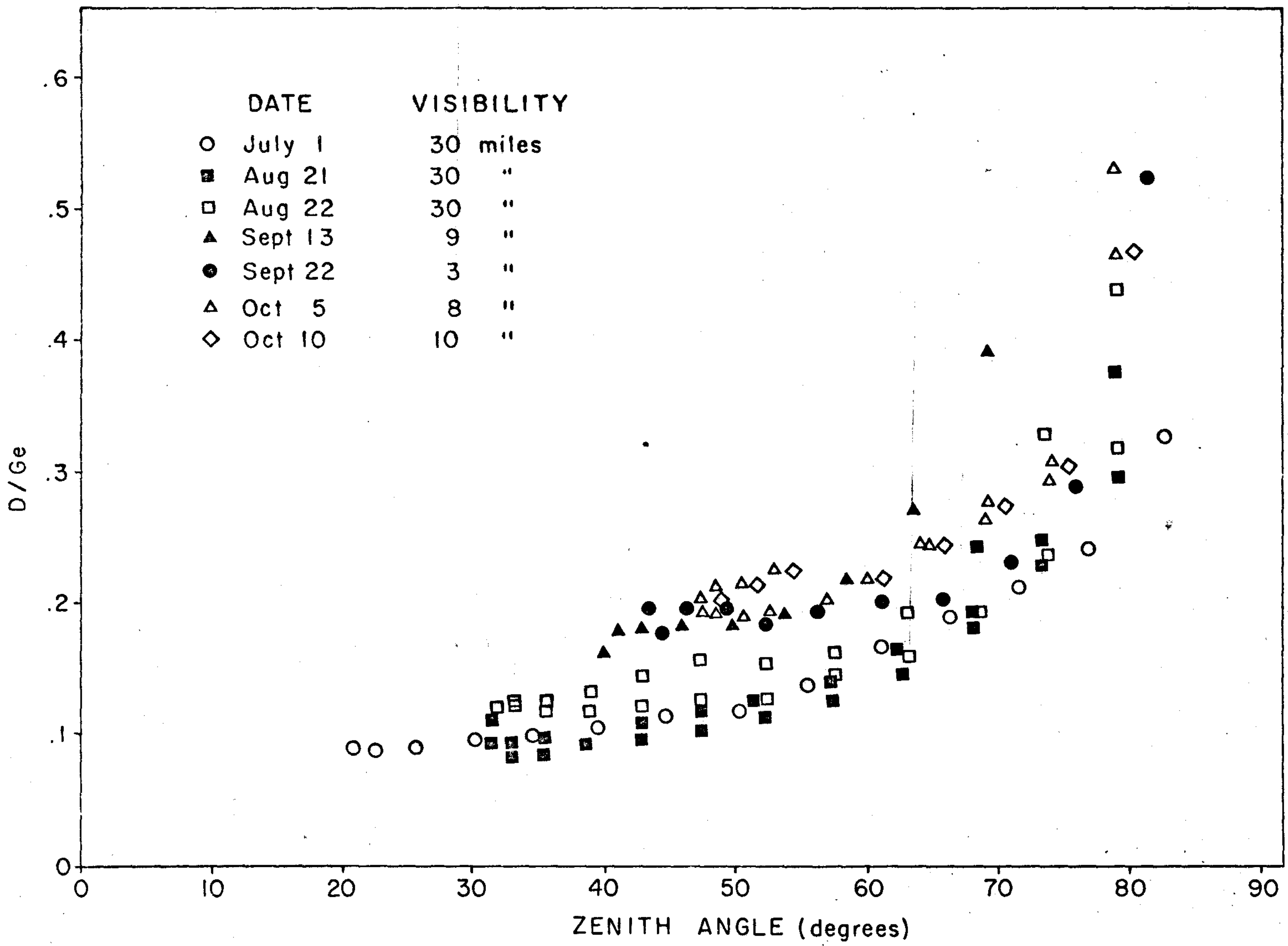

It is clearly seen from Figure 26 that convergence occurs at a value slightly larger than 6.6%, the value predicted theoretically for completely isotropic diffuse radiation. The difference is likely to be attributed to a small but well defined backscatter effect.

Assuming then that the albedo of diffuse radiation is indeed 6.6%, the theoretical reflection from a horizontal thin film of water can be calculated for all the albedo values obtained experimentally. The difference between the measured and calculated must be due to extraneous influences in the water, mainly wave effect and backscatter. Neglecting wave effect the backscatter term B can be given as:-

$$B = aGe - I_e R_F \cos Z - 0.066D; \qquad (51)$$

Although separation of the backscatter and wave effect is strictly not possible, conditions can be chosen so that the wave effect is small. The backscatter can then be estimated using equation 51 if the following assumption are made:-

a) For wave heights less than 5 cm and zenith angles less than 30°, the effect of waves on the albedo is negligible,

b) The albedo of diffuse radiation is 6.6% regardless of the nature of the diffuse radiation.

The first assumption is supported by the theoretical models of Burt (1954) and Cox and Munk (1956) who showed that even for considerable water roughness, there would not be any significant change in the albedo for zenith angles less than 30°. Thus, for this particular analysis albedo measurements were taken which satisfied the first condition. Any discrepancies arising from the second assumption were minimized by omitting

Figure 26

DEPENDENCE OF ALBEDO ON DIFFUSE RADIATION

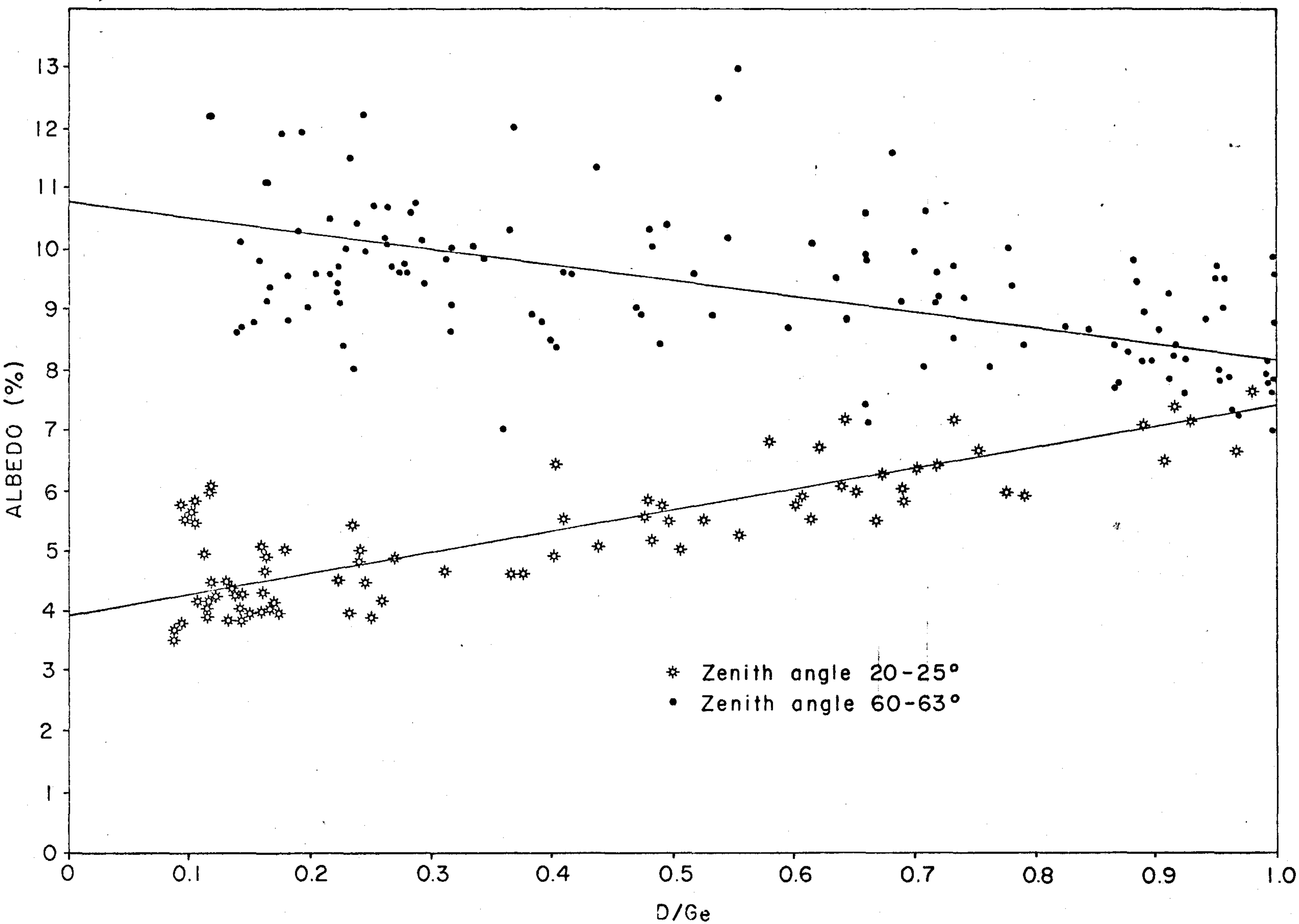

from the analysis conditions in which the diffuse radiation exceeded 20% of the global radiation. In this case then an uncertainty of a few percent in the albedo of diffuse radiation will not affect significantly the overall albedo. Figure 27 shows a frequency distribution for the residual backscatter radiation. An average backscatter of 1.7% was obtained which agrees well with previous measurements.

Finally, an approximate estimate of the wave effect can be attempted if the assumption is made that the backscatter is essentially constant for varying zenith angles. Equation 50 can be rearranged to give:-

$$R' = \frac{aGe - DR_D' - B}{Ie} ; \tag{52}$$

Since a, Ge, D and Ie are obtained from direct measurements and Rd and B have been calculated, then R' can be obtained. For purposes of comparison it is more practical to define a new reflection R'' such that:-

$$R'' = \frac{R'}{\cos Z} ; \tag{53}$$

Thus, for a perfectly smooth horizontal surface:-

$$R'' = \frac{R_F \cos Z}{\cos Z} = R_F . \tag{54}$$

Two periods of "calm" and "rough" wave conditions were then selected and the differences ($R''-R_F$) was plotted as a function of zenith angle. "Calm" conditions were assumed at wave heights of less than 5 cm while rough conditions were assumed to exist at wave heights over 30 cm. Initial results were

Figure 27

BACKSCATTERED RADIATION FROM WATER SURFACE EXPRESSED AS PERCENT OF INCOMING GLOBAL RADIATION. ZENITH ANGLE=20-30°

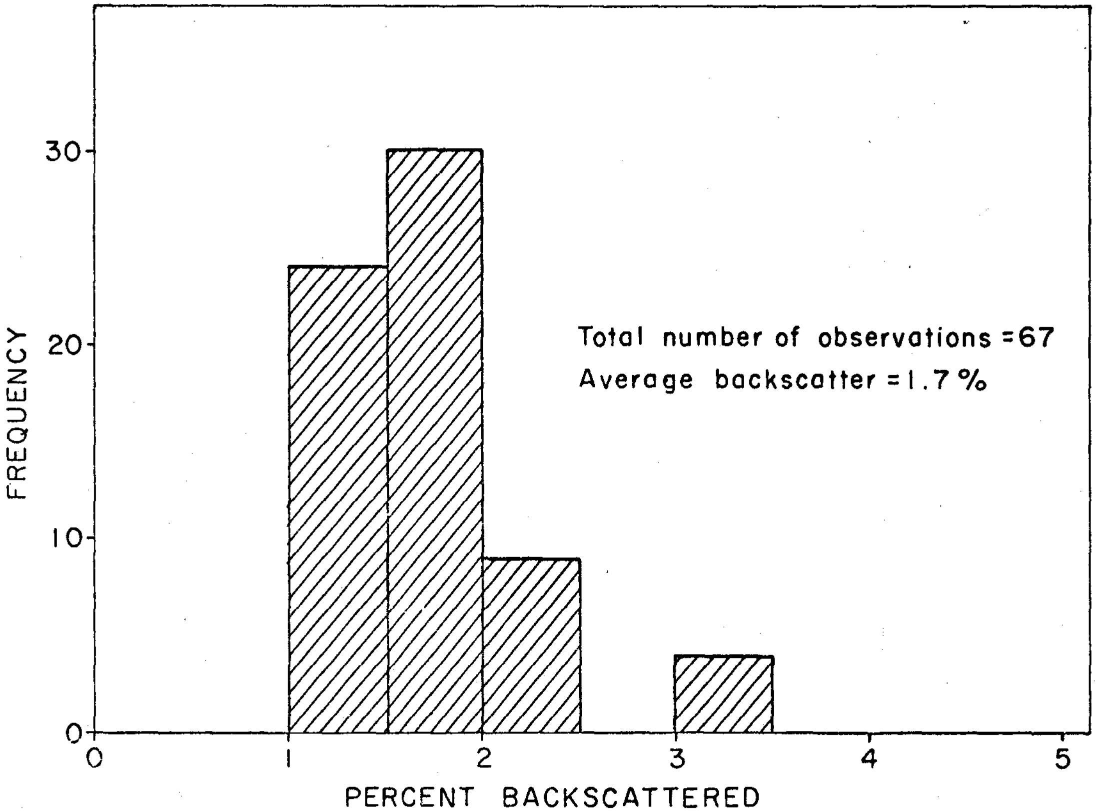

unexpected. The differences proved to be consistently positive for rough conditions and increased with the zenith angle. For calm conditions the differences were slightly negative at low zenith angles but increased regularly with the zenith angle. Originally it was thought that the cosine error might account for the trend. This error arises as a departure of a particular pyranometer from a cosine response when irradiated by direct beam radiation. Although a cosine correction for the particular pyranometer used was not available, the individual departures for a particular make of instrument are not expected to be large. A representative cosine correction was then applied to the direct beam incoming radiation. The results did not show a significant departure from the original trend. The data was then further refined by removing values of global radiation with diffuse radiation greater than 75% of the total energy. This was done to avoid small values of $\dot{I}e$ in equation 52 which would give an erroneously large value of R''. Figure 28 shows the behaviour of $R''-R_F$ with these two corrections taken into account. The consistent positive values for both types of wave conditions indicate that the effect might not be instrumental. After some consideration of the theoretical models, this writer feels that it is not correct to expect agreement between the theory and these measurements. In particular the previous theoretical models consider the entire flux reflected from an arbitrary wave shape. This is not necessarily equal to the total reflected flux incoming on a small horizontal detector. In the case of a perfectly diffuse (Lambertian) surface the equality will be valid. This will not occur with water surfaces which are non-Lambertian. To summarize, for large zenith angles and under cloudless skies there

Figure 28
WAVE EFFECT ON THE ALBEDO

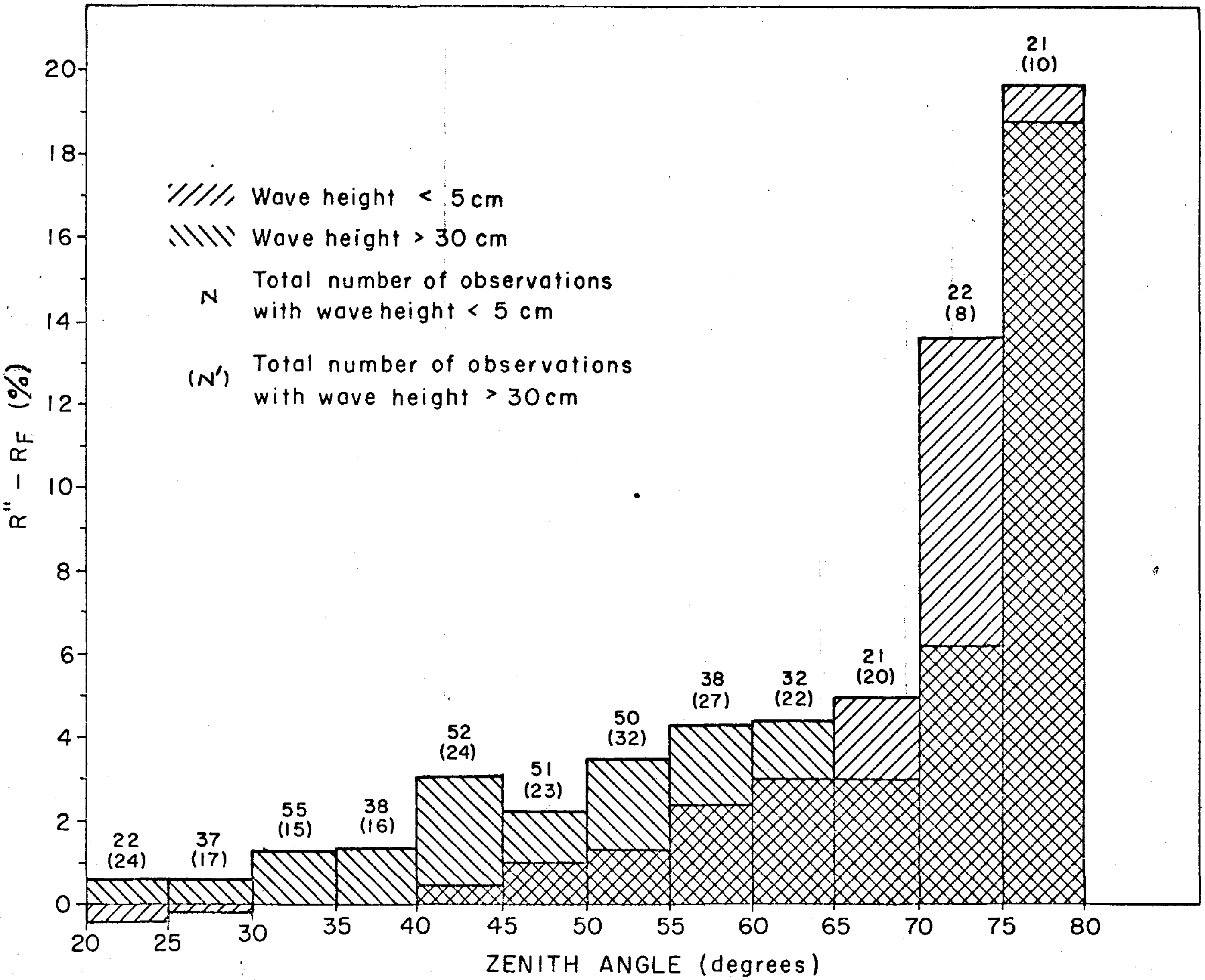

seem to be two opposing trends which will affect the albedo. The large and quite diverse increase in diffuse radiation will lower a and the effect of undulations on the surface seem to cause an increase in a. Although the second effect has not been rigorously shown, at worst no negative differences as predicted theoretically were observed. It is likely that the diffuse albedo is the dominant of the two effects and will thus account for the large number of experimental points beneath the theoretical Fresnel curve.

Under cloudy conditions the amount of incoming diffuse radiation will depend on the cloud amount and characteristics. This will result in an increase in albedo for low zenith angles and a decrease for high. Anderson (1954) obtained albedo measurements under both low and high clouds and for three different cloud covers. Since his results for the high and low clouds did not differ greatly, it was decided in this study to simplify the analysis and group all the albedo values under three different types of total cloud cover. In a manner similar to Anderson's, the cloud cover was subdivided into three main categories: scattered (1/10 to 5/10), broken (6/10 to 9/10) and overcast (10/10). Figures 29, 30 and 31 show the results. For scattered cloud cover a follows the clear day albedo closely. The diurnal change is reduced with considerable scatter under broken clouds and in the overcast case there is little diurnal change from the mean value of 7.5%.

To conclude daily albedos will be briefly considered. Figure 32 shows the seasonal trend for all daily data. Values range between 7% for early July and 11% for the middle of November. Superimposed on this trend is a considerable daily scatter caused primarily by cloud and to a lesser extent by wave action and water turbidity.

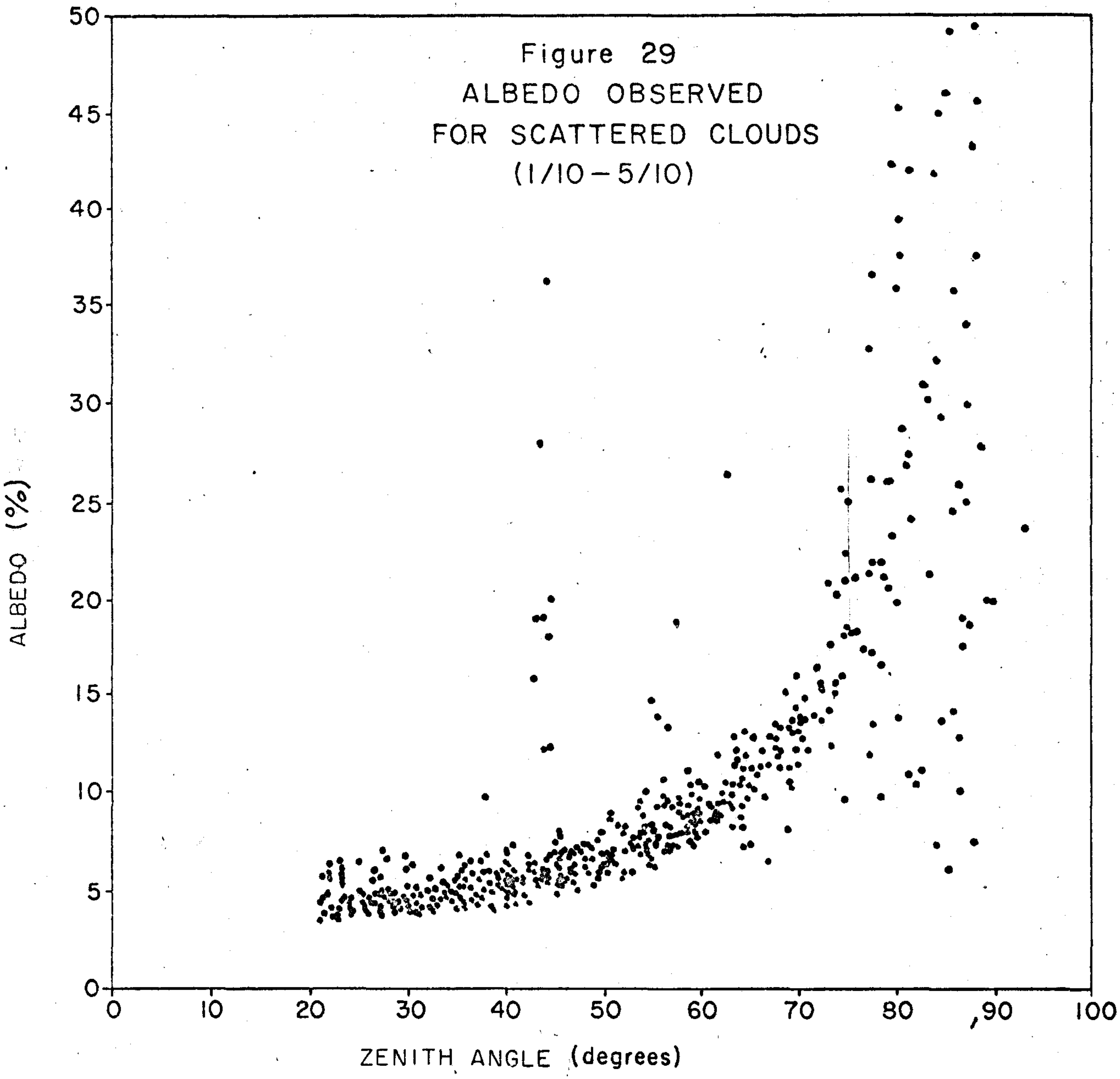

Figure 29
ALBEDO OBSERVED
FOR SCATTERED CLOUDS
(1/10 – 5/10)

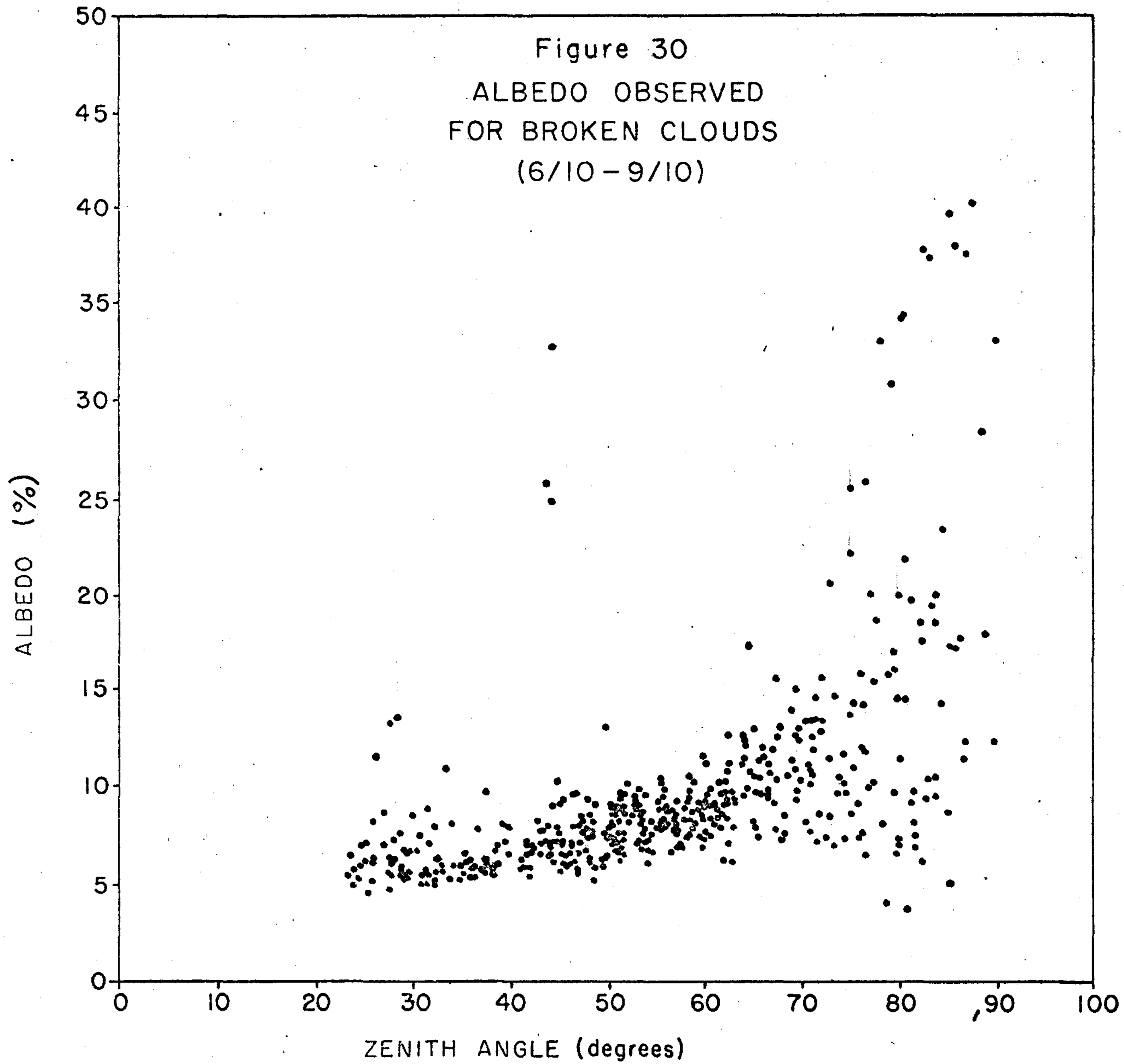

Figure 30
ALBEDO OBSERVED
FOR BROKEN CLOUDS
(6/10 – 9/10)

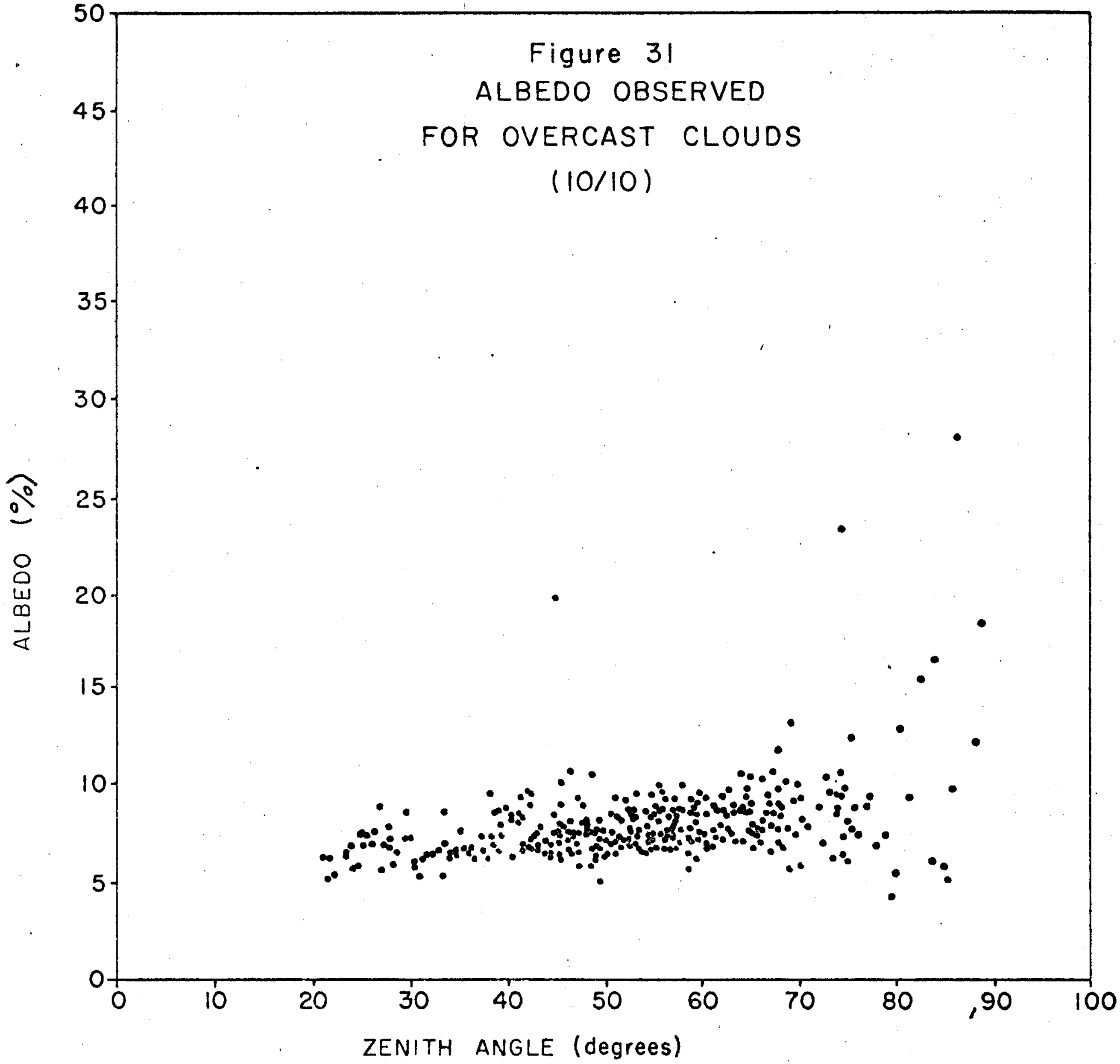

Figure 31
ALBEDO OBSERVED
FOR OVERCAST CLOUDS
(10/10)

Figure 32

DAILY ALBEDOS OBSERVED THROUGHOUT THE SEASON

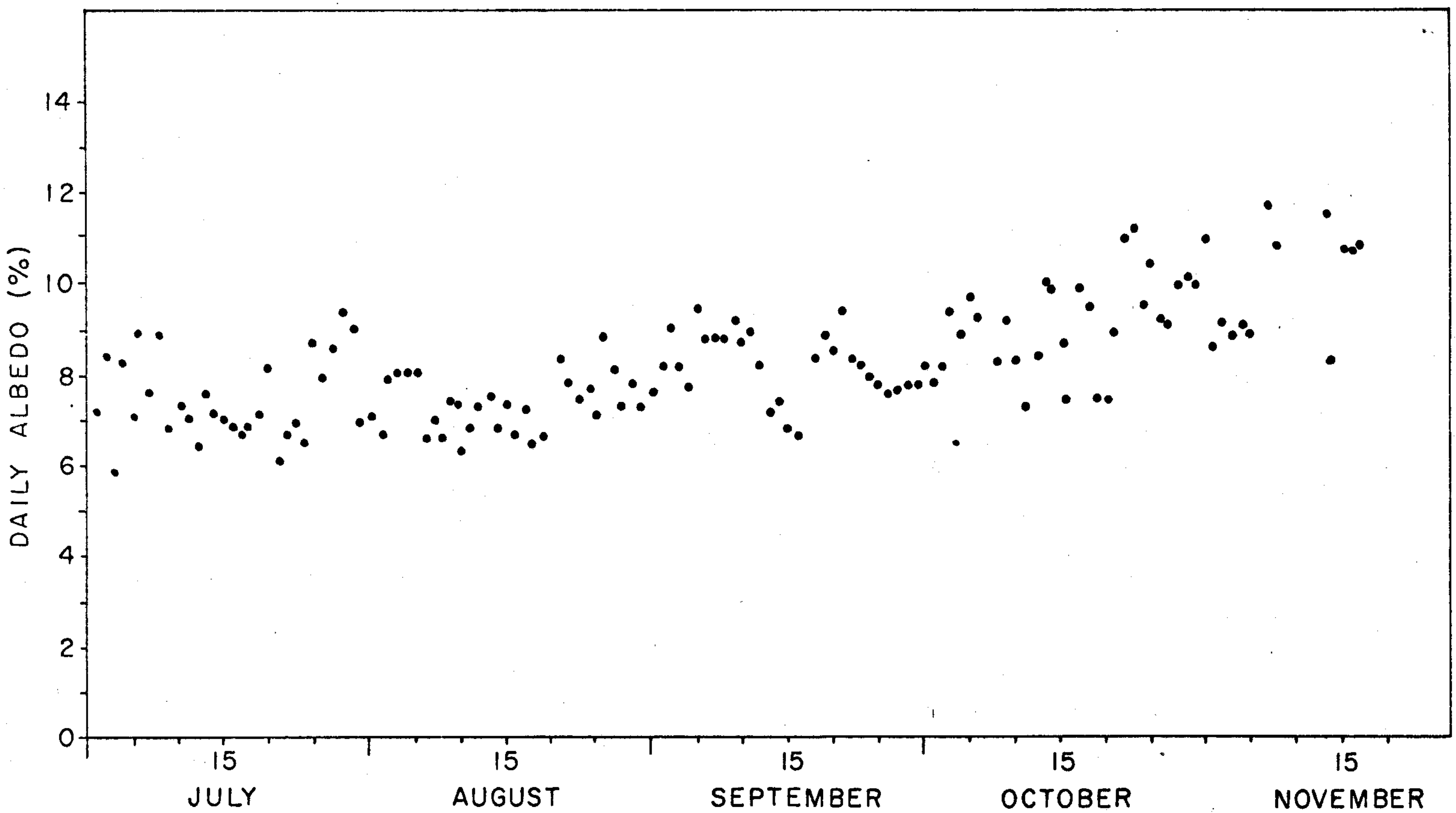

CHAPTER VI

CONCLUSION

The following main points can be inferred as a result of this analysis:-

1. Large variations occur in the aerosol absorption and scattering terms during cloudless days. These variations are of the same order as differences between the Houghton and McDonald water vapor absorption estimates. Since aerosol depletion cannot be properly predicted at present, the use of either of the two water vapor deletion relations is arbitrary.

2. The variation in time of precipitable water vapor must be investigated. The limited number of radiosonde ascents done at the Grimsby site indicate large changes in precipitable water vapor on a diurnal basis. These could have a significant effect on the prediction of global radiation.

3. The depletion of solar radiation under cloudless skies is a conservative process and thus half-hourly fluxes of global radiation can be predicted with an accuracy slightly better than 0.05 cal cm^{-2} min^{-1}. The Houghton and Lettau relations predict best while the London model with its allowance of diffuse absorption and non-isotropic scattering tends to underpredict.

4. The main difficulty in the prediction of global radiation

under cloud conditions lies in determining the cloud transmission properties. The linear predictive models employ a total cloud cover and an empirically determined cloud transmission ε. Because of the large range of cloud types observed in half hourly predictions, such an expression will evidently have large prediction errors. The situation is only slightly improved by allowance for cloud type transmission since this term probably depends on the local climate. Further investigations are needed.

5. The Layer model and the non-linear models of Laevastu and Mateer predict best for half-hourly fluxes. For daily average fluxes the Mateer and Laevastu relations predict most satisfactorily; while for five-day and monthly averages the Layer and Mateer expressions give predictions closest to the measured values.

6. Under cloudless conditions and for zenith angles less than 70°, measured albedo values are higher than the theoretical Fresnel reflection by about 2%. The albedo of diffuse radiation and wave effects tend to be the dominant processes for zenith angles larger than 70° so that large scatter may result.

7. Under conditions of large overcast with totally diffuse incoming radiation, an albedo of between 7 to 8% was obtained. This corresponds approximately to the theoretical estimate of 6.6% (for diffuse isotropic radiation) plus a backscatter term which was observed to be slightly less than 2%. There is an increasing dependence of albedo on zenith angle for decreasing cloud amount.

REFERENCES

Abbot, C. G. and L. B. Aldrich, 1932: An improved water flow pyrheliometer and the standard scale of solar radiation, Smithsonian Inst. Misc. Collections, 87, No. 15, 8 pp.

Abbot, C. G., L. B. Aldrich, and A. G. Frailand, 1954: Concerning Smithsonian pyrheliometry, Smithsonian Inst. Misc. Collections, 123, No. 5, 4 pp.

Anderson, E. R., 1954: Water Loss Investigations: Lake Hefner Studies, Technical Report, U. S. Geol. Surv. Prof. Paper 269, 71-119.

Ångström, A., 1964: The parameters of atmospheric turbidity, Tellus 16, 64-75.

___________, 1962: Atmospheric turbidity, global illumination and planetary albedo of the earth, Tellus 14, 435-450.

___________, 1924: Solar and terrestrial radiation, Quart. J. R. Meteor. Soc., 50, 121-125.

Atkins, W. and H. Poole, 1940: A cubical photometer for studying the angular distribution of submarine daylight, J. Mar. Biol. Assoc., 24, 271-281.

Beard, J. and J. Wiebelt, 1966: Reflectance of a water wave surface as related to evaporation suppression, J. Geophys. Res., 71, 3843-3847.

Berliand, T. G., 1960: Methods for climatological computations of global radiation, Meteor. Hydrol., 6.

Budyko, M., 1956: The Heat Balance of the Earth's Surface, (Translated by U. S. Dept. of Commerce, Washington, D.C., 1958, 259 pp.).

Burt, W. V., 1954: Albedo over wind roughened waters, J. Meteor., 11, 283-290.

___________, 1953: A note on the reflection of diffuse radiation from the sea surface, Trans. A. Geophys. Union, 34, 199-200.

Centeno, M., 1941: Refractive index of liquid water in the near infra-red spectrum, J. Opt. Soc. A., 31, 244-251.

Chandrasekhar, S., 1950: Radiative Transfer, Clarendon Press, Oxford, 385 pp.

Climatic Atlas of the United States, 1968: Edited by Environmental Sci. Services Admin., pub. by U.S. Dept. of Commerce.

Conover, J. H., 1965: Cloud and terrestrial albedo determinations from Tiros satellite pictures, J. Appl. Meteor., 4, 378-386.

Cox, C. and W. V. Munk, 1956: Slopes of the sea surface as deduced from photographs of the sun glitter, Bull. Scripps Inst. Ocea., 6, 401-488.

Dave, J. V. and Z. Sekera, 1959: Effect of ozone on the total sky and global radiation, J. Meteor., 16, 211-212.

Davies, J. A., P. J. Robinson and M. Nunez, 1970: Radiation Measurements over Lake Ontario and the Determination of Emissivity, Dept. of Geography, McMaster Univ., Report HO 81276, 85 pp.

Deirmendjian, D., 1969: Electromagnetic Scattering on Spherical Polydispersions, Elsevier Pub. Co., 290 pp.

Deirmendjian, D. and Z. Sekera, 1954: Global radiation resulting from multiple scattering in a Rayleigh atmosphere, Tellus 6, 382-298.

Drummond, A. J., 1970: Precision radiometry and its significance in atmospheric and space physics, Advances in Geophysics, 14, 1-52.

______________, 1956: On the measurement of sky radiation, Archiv. Meteor. Geophys. Biokl. (B), 7, 413-436.

Feigel'son, E. M., 1966: Light and Heat Radiation in Stratus Clouds, (Translated by Israel Program for Scientific Translation, 245 pp.).

Fowle, F. E., 1915: The transparency of aqueous vapor, Astrophys. J., 42, 394-411.

____________, 1913: The non-selective transmissibility of radiation through dry and moist air, Astrophys. J., 38, 392-406.

____________, 1912: The spectroscopic determination of aqueous vapor, Astrophys. J., 35, 149-162.

Fritz, S., 1958: Absorption and scattering in clouds of large water drops, J. Meteor., 15, 51-58.

_________, 1954: Scattering of solar energy by clouds of large water drops, J. Meteor., 11, 291-300.

Fritz, S. and T. H. McDonald, 1951: Measurements of absorption of solar radiation by clouds, Bull. A. Meteor. Soc., 32, 205-209.

Gates, D. M., 1965: Radiant energy, its receipt and disposal, Meteor. Monographs, 6, No. 28, pp. 1-26, pub. by American Meteor. Soc., Boston, Mass.

Griggs, M., 1968: Aircraft measurements of albedo and absorption of stratus clouds, and surface albedos, J. Appl. Meteor., 7, 1012-1017.

Haltiner, J. H. and F. L. Martin, 1957: Dynamic and Physical Meteorology, McGraw-Hill Pub. Co., 470 pp.

Haurwitz, B., 1948: Insolation in relation to cloud type, J. Meteor., 5, 110-113.

Hay, J. E., 1970: Modelling the Radiation Climate of Canada, report presented at the Annual Conference, Canadian Association of Geographers, Winnipeg, 24 pp.

Hewson, E. W., 1942: Reflection, absorption and transmission of solar radiation by fog and cloud, Quart. J. R. Meteor. Soc., 69, 47-62.

Houghton, H. G., 1954: On the annual heat balance of the northern hemisphere, J. Meteor., 11, 1-9.

Idso, S. B., 1970: The transmittance of the atmosphere for solar radiation on individual clear days, J. Appl. Meteor., 9, 239-241.

__________, 1969: Atmospheric attenuation of solar radiation, J. Atmos. Sci., 26, 1088-1095.

Jerlov, N. G., 1968: Optical Oceanography, Elsevier Ocea. Series, 5, 194 pp.

Kimball, H. H., 1930: Measurements of solar radiation intensity and determinations of its depletion by the atmosphere, Monthly Wea. Rev. 58, 43-52.

__________, 1928: Amount of solar radiation that reaches the surface of the earth on the land and sea and methods by which it is measured, Monthly Wea. Rev., 58, 43-52.

Klein, W. H., 1948: Calculation of solar radiation and the solar heat load on man, J. Meteor., 5, 119-129.

Kondrat'yev, K. Ya. and G. A. Nikolsky, 1970: Solar radiation and solar activity, Quart. J. R. Meteor. Soc., 96, 509-522.

Kondrat'yev, K. Ya., 1969: Radiation in the atmosphere, Academic Press, 912 pp.

Laevastu, T., 1960: Factors affecting the temperature of the surface layers of the sea, Societas Scientiarum Fennica. Commentationes Physico-Mathematicae, XXV, 136 pp.

Lettau, H. and K. Lettau, 1969: Shortwave radiation climatonomy, Tellus, 21, 208-222.

Linke, F., 1942: Die sonnenstrahlung und ihre schwächung in der atmosphäre, Handbuch der Geophysik, Berlin, 8, 239-332.

List, R. J., 1966: Smithsonian Meteorological Tables, Smithsonian Press, Washington, 527 pp.

London, J., 1957: A Study of the Atmospheric Heat Balance, Final Report, Project 131, N.Y.U. Dept. of Meteor. and Ocean., 74 pp.

Mason, B. J., 1962: Clouds, Rain and Rainmaking, Cambridge Univ. Press, 144 pp.

Mateer, C. L., 1963: On the relationship between global radiation and cloudiness at ocean station P, Archiv. Meteor. Geophys. Biokl. (B), 12, 482-490.

McDonald, J. E., 1960: Direct absorption of solar radiation by atmospheric water vapor, J. Meteor., 17, 319-328.

Monteith, J. L., 1962: Attenuation of solar radiation: A climatological study, Quart. J. R. Meteor. Soc., pp. 508-521.

____________, 1959: A solarimeter for field use, J. Sci. Instr., 36, 341-346.

Mügge, R. and F. Möller, 1932: Zur berechnung von strahlungsströmen und temperaturanderungen in atmosphären von beliebigem aufbau. Z. Geophys., 8, 53-64.

Neiburger, M., 1949: Reflection, absorption and transmission of insolation by stratus clouds, J. Meteor., 6, 98-104.

____________, 1948: Reflection of diffuse radiation by the sea surface, Trans. A. Geophys. Union, 29, 647-652.

Neumann, G. and R. Hollman, 1961: On the albedo of the sea surface, Union Geod. Geophys. Intern. Monographie, 10, 72-83.

Neumann, J., 1954: Insolation in relation to cloud type, Monthly Wea. Rev., 82, 317-319.

Ny, T., and S. Choong, 1933: Title not available, Chinese J. Phys., 1, 38.

Paltridge, G. W., R. A. Hamilton and R. H. Collingbourne, 1969: A note on the calculation of aerosol absorption from solar radiation measurements, Quart. J. R. Meteor. Soc., 95, 650-652.

Powell, N. M. and G. L. Clarke, 1936: The reflection and absorption at the surface of the ocean, J. Opt. Soc. A., 26, 111-120.

Reitan, C. H., 1960: Distribution of precipitable water vapor over the United States, Bull. A. Meteor. Soc., 41,79-87.

Robinson, G. D., 1963: Absorption of solar radiation by atmospheric aerosols as revealed by measurements at the ground, Archiv. Meteor. Geophys. Biokl. (B), 12, 19-40.

_______________, 1958: Some observations from aircrafts of surface albedo, Archiv. Meteor. Geophys. Biokl. (B), 9, 29-41.

Robinson, N., 1966: Solar Radiation, Elsevier Pub. Co., 347 pp.

Stair, R. and R. G. Johnson, 1956: Preliminary spectroradiometric measurements of the solar constant, J. Res. Nat. Bur. Std., 57, 205-211.

Tabata, S., 1964: Insolation in relation to cloud amount and sun's altitude, Univ. of Tokyo Geophys. Notes, 17, 202-210.

Vowinckel, E. and S. Orvig, 1962: Relation between solar radiation income and cloud type in the artic, J. Appl. Meteor., 1, 552-559.

Yamamoto, G., 1962: Direct absorption of solar radiation by atmospheric water vapor, carbon dioxide and molecular oxygen, J. Atmos. Sci., 19, 182-188.

Yamamoto, G. and G. Onishi, 1952: Absorption of solar radiation by water vapor in the atmsophere, J. Meteor., 9, 415-421.